

AD-A151 709

ADVANCED CAPACITORS(U) HUGHES AIRCRAFT CO EL SEGUNDO CA

1/3

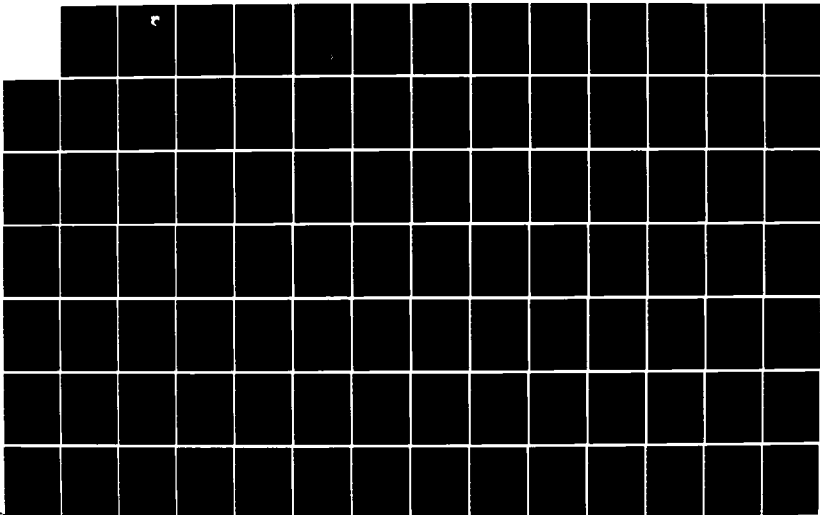
ELECTRO-OPTICAL AND DATA SYSTEMS GROUP
J B ENNIS ET AL OCT 84 HAC-FR84-76-621

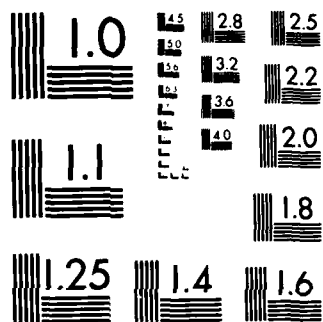
UNCLASSIFIED

AFWAL-TR-84-2058 F33615-79-C-2081

F/G 9/1

NL





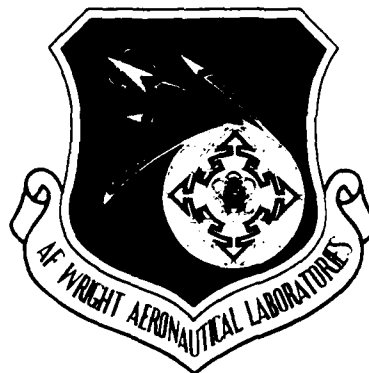
MICROCOPY RESOLUTION TEST CHART
NATIONAL BUREAU OF STANDARDS 1963 A

AD-A151 709

(2)

AFWAL-TR-84-2058

ADVANCED CAPACITORS



Joel B. Ennis and
Robert S. Buritz

Hughes Aircraft Company
Electro-Optical and Data Systems Group
El Segundo, California 90245

October 1984

DTIC
MAR 27 1985
B

Final Report for Period April 1980 to June 1984.

Approved for public release; distribution unlimited.

DTIC FILE COPY

AERO PROPULSION LABORATORY
AIR FORCE WRIGHT AERONAUTICAL LABORATORIES
AIR FORCE SYSTEMS COMMAND
WRIGHT-PATTERSON AIR FORCE BASE, OHIO 45433


85 03 12 110

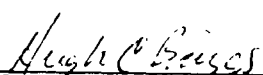
NOTICE

When Government drawings, specifications, or other data are used for any purpose other than in connection with a definitely related Government procurement operation, the United States Government thereby incurs no responsibility nor any obligation whatsoever; and the fact that the government may have formulated, furnished, or in any way supplied the said drawings, specifications, or other data, is not to be regarded by implication or otherwise as in any manner licensing the holder or any other person or corporation, or conveying any rights or permission to manufacture use, or sell any patented invention that may in any way be related thereto.


This report has been reviewed by the Office of Public Affairs (ASD/PA) and is releasable to the National Technical Information Service (NTIS). At NTIS, it will be available to the general public, including foreign nations.

This technical report has been reviewed and is approved for publication.


NEAL C. HAROLD, Lt, USAF
Power Systems Branch
Aerospace Power Division


HUGH C. BRIGGS, Major, USAF
Chief, Power Systems Branch
Aerospace Power Division

FOR THE COMMANDER


JAMES D. REAMS
Chief, Aerospace Power Division
Aero Propulsion Laboratory

"If your address has changed, if you wish to be removed from our mailing list, or if the addressee is no longer employed by your organization please notify AFWAL/POOS, W-PAFB, OH 45433 to help us maintain a current mailing list".

Copies of this report should not be returned unless return is required by security considerations, contractual obligations, or notice on a specific document.

UNCLASSIFIED

SECURITY CLASSIFICATION OF THIS PAGE

REPORT DOCUMENTATION PAGE

1a. REPORT SECURITY CLASSIFICATION UNCLASSIFIED			1b. RESTRICTIVE MARKINGS	
2a. SECURITY CLASSIFICATION AUTHORITY			3. DISTRIBUTION/AVAILABILITY OF REPORT	
2b. DECLASSIFICATION/DOWNGRADING SCHEDULE			Approved for public release; Distribution unlimited.	
4. PERFORMING ORGANIZATION REPORT NUMBER(S) FR84-76-621			5. MONITORING ORGANIZATION REPORT NUMBER(S) AFWAL-TR 84-2058	
6a. NAME OF PERFORMING ORGANIZATION Hughes Aircraft Co. Electro-Optical Group		6b. OFFICE SYMBOL (If applicable)		7a. NAME OF MONITORING ORGANIZATION Aero Propulsion Laboratory (AFWAL/POOS) Air Force Wright Aeronautical Laboratories
6c. ADDRESS (City, State and ZIP Code) P.O. Box 902 El Segundo, CA 90245			7b. ADDRESS (City, State and ZIP Code) Wright-Patterson AFB, OH 45433	
8a. NAME OF FUNDING/SPONSORING ORGANIZATION		8b. OFFICE SYMBOL (If applicable)		9. PROCUREMENT INSTRUMENT IDENTIFICATION NUMBER F33615-79-C-2081
8c. ADDRESS (City, State and ZIP Code)			10. SOURCE OF FUNDING NOS.	
			PROGRAM ELEMENT NO. 31	PROJECT NO. 45
			TASK NO. 32	WORK UNIT NO. 55
11. TITLE (Include Security Classification) (U) Advanced Capacitors				
12. PERSONAL AUTHOR(S) Joel B. Ennis and Robert S. Buritz				
13a. TYPE OF REPORT Final		13b. TIME COVERED FROM Apr80 to Jun84		14. DATE OF REPORT (Yr., Mo., Day) October 1984
15. PAGE COUNT 189				
16. SUPPLEMENTARY NOTATION				
17. COSATI CODES			18. SUBJECT TERMS (Continue on reverse if necessary and identify by block number)	
FIELD 0901	GROUP 0903	SUB GR 0905	Capacitor, pulse power, dielectric systems, pulse capacitor, marx bank, pulse forming network	
19. ABSTRACT (Continue on reverse if necessary and identify by block number)				
<p>This report contains a description of an experimental development program conducted by Hughes Aircraft Company to develop and test advanced dielectric materials for capacitors for airborne power systems. Five classes of capacitors were considered: high rep rate and low rep rate capacitors for use in pulse-forming networks, high voltage filter capacitors, high frequency AC capacitors for series resonant inverters, and AC filter capacitors. To meet these requirements, existing dielectric materials were modified and new materials were developed.</p> <p>The initial goal of the program was to develop an improved polysulfone film with fewer imperfections that could operate at significantly higher electrical stresses. At the beginning of the program, low breakdown strength was thought to be related to inclusions of conductive particles, thin spots, or holes in the dielectric. Many experiments were performed to evaluate the effect of filtration of the casting solution. As these experiments proceeded, it became apparent that mere filtration and attention to the details</p>				
20. DISTRIBUTION/AVAILABILITY OF ABSTRACT UNCLASSIFIED/UNLIMITED <input checked="" type="checkbox"/> SAME AS RPT <input type="checkbox"/> DTIC USERS <input type="checkbox"/>			21. ABSTRACT SECURITY CLASSIFICATION UNCLASSIFIED	
22a. NAME OF RESPONSIBLE INDIVIDUAL REX L. SCHLICHER, Capt., USAF			22b. TELEPHONE NUMBER (Include Area Code) (513) 237-8766	22c. OFFICE SYMBOL AFWAL/POOS-2

DD FORM 1473, 83 APR

EDITION OF 1 JAN 73 IS OBSOLETE

UNCLASSIFIED
SECURITY CLASSIFICATION OF THIS PAGE

SECURITY CLASSIFICATION OF THIS PAGE

Financial constraints prevented further development of the high frequency, AC inverter capacitor due to lack of funding. The untested design is proposed for future study.

A-1

DTIC
ELECTE
MAR 27 1985
B

SECURITY CLASSIFICATION OF THIS PAGE

SUMMARY

This report contains a description of an experimental development program conducted by Hughes Aircraft Company to develop and test advanced dielectric materials for capacitors for airborne power systems. Five classes of capacitors were considered: high rep rate and low rep rate pulse capacitors for use in pulse-forming networks, high voltage filter capacitors, high frequency AC capacitors for series resonant inverters, and AC filter capacitors. To meet these requirements, existing dielectric materials were modified, and new materials were developed.

The initial goal of the program was to develop an improved polysulfone film with fewer imperfections that could operate at significantly higher electrical stresses. At the beginning of the program, low breakdown strength was thought to be related to inclusions of conductive particles, thin spots, or holes in the dielectric. Many experiments were performed to evaluate the effect of filtration of the casting solution. As these experiments proceeded, it became apparent that mere filtration and attention to the details of maintaining a particle-free film were not the entire solution to the breakdown problem. From a series of experiments, the film samples were found to contain mobile charge carriers, as dissolved ionic impurities, that move through the dielectric when voltage is applied and cause distortion and enhancement of the electric field. It was shown that these contaminants enter the film via the resin and solvent, and that they can be partially removed. As far as developed, however, these treatments did not significantly improve the breakdown characteristics. It still must be determined to what extent the impurities must be removed.

The technique of casting films on a roughened drum was demonstrated, and found useful in preparing textured films. -- This is the first step toward a replacement for Kraft paper.

A new material, Ultem[®], was proposed for use in high energy density capacitors. This new polyetherimide resin has properties similar to polysulfone and polyimide, with improvement in breakdown characteristics and temperature capability. This material was selected for further study and evaluation in model capacitor designs.

Test fixtures were built for life tests of four types of capacitors under actual service conditions. Samples of each type of capacitor were assembled and tested according to plan. In some cases, a second design was built and tested after life tests and failure analyses had been performed on the original design.

Failures in the pulse capacitors occurred short of the lifetime goal, and were related to overheating. The second DC filter design achieved only a 150 hour life at a packaged energy density of 100 J/lb. Ultem was found to be superior to commercial polysulfone film in the 400 Hz AC filter capacitor application.

Financial constraints prevented further development of the high frequency, AC inverter capacitor due to lack of funding. The untested design is proposed for future study.

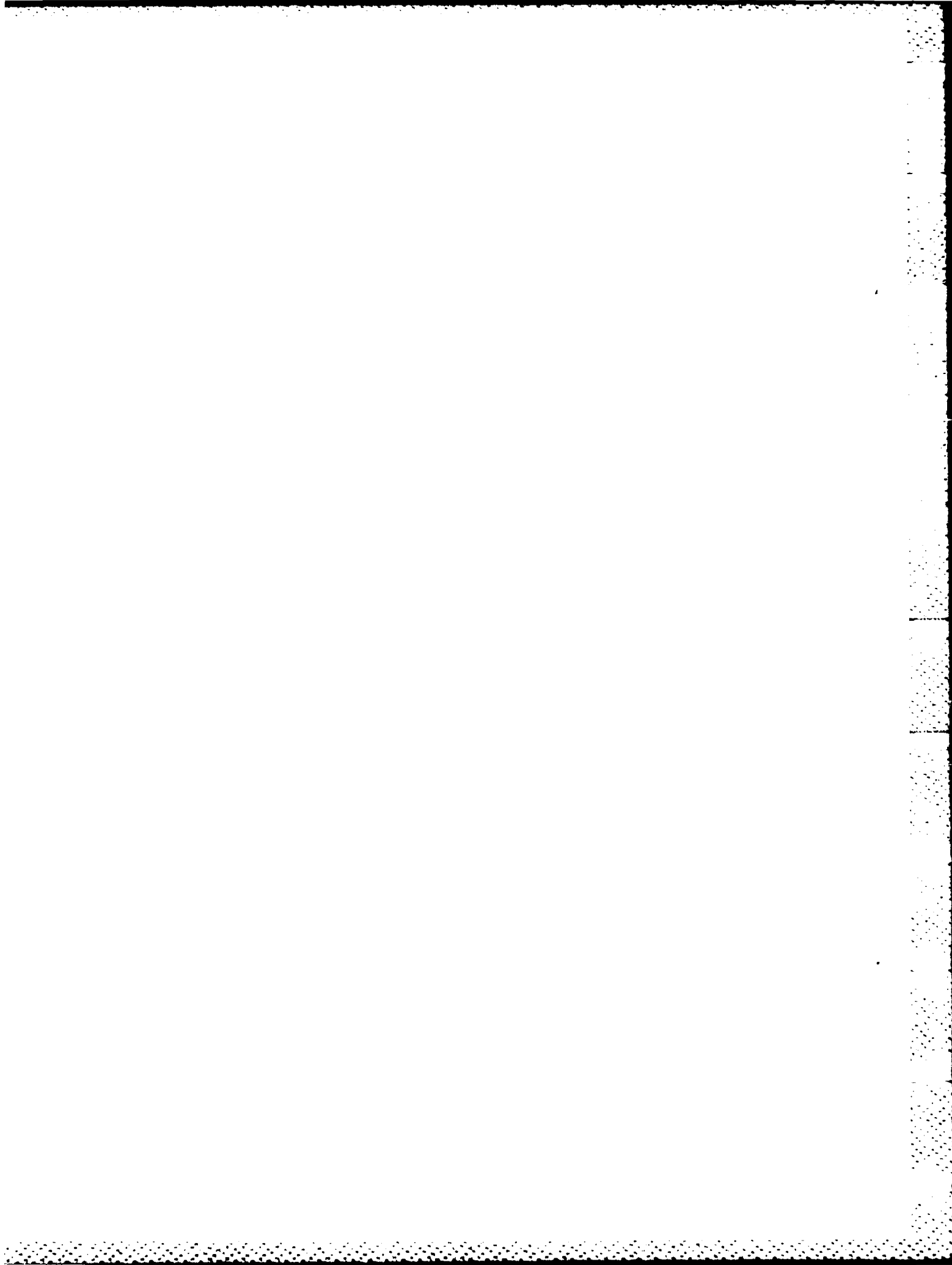
Ultem is a registered trademark of General Electric.

FOREWORD

This report presents the progress made by the Hughes Aircraft Company in the developing and testing of dielectric materials for capacitors under Contract F33615-79-C-2081, supported by the Air Force Aero Propulsion Laboratory at Wright-Patterson AFB, OH. Mr. Michael P. Dougherty monitored the program from its inception until 1982, when it was transferred to Capt. Gerald Clark and in 1983 to Capt. Rex Schlicher. Dr. Robert D. Parker was the Program Manager at Hughes from contract go-ahead until February 1982. Currently the Program Manager is Mr. Robert S. Buritz. Mr. Joel B. Ennis joined the program as Principal Investigator in August 1983.

Phase I - Material Testing and Selection was conducted by Hughes at its Culver City, California facility. A significant portion of the effort of Task III - Material Fabricating, Testing, and Final Selection was contracted to the Schweitzer Division of the Kimberly-Clark Corporation at Lee, MA. Schweitzer developed and prepared improved film insulating materials, assisted in the definition of the most productive technical approaches, and performed preliminary testing. Dr. W. Selke, Director of Research, Mr. E.P. Bullwinkel and Dr. A.R. Taylor were responsible for the material development and testing conducted at Schweitzer.

Phase II - Capacitor Pad Design and Testing was conducted by Hughes at its new El Segundo, CA facility. The 400 Hz AC filter capacitors were fabricated by Component Research Company, Inc., Santa Monica, CA. Mr. Hillel Kellerman, Vice President, was very helpful in providing assistance for this effort at Component Research.



CONTENTS

1.0	INTRODUCTION	1-1
1.1	Capacitor Considerations	1-3
1.2	High Repetition Rate Pulse Capacitor	1-3
1.3	Low Repetition Rate Pulse Capacitors	1-5
1.4	DC Filter Capacitor	1-6
1.5	High Frequency AC Capacitor	1-8
1.6	AC Filter Capacitor	1-9
1.7	Program Summary	1-10
	1.7.1 Phase I - Material Testing and Selection	1-10
	1.7.2 Phase II - Capacitor Pad Design and Testing	1-11
2.0	TECHNICAL BACKGROUND	2-1
2.1	Dielectric Design Theory	2-1
2.2	Failure Mechanisms	2-6
	2.2.1 Electrical Failure	2-6
	2.2.2 Thermal Failure	2-8
	2.2.3 Dielectric Flaws	2-11
	2.2.4 Manufacturing Flaws	2-12
	2.2.5 Mechanical Failure	2-13
3.0	PRELIMINARY MATERIAL/DIELECTRIC SYSTEMS SELECTION	3-1
3.1	Candidates for Improvement	3-1
	3.1.1 Higher Quality Films	3-2
	3.1.2 Denser Kraft Paper	3-3
	3.1.3 Kraft Paper Replacement	3-4
	3.1.4 Film Lamination	3-5
	3.1.5 High Dielectric Constant Impregnants	3-5
3.2	Expected Improvements	3-7
3.3	Preliminary Candidate Systems and Estimates	3-8
	3.3.1 High Repetition Rate Capacitor	3-8
	3.3.2 Low Repetition Rate Capacitor	3-8

CONTENTS (Continued)

	3.3.3	DC Capacitor	3-9
	3.3.4	High Frequency AC Capacitor	3-9
4.0		MATERIAL TEST PLAN	4-1
	4.1	Introduction	4-1
	4.2	Developmental Testing	4-1
	4.3	Parametric Characterization	4-2
	4.4	Acceptance Testing	4-2
	4.5	Test Procedures	4-2
	4.6	Requirements	4-2
	4.7	Using the Test Plan	4-4
5.0		MATERIAL FABRICATION AND TESTING	5-1
	5.1	Introduction	5-1
	5.2	Voltage Breakdown Testing	5-2
	5.3	Measurement of Ionic Contaminants in Polymer Solutions and Solvents	5-9
	5.4	Polymer Film Conductivity	5-11
	5.5	Filtration Studies	5-11
	5.6	Charge Mobility Experiments	5-14
		5.6.1 Small Area Tests	5-14
		5.6.2 Time-Dependent Breakdown	5-16
		5.6.3 Film Conductivity	5-19
	5.7	Decontamination Procedures	5-19
	5.8	Polyetherimide Film	5-24
	5.9	Textured Film	5-26
6.0		FINAL SELECTION	6-1
	6.1	Recommended Dielectric Systems and Revised Estimates	6-1
		6.1.1 High Repetition Rate Capacitor	6-1
		6.1.2 Low Repetition Rate Capacitor	6-2
		6.1.3 DC Filter Capacitor	6-2
		6.1.4 High Frequency AC Capacitor	6-2
7.0		MATERIAL CHARACTERIZATION	7-1
	7.1	Tests on Plastic Films	7-1
		7.1.1 Ultem Polyetherimide	7-2
		7.1.2 Kimfone Polysulfone	7-7
		7.1.3 Billore Biaxially Oriented Polypropylene	7-7
		7.1.4 Fluorofilm-C Polytetrafluoroethylene	7-7

CONTENTS (Continued)

7.2	Tests on Dielectric Liquids	7-7
7.2.1	BASF Platinol DOP	7-11
7.2.2	Dow Corning DC-200 Silicone	7-11
7.2.3	Helix FE-4 Fluoropropane Ether	7-11
7.3	Kraft Papers	7-11
7.4	Wetting Study	7-16
7.5	Textured Film Study	7-19
8.0	CAPACITOR PAD DESIGNS	8-1
8.1	Capacitor Pad Test Plan	8-1
8.2	Design Considerations	8-2
8.2.1	High Repetition Rate Pulse Capacitor	8-2
8.2.2	Low Repetition Rate Pulse Capacitor	8-4
8.2.3	DC Filter Capacitor	8-5
8.2.4	High Frequency AC Capacitor	8-6
8.2.5	AC Filter Capacitor	8-7
8.3	Material Selection	8-9
8.3.1	High Repetition Rate Pulse Capacitor	8-9
8.3.2	Low Repetition Rate Pulse Capacitor	8-13
8.3.3	High Frequency AC Capacitor	8-13
8.3.4	AC Filter Capacitor	8-14
8.4	Capacitor Section Size	8-15
8.5	Dielectric Designs	8-16
8.5.1	High Repetition Rate Pulse Capacitor	8-21
8.5.2	Low Repetition Rate Pulse Capacitor	8-21
8.5.3	DC Filter Capacitor	8-24
8.5.4	High Frequency AC Capacitor	8-24
8.5.5	AC Filter Capacitor	8-26
8.6	Pad Designs	8-26
9.0	MANUFACTURING PROCEDURES	9-1
9.1	Pad Winding	9-1
9.2	Pad Pressing	9-4
9.3	Assembly into the Can	9-5
9.4	Oil Filtration and Testing	9-7
9.5	Pre-Impregnation Testing	9-8
9.6	Impregnation and Sealing	9-8
9.7	Conclusions	9-10
10.0	CAPACITOR PAD TESTING	10-1
10.1	Parametric Measurements	10-1

CONTENTS (Continued)

10.1.1	Capacitance and Dissipation Factor	10-1
10.1.2	Equivalent Series Resistance	10-4
10.1.3	Insulation Resistance	10-4
10.1.4	Dielectric Withstand Voltage	10-6
10.1.5	AC Filter Capacitor Tests	10-7
10.2	Life Test Fixtures	10-8
10.2.1	Pulse Capacitors	10-8
10.2.2	DC Filter	10-11
10.2.3	High Frequency AC	10-12
10.2.4	AC Filter	10-14
10.3	Temperature Rise Study	10-15
10.4	Life Tests	10-21
10.4.1	High Repetition Rate Pulse Capacitor	10-21
10.4.2	Low Repetition Rate Pulse Capacitor	10-23
10.4.3	DC Filter Capacitor	10-28
10.4.4	AC Filter Capacitor	10-28
10.5	Failure Analyses	10-30
10.5.1	High Repetition Rate Pulse Capacitors	10-30
10.5.2	Low Repetition Rate Pulse Capacitors	10-31
10.5.3	DC Filter Capacitors	10-33
10.5.4	AC Filter Capacitors	10-33
11	CONCLUSIONS	11-1
	REFERENCES	R-1
	APPENDIX	A-1

1.5 HIGH FREQUENCY AC CAPACITOR

This capacitor is used in a series resonant inverter circuit to provide a resonant impedance for the storage of energy. The AC voltage signal at 10 kHz is at 1060 VRMS and results in a current flow of over 480 ARMS. Thus, this 8 μ F capacitor must handle more than 500,000 VAR. The specifications for this capacitor are summarized in Table 4.

TABLE 4. HIGH FREQUENCY AC CAPACITOR SPECIFICATIONS

Parameter	Value	Unit
Capacitance	8	μ F
Voltage		
Peak	1500	Volts
RMS	1060	Volts
Current		
Peak	679	Amperes
RMS	480	Amperes
Frequency	10	kHz
Duty Cycle	Continuous	
Dissipation Factor	<0.0001	
Energy Density (goal)	50	J/lb

The energy density goal was set at 50 J/lb. Converted to "power" density, this figure translates to $5.7 \cdot 10^6$ VAR/lb of capacitor!

Recently, White and Galperin at Maxwell Laboratories reported on the design of a similar capacitor for NASA-Lewis.⁹ The capacitance was 0.83 μ F, operating at 600 VDC plus 600 VRMS at 40 kHz with a current of 125 ARMS. The capacitor was vacuum qualified and designed to operate with a 60°C baseplate temperature and had a dielectric of polypropylene impregnated with monoisopropyl biphenyl (MIPB). This capacitor was operating with 75,000 VAR of reactive (wattless) power. This unit weighed about 7.5 pounds, so the energy density was about 0.12 J/lb.¹⁰ This can be considered the state of the art.

TABLE 3. DC FILTER CAPACITOR SPECIFICATIONS

Parameter	Value	Unit
Capacitance	0.4	μ F
Working Voltage	25	kV
Ripple voltage	21	VRMS
Ripple Frequency	20	kHz
Current	5.3	ARMS
Duty Cycle	Continuous	
Dissipation Factor	≤ 0.002	
Energy Density (goal)	100	J/lb

An off-the-shelf capacitor of this type is typically designed for a lifetime of at least 10,000 hours and often 20 years. Because of this, energy densities may be low even though the application is relatively benign. For example, General Electric produces capacitors of this type designed for 60,000 hour life at 50°C which have energy densities of 12 to 32 J/lb, depending on the capacitance.⁸ Hughes has produced small capacitors of this type capable of meeting stringent military standards with energy densities up to 26 J/lb.

Improvements in the energy density of this capacitor must either come from decreased life or improved materials capable of providing the same lifetimes at much greater stresses. Failures in these capacitors are not due to partial discharges at foil edges or thermal degradation, but are generally due to flaws in the dielectric materials. Microscopic conducting paths through the insulation rapidly overheat and breakdown follows. These conducting paths may originate in a number of ways, but mechanical stress points on wrinkles or winding folds are common failure locations, indicating that stretching, thinning, or microcracking of polymer films is ultimately responsible.

TABLE 2. LOW REPETITION RATE PULSE CAPACITOR SPECIFICATIONS

Parameter	Value	Unit
Energy Stored	1760	Joules
Peak Voltage	40	kV
Voltage Reversal	≥ 20	Percent
Capacitance	2.2	μF
Peak Current	52.6	kA
Pulse Rise Time	2	μsec
Capacitor Inductance	≤ 20	μH
Pulse Repetition Rate	50	pps
Burst Length	60	Seconds
Duty Cycle	≤ 2	Hours
Life	10^6	Pulses
Shelf Life	> 1	Year
Ambient Temperature	≤ 72	$^{\circ}\text{C}$
Energy Density (goal)	500 10	J/lb J/in ³

and less than 15 minutes off, and which achieved energy densities of 28 J/lb at lifetimes of better than 10^7 shots. This work was aimed at comparisons of impregnating liquids and other dielectric materials in achieving long lifetimes. Dodecyl benzene out-performed both mineral oil and dioctyl phthalate oils for long life.

1.4 DC FILTER CAPACITOR

This capacitor is used to filter out ripple from a DC power supply. The DC voltage is 25 kV, with a 21 VRMS AC signal at 20 kHz to be filtered out. The operation of this capacitor, unlike the previous two pulse capacitors, is continuous. Since a relatively small amount of current passes through the conductors of this component, heating is not a problem. Details of the specifications for this capacitor are given in Table 3.

In a previous program conducted by Hughes ("Capacitors for Aircraft High Power," F33615-75-C-2021) for the Aero Propulsion Laboratory, pulse discharge capacitors were developed for the same PFN application. These achieved a packaged energy density of 77 J/lb at a lifetime of 10^5 shots. The dielectric was Kraft and polysulfone.¹

Major problems inherent in high average power capacitors are heat generation, thermal stability, and heat removal. Insulation materials are selected for low dissipation factors and high temperature capability. Heat removal is accomplished through packaging design and electrode terminations. Both polysulfone and polyetherimide films selected for use on this program have moderate dissipation factors and moderate thermal stability.

1.3 LOW REPETITION RATE PULSE CAPACITORS

This capacitor is intended for use in a 6-section PFN designed to deliver 10.6 kJ of energy to a load in a rectangular pulse 20 μ s wide. The PFN would be charged to 40 kV and discharged 50 times per second. The required life is 10^6 pulses when operating in a "burst" mode duty cycle of 1 minute on and up to 2 hours cool down time. Further specifications are given in Table 2.

Because this capacitor operates at a much lower repetition rate than the previously described component, heating problems are greatly reduced. This provides the opportunity to work the dielectric at higher stress levels and achieve significantly greater energy densities.

In earlier work, Hoffman and Ferrante achieved 141 J/lb at 50 kV using an unspecified paper/plastic mineral oil dielectric tested under undisclosed conditions.⁶ In an effort to develop components for airborne use, Hoffman was able to build capacitors which stored 218 J/lb at a few pulses per second, and 120 J/lb at "moderate" repetition rates.⁷

On the earlier Hughes program, lifetimes of 10^4 to 10^5 shots were achieved in model capacitors having an unpackaged energy density of 87 J/lb. These were tested at a repetition rate of 50 pps for 1 minute and then cooled for 1 hour.¹ Since that time, IR&D work has produced a number of capacitors which were tested at repetition rates of 30 pps, duty cycles of 1 minute on

TABLE 1. HIGH REPETITION RATE PULSE CAPACITOR SPECIFICATIONS

Parameter	Value	Unit
Energy Stored	250	Joules
Peak Voltage	15	kV
Voltage Reversal	≥ 20	Percent
Capacitance	2.2	μF
Peak Current	20	kA
Pulse Rise Time	2	μsec
Capacitor Inductance	≤ 20	μH
Pulse Repetition Rate	300	pps
Burst Length	60	Seconds
Duty Cycle	≤ 2	Hours
Life	10^6	Pulses
Shelf Life	> 1	Years
Ambient Temperature	≤ 72	$^{\circ}\text{C}$
Energy Density (goal)	≥ 300 ≥ 3	J/lb J/in ³

development effort, Dailey and White reported capacitors achieving a 10^5 pulse life at 50 J/lb when operating at 250 pps in 60-second bursts, and 76 J/lb at 100 pps in 30-second bursts.² Creedon and Fitch reported (in 1976) the development of a 6-section PFN employing 0.75 μF , 40 kV capacitors which had a lifetime of well over 10^5 shots at an energy density of 42 J/lb while operating at 125 pps in 30 to 75 second bursts.³ These capacitors were of Kraft/polycarbonate/castor oil construction and the PFN was developed for the US Army's ERADCOM. Subsequent increases in energy density were achieved by going to a polypropylene dielectric, but Army goals of 150 J/lb and 250,000 shot life have not been met.⁴ During the latter part of this program, G. Howard Mauldin at Sandia National Laboratories reported achieving lifetimes of 10^5 to 10^7 shots and energy densities of about 50 J/lb at 100 to 500 pps continuous.⁵ This was achieved using polysulfone film impregnated with a fluorocarbon liquid.

lifetime were sought for four different capacitor applications. Another objective was to determine whether Ultem polyetherimide film could be used as a replacement for polysulfone in certain high temperature environments.

1.1 CAPACITOR CONSIDERATIONS

Several types of capacitor applications were considered during this program. These were: 1) a high repetition rate (300 pps) pulse capacitor, 2) a low repetition rate (50 pps) pulse capacitor, 3) a DC filter capacitor, 4) a high frequency series resonant inverter capacitor, and 5) a 400 Hz AC filter capacitor. The latter application was added late in the program. The first four applications were expected to be met by oil impregnated, wound film-paper-foil capacitors, while the fifth item was to be a dry metallized film capacitor. The latter was the only one of the five which did not have an operating voltage of at least 1000 volts.

Each of these capacitor applications is a distinct and unique design problem, although the two pulse capacitors have much in common. Throughout this report, the five capacitors will be considered individually, reflecting the philosophy of the development effort. In the following sections, the specifications and goals for each capacitor are detailed, as well as historical background on previous progress in the development of each class of capacitor, providing a reference point as to the state of the art before this program.

1.2 HIGH REPETITION RATE PULSE CAPACITOR

This capacitor is intended for use in 6-section pulse forming networks (PFNs), capable of providing 1.5 kJ of energy to a load in a rectangular pulse 20 μ s wide. The PFN would be charged to a peak voltage of 15 kV and discharged 300 times per second. The required lifetime is 10^6 pulses when operating in a "burst" mode duty cycle of 1 minute on and up to 2 hours cool down time. Further specifications are given in Table 1.

Previous work on high repetition rate pulse capacitors has not provided a component which could simultaneously meet both the energy density goal and lifetime needed for airborne military systems. In an airborne component

increase, unless changes are made in the way the capacitors are constructed. Therefore, the essential problem is to increase the amount of energy which can be stored by a given volume or weight of dielectric. Because this "energy density" is a function of the square of the magnitude of the electric field applied, this program was aimed at increasing the value of the electric field which could be applied across the dielectric of a practical capacitor without a catastrophic breakdown.

The intrinsic dielectric strengths of the films available for use in capacitors range from 3.1 MV/cm (8 kV/mil) to 5.9 MV/cm (15 kV/mil), so energy densities in the range 100 J/kg (500 J/lb) to 3850 J/kg (1750 J/lb) should be possible. Since these numbers are far in excess of those reported in the literature, it is pertinent to ask the reason for the large difference.

Two problems faced in achieving higher energy densities are electrical breakdown and thermal failure. Some capacitors used for pulsed-energy storage fail because corona arising in manufacturing anomalies or material defects eventually punctures the insulation, resulting in a shorted unit. The second type of failure results from dissipation of relatively large amounts of power in a poorly cooled volume. This failure can take the form of thermal runaway, insulation failure because of very great local hot-spot temperatures, or excessive thermal expansion. This last failure mode is sometimes quite dramatic; the capacitor case suddenly ruptures from the internal pressure.

The AFAPL-funded program previously conducted by Hughes resulted in the elimination of manufacturing defects and many material problems.¹ Failures in high repetition rate units are now observed to occur at fields in excess of 4.97 MV/cm (5 kV/mil) and to be about equally distributed between wearout because of corona at the foil edge and random dielectric failure. Random dielectric failure is caused primarily by dielectric material flaws, such as pinholes, conducting particle inclusions, variations in thickness, and thermally activated flaws. One of the objectives of this program was to reduce the random dielectric failures by developing materials of higher quality and better dielectric properties than those previously available. Based on the projected results of such an effort, large increases in the energy density for a given

1.0 INTRODUCTION

A need for large amounts of electrical power in a number of airborne and space military systems has been envisioned for some time. A technical barrier which has always stood in the way of such systems has been the required volume and weight of the power source and power conditioning subsystem. The purpose of this program was to address the power conditioning subsystem of such a high power system in an effort to reduce its weight. Particular attention was given the capacitive components which are used as energy storage devices.

Applications of this technology exist in the future development of directed-energy weapons such as lasers, high power radars, and radio frequency noise generators (jamming equipment) as well as any other devices or systems with large power requirements in an airborne or space environment.

Capacitors are essentially electrical components which store energy in the form of an electric field in an insulator between two electrodes. In contrast, inductors store energy in the form of a magnetic field. Capacitors are used in circuits in many different ways, and are exposed to different types of electrical stresses depending on the application. This program was concerned with:

1. Capacitors used to store energy over a relatively long period of time and then deliver that energy to a load in a short pulse.
2. Capacitors used to reduce irregularities in a DC or AC voltage.
3. Capacitors used to cyclically store energy and exchange it with an inductor in a resonant circuit.

The size and weight of capacitors generally increase as the amount of energy they can store increases. Thus, as power and energy requirements increase in military systems, the size and weight of the capacitors used will

TABLES (Continued)

Table		Page
26	Contact Angle (θ) Measurements	7-18
27	Solid-Vapor Surface Tension of Liquids	7-20
28	Surface Tension of Selected Polymers	7-21
29	Power Dissipated Versus DF	8-7
30	Polymer Films Considered	8-10
31	Dielectric Liquids Considered	8-10
32	Comparison of Polysulfone and Polyetherimide Films . . .	8-12
33	High Repetition Rate Pulse Capacitor Dielectric Systems	8-22
34	Low Repetition Rate Pulse Capacitor Dielectric Systems	8-23
35	DC Filter Capacitor Dielectric Systems	8-25
36	High Frequency AC Capacitor Dielectric Systems	8-27
37	AC Filter Capacitor Dielectric Systems	8-28
38	DOP Filtration Test Results	9-9
39	Capacitance Measurements	10-2
40	Dissipation Factor Measurements	10-3
41	Resistance Parameter Measurements	10-5
42	Comparison of TC Test Capacitors	10-16
43	Life Test Results — High Repetition Rate Pulse Capacitors	10-24
44	Life Test Results — Low Repetition Rate Pulse Capacitors	10-25
45	Life Test Results — DC Filter Capacitors	10-29
46	Comparison of Program Goals and Values Achieved	11-3

TABLES (Continued)

Table		Page
26	Contact Angle (θ) Measurements	7-18
27	Solid-Vapor Surface Tension of Liquids	7-20
28	Surface Tension of Selected Polymers	7-21
29	Power Dissipated Versus DF	8-7
30	Polymer Films Considered	8-10
31	Dielectric Liquids Considered	8-10
32	Comparison of Polysulfone and Polyetherimide Films . . .	8-12
33	High Repetition Rate Pulse Capacitor Dielectric Systems	8-22
34	Low Repetition Rate Pulse Capacitor Dielectric Systems	8-23
35	DC Filter Capacitor Dielectric Systems	8-25
36	High Frequency AC Capacitor Dielectric Systems	8-27
37	AC Filter Capacitor Dielectric Systems	8-28
38	DOP Filtration Test Results	9-9
39	Capacitance Measurements	10-2
40	Dissipation Factor Measurements	10-3
41	Resistance Parameter Measurements	10-5
42	Comparison of TC Test Capacitors	10-16
43	Life Test Results — High Repetition Rate Pulse Capacitors	10-24
44	Life Test Results — Low Repetition Rate Pulse Capacitors	10-25
45	Life Test Results — DC Filter Capacitors	10-29
46	Comparison of Program Goals and Values Achieved	11-3

LIST OF TABLES

Table		Page
1	High Repetition Rate Pulse Capacitor Specifications . . .	1-4
2	Low Repetition Rate Pulse Capacitor Specifications . . .	1-6
3	DC Filter Capacitor Specifications	1-7
4	High Frequency AC Capacitor Specifications	1-8
5	AC Filter Capacitor Specifications.	1-9
6	Field Distribution in Pulse Discharge Component	3-3
7	Properties of Impregnants	3-6
8	Test Procedures for Films	4-3
9	Test Procedures for Oils	4-3
10	Test Procedures for Papers	4-4
11	Particle Analyses of Filtered Casting Solutions	5-12
12	Dissipation Factor Measurements for Various Solutions . .	5-22
13	SAT Breakdown for Treated Films	5-22
14	Properties of Ultem [®] and Polysulfone Resin	5-25
15	Ultem 24GA Properties	7-3
16	Breakdown Strength of Ultem	7-5
17	Insulation Resistance of Ultem	7-6
18	Properties of 24GA Kimfone Polysulfone	7-8
19	Properties of Polypropylene Film	7-9
20	Properties of 25GA Fluorofilm-C	7-10
21	Properties of BASF Platinol DOP	7-12
22	Properties of DC-200	7-13
23	Properties of Helix FE-4 Fluoropropane Ether	7-14
24	Norden Kraft 30 GA Properties	7-15
25	Liquid-Vapor Surface Tension of Liquids	7-17

ILLUSTRATIONS (Continued)

Figure		Page
41	DC Filter Capacitor Test Fixture	10-12
42	High Frequency AC Test Fixture Design	10-13
43	AC Filter Capacitor Test Circuit	10-15
44	Temperature Rise Versus Total Power in Pulse Capacitors	10-17
45	Dependence of ESR on Voltage	10-18
46	Normalized Plot Showing Cooling of Capacitors with Time	10-20
47	Temperature Rise Versus Peak Voltage	10-22
48	Weibull Plot of Low Rep Rate Pulse Capacitor Life Test Data	10-26
49	Capacitor Failure Rate Distribution	10-28
50	Weibull Plot of DC Filter Capacitor Life Test Data . . .	10-34

ILLUSTRATIONS (Continued)

Figure		Page
21	Current Density Versus Time for Commercial Polysulfone Film	5-20
22	Current Density Versus Voltage Stress for Commercial Polysulfone Film	5-20
23	Current Density Versus Voltage Stress for Treated and Untreated Film	5-23
24	Large Area Breakdown Versus Voltage Stress	5-24
25	Large Area Breakdown Counts/Meter ² Versus Voltage Stress Ultem® Film	5-25
26	Ultem Dielectric Constant	7-4
27	Ultem Dissipation Factor	7-4
28	Profilometer Profile Measurements of Ultem Films	7-22
29	Original High Repetition Rate Pulse Capacitor for 2.2 μ F Pad Arrangement	8-15
30	High Repetition Rate Pulse Capacitor 1.1 μ F Pad Arrangement	8-16
31	Average Direct Voltage Breakdown Strength for Typical Capacitor Dielectric Pads Built Up With Five Different Capacitor Paper Thicknesses Showing Effects of Varying Number of Paper Sheets Between Electrodes	8-19
32	The Dielectric Strength of Several Films Versus Thickness	8-20
33	Capacitor Winding Machine	9-3
34	Pad Test Configuration	9-6
35	Reusable Test Vessel Assembly	9-6
36	Oil Filtration System	9-7
37	Leakage Current and Dielectric Withstand Voltage Test Circuit	10-6
38	Histogram of Leakage Current Data for Ultem and Kimfone Metallized Film Capacitors	10-8
39	Histogram of Leakage Current Data	10-9
40	Discharge Voltage and Current Waveforms for (a) 2.2 μ F and (b) 1.1 μ F Pad Test Configurations	10-10

LIST OF ILLUSTRATIONS

Figure		Page
1	Density Versus Field for Two Dielectric Systems	2-2
2	Polyvinylidene Film Dissipation Factor Versus Frequency	2-9
3	Typical Dissipation Factor Versus Temperature	2-9
4	Dielectric Strength Versus Temperature of Various Capacitor Dielectrics	2-10
5	Typical Large Area Breakdown Test Results	3-7
6	Density of Defects in Polysulfone Films	5-3
7	Aqueous Line Contact Electrodes	5-4
8	Nondestructive VBT	5-5
9	Energy Dissipation in Sample	5-6
10	Electrode Circuits	5-7
11	Waveforms	5-8
12	Surface Discharge - Free Electrode System	5-9
13	Ion Pair Dissociation Versus Liquid Dielectric Constant	5-11
14	Breakdowns Versus Voltage Stress	5-13
15	Breakdown Voltage Stress Versus Time of Applied Bias Voltage	5-14
16	Charge Distribution Within "Polarized" Dielectric	5-15
17	Percent of Ultimate Breakdown Voltage Under Ramp Conditions Versus Time of Application of DC Voltage Small Area Test	5-16
18	Field Distortion Versus Time	5-17
19	Time-Dependent Breakdown Cumulative Counts/Meter ³ Versus Time of Application of Voltage	5-17
20	Cumulative Breakdowns Versus Time of Application of Voltage	5-18

1.6 AC FILTER CAPACITOR

This capacitor is used as filter for the output of a 400 Hz generator in aircraft. The voltage is low compared with the capacitors listed above, being only 140 VRMS. About 35 ARMS of current flows through the capacitor electrodes. The operating temperature limit currently extends to 125°C, but future systems may require capacitors rated at up to 200°C.

The original design for this capacitor consisted of a large number of metallized polysulfone film capacitors in parallel, contained with a hermetically sealed metal case. Problems with yields were experienced by suppliers of the component and subsystem to the Air Force. The capacitor specification for this program was General Electric Drawing No. 144A9644, Revision AA. Its requirements are summarized in Table 5.

TABLE 5. AC FILTER CAPACITOR SPECIFICATIONS

Parameter	Value	Unit
Capacitance (1 kHz)	120	μF
Tolerance	-5, +15	Percent
Voltage (RMS)	140	Volts
Capacitor Current (RMS)	35	Amperes
Feedthrough Current (RMS)	150	Amperes
Surge Current (1)	209	Amperes
Surge Duration (1)	5	Seconds
Surge Current (2)	165	Amperes
Surge Duration (2)	5	Minutes
Frequency	400	Hz
Operating Temperature	-55 to +125	°C
Storage Temperature	-65 to +125	°C
Dissipation Factor (1 kHz)	0.0025	-
Insulation Resistance (200 VDC, 5 min)	>1667 >200,000	MΩ MΩ-μF
Dielectric Withstand Voltage (RMS)	168	Volts

The work on this capacitor was aimed at comparing polysulfone and polyetherimide films for the high temperature application. Reliability and endurance were more critical than increased energy density.

1.7 PROGRAM SUMMARY

The program was divided into two sequential phases composed of a total of five tasks. This report is a description of the developmental effort and testing conducted by Hughes. A significant portion of the effort of Task III was contracted to the Schweitzer Division of Kimberly-Clark Corporation. The program is briefly summarized below.

1.7.1 Phase I - Material Testing and Selection

Task I - Preliminary Material/Dielectric Systems Selection. The most promising existing material candidates for modification and development were determined for the improvement of energy density in each of the four operating regimes. Preliminary candidate dielectric systems were proposed.

Task II - Material Test Plan. A comprehensive test plan was devised for evaluating the materials identified for modification and development. It allows the assessment of improvement in materials being developed, identified parameters of particular interest to the capacitor designer for evaluation, and provides specific acceptance test criteria.

Task III - Material Fabrication, Testing, and Final Selection. Test procedures for small and large area breakdown tests were developed. It was shown that breakdowns below the intrinsic level are not caused entirely by inclusions of conductive particles but by dissolved ionic impurities. A new material was proposed for use in high energy density capacitors, and samples were fabricated suitable for use in capacitors. Ample quantities of the new material were manufactured for the next phase. Final dielectric systems were recommended. The two required presentations were made.

1.7.2 Phase II - Capacitor Pad Design and Testing

Task I - Capacitor Pad Design and Test Plan. Capacitor pads were designed for the five service regimes, and the designs documented. The special techniques developed on the previous program were employed, including constant tension flat mandrel winding and high purity impregnation. Test plans for pad evaluation were prepared. The test bay developed during the previous program was used for the pulse capacitor tests. Other test fixtures were constructed for life testing the other components.

Task II - Capacitor Pad Fabrication and Testing. In this task, new materials were tested by fabricating and testing capacitor pads for four of the five service regimes. Failures were analyzed and documented so that future improvements may be made.

2.0 TECHNICAL BACKGROUND

2.1 DIELECTRIC DESIGN THEORY

From the standpoint of basic electrostatics, the design of a high energy-density capacitor is deceptively simple. The energy density D is the stored energy divided by the weight:

$$D = CV^2/2W \quad (2-1)$$

where:

- C = capacitance,
- V = applied voltage,
- W = weight of the capacitor.

For the most elementary model (a two-electrode planar capacitor where edge corrections are neglected) this equation can be written as:

$$D = (\epsilon AV^2)/(2tW) \quad (\text{J/g}) \quad (2-2)$$

where:

- ϵ = the dielectric constant,
- A = the area of one plate,
- t = dielectric thickness.

If most of the capacitor weight is in the dielectric, the second equation becomes:

$$D = (\epsilon E^2)/2d \quad (\text{J/g}) \quad (2-3)$$

where:

E = the electric field

d = the density of the dielectric.

The assumption made to derive this equation is fairly appropriate for large-valued high-voltage capacitors. The resulting simplified equation is helpful in estimating progress during the development process. Clearly the energy density in the dielectric must be greater than that required for the complete component to allow for the weight of the case, termination, and foils.

Equation 2-3 can be plotted for different values of ϵ and d such as might be obtained for various dielectric sandwiches used in high energy density capacitors, as in Figure 1. The upper curve represents a polyvinylidene fluoride system, while the lower curve is representative of a polysulfone system for use where large power transfer is required. It can be seen that

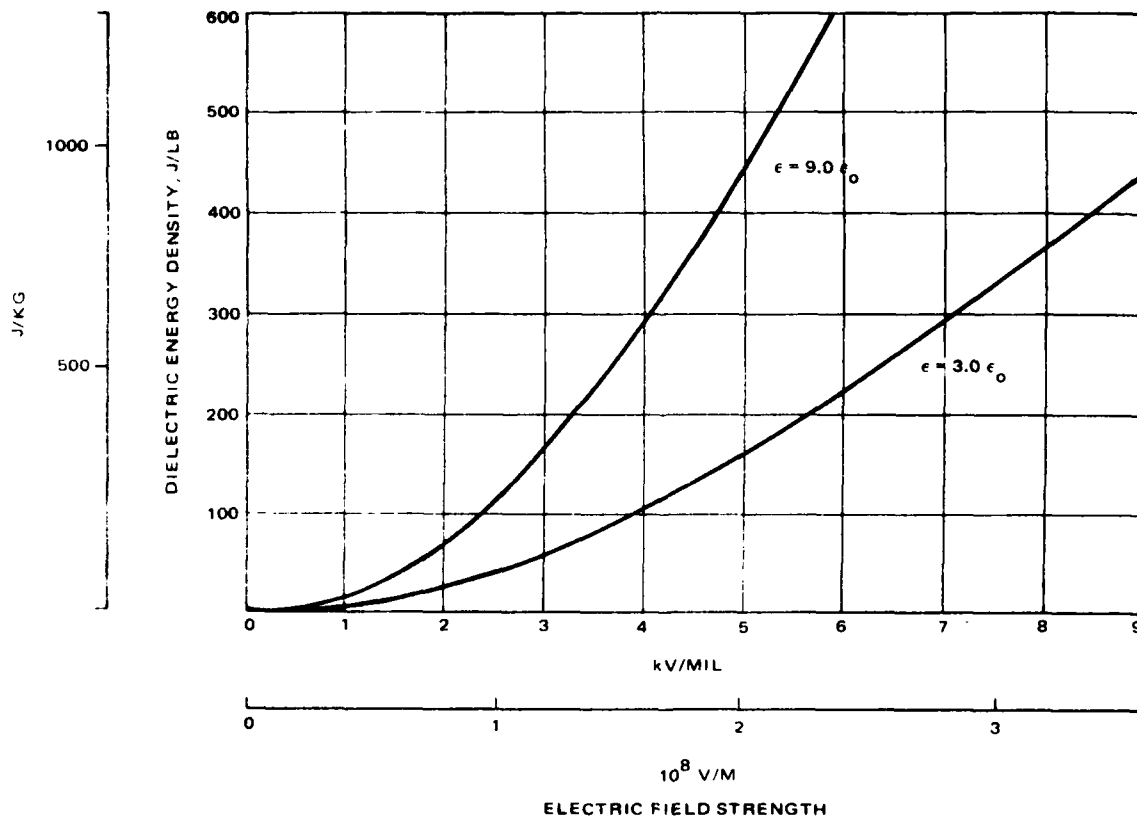


Figure 1. Energy density versus field for two dielectric systems.

only a moderate field strength is required to meet the goal set for the DC filter capacitor (220 J/kg), but a much larger field is required to achieve the goal set for the low repetition rate pulse capacitor (1100 J/kg).

For detailed design, a more realistic equation that accounts for foil weight is necessary:

$$ED = \epsilon/2 \frac{E^2}{(d_d + t_f d_f / t_d)} \quad (\text{J/g}) \quad (2-4)$$

This expression takes into account the sometimes appreciable foil weight but ignores margins, tabs, and terminations.

For pulse capacitors made from three different kinds of dielectric, the field in dielectric A can easily be shown to be:

$$E_A = \frac{\epsilon_B \epsilon_C V}{\epsilon_A \epsilon_B t_C + \epsilon_A \epsilon_C t_B + \epsilon_B \epsilon_C t_A} \quad \left(\frac{V}{\mu m} \right) \quad (2-5)$$

where:

- A, B and C = the three different dielectrics
- ϵ = the dielectric constant,
- t = thickness
- V = the total applied voltage.

The effect of this field division is to drive the electric field in the material with the lower dielectric constant to a value larger than would be expected if a simple average is calculated.

For the DC capacitor, after the component comes to a steady state condition, the fields in the three layer situation are:

$$E_A = \frac{\rho_A V}{\rho_A t_A + \rho_B t_B + \rho_C t_C} \quad \left(\frac{V}{\mu m} \right) \quad (2-6)$$

where ρ is the volume resistivity and the other symbols are given above.

As a result, a disadvantage exists in using more than one material in a dielectric. Given a particular thickness of dielectric, t , the field in the single-material dielectric is the average field, V/t . The energy density is proportional to $(V/t)^2$. The highest energy density is achieved when (V/t) is the breakdown strength of the material, and this is known as the ultimate energy density of that material. The most desirable way to make a high energy density capacitor is to use a single material with the greatest ultimate energy density. If two materials are used, the field in the more highly stressed material (lower ϵ in the pulse discharge case, greater ρ in the slow charging case) will be greater than the average field (V/t) . Because the breakdown of this material will still occur when the field across the material is the value of the breakdown strength, the allowable voltage is smaller, and the energy density of the system is usually reduced from the single material. An alternate explanation is that the two materials correspond to two capacitors in series, one of which can be stressed higher, and has a higher energy density than the other. This arrangement is obviously less efficient than two capacitors made using the better dielectric. In paper/film/oil capacitors, the situation is worse because there are three dielectric components.

Yet, there are good reasons for including three materials in a wound capacitor operating at high voltage and high stress. The liquid fills the spaces in the winding which would otherwise be voids, and would be susceptible to corona. Rough surfaced Kraft paper is interleaved between films and foils to permit penetration and retainment of impregnant in the winding. Using special processing techniques, all-film windings can be completely impregnated. Generally, these capacitors had shown extremely steep life versus stress curves. This characteristic is indicative of a corona failure mechanism. A possible explanation is that the electrostrictive forces, which sometimes produce audible clicking during pulsing, tend to squeeze out the liquid and leave voids when the voltage is relaxed on discharge (even when the winding is initially impregnated completely). However, progress is being made at solving this problem through the use of high-wetting liquids, low tension windings, and hydrostatic pressurization.

In order to maximize the energy density of the triple dielectric system, materials and thicknesses must be combined to achieve the most efficient use of each layer. Such factors as the density of the paper, the total number of

layers, the variation of dielectric strength with gauge, and so on, must all be factored in. A computer program has proven to be extremely useful for this type of analysis at Hughes.

In reality, the energy density requirements are not difficult to meet. The real problem is to simultaneously achieve both the energy density and the lifetime goals. The life, L , of a capacitor dielectric in relation to the applied field, E , is often represented by the equation

$$L = CE^{-n} \quad (2-7)$$

where C and n are constants particular to the given dielectric.

This equation reflects the fact that the life of a capacitor will drastically decrease as its energy density is increased by simply raising the voltage. To improve both life and energy density, the constants C and/or n must be altered by way of improving the breakdown strength or permittivity on the one hand, or by suppressing the processes which cause failure on the other.

To accomplish the desired goal of increasing energy density without sacrificing lifetime, tradeoffs between ideal dielectrics for energy density and for corona suppression have to be carefully considered. The ideal dielectrics, unfortunately, are not the same for each consideration. The relationship between the corona inception voltage (CIV) and the dielectric strength of a capacitor is far from straightforward. For example, the CIV for paper impregnated with diphenyl chloride drops with increasing paper density, while breakdown voltage increases. Reversed trends are also evident with respect to temperature.^{11,12} However, these problems can be resolved by means of material selection or modification and, to some extent, by changing the foil edge shape. Certain polymers show remarkable resistance to corona degradation relative to some others,¹³ and the same is true for impregnants.¹⁴

The foil edge is the location of strong and divergent electric fields. Several authors have treated the computation of the peak field for various shapes, and have examined means of grading the field using more conductive or higher permittivity impregnants.^{15,16} Parker, in work done at Hughes, examined

a number of means of treating the foil edge to obtain a smooth, cylindrical shape.¹⁷ Some capacitor manufacturers have folded foil to accomplish this result. Field grading by means of the impregnant's time constant for relaxation may be possible, but the high energy dissipation which would accompany this choice is often not acceptable. Minimizing foil weight requires minimal foil thickness and this usually makes foil folding unattractive.

2.2 FAILURE MECHANISMS

Success in achieving the energy density and life of the capacitors required for future systems will only come from an understanding of the processes which lead to failure and an adequate program to defeat these processes. A general overview of failure mechanisms in capacitor dielectrics is given below.

2.2.1 Electrical Failure

Electrical failure in a large pulse-discharge energy storage capacitor almost invariably takes the form of corona leading to the establishment of conducting paths, puncture of the insulation, breakdown, and a shorted section. An electric field across the dielectric also produces an electric field in the gas that fills any voids, bubbles, or other insulation imperfections. The gas breaks down at a lower electric field than the other dielectric if the characteristic dimension of the imperfection is in the right range. In addition, the field in the gas is enhanced by the difference between the dielectric constants of the gas and the other insulation. At a critical electric field, a breakdown, or partial internal discharge, will occur in the void. The breakdown is of quite high temperature and tends to burn the insulation.

In a solid dielectric, the repeated breakdowns carbonize the insulation and enlarge the void along the direction of the electric field lines. The void grows with time and breaks down at a lower field strength and higher current. An increasingly larger amount of damage is caused and the situation gets worse. Failure occurs by shorting across the enlarged carbonized void.

The liquid insulations normally used in high voltage capacitors present a different problem as there is a considerable amount of electric-field related

failure modes. In the simplest case, if the dielectric is organic, the corona carbonizes the fluid. The particles of carbon line up along the electric field lines and cause repeated breakdowns at decreasing fields and finally failure. For inorganic liquids, the effects depend upon liquid type and sometimes exact composition. They range from decomposition with release of HF gas, to flocculation, to lowered breakdown strength. The decomposition products often attack the plastic or cellulose chemically, rapidly accelerating the rate of failure.

Ancillary effects in liquids contribute to electrical failure. Very high electric fields or fields with large divergence, particularly at a point or rough edge of foil or tab, may cause the spontaneous evolution of gas bubbles, either from solution or from decomposition, depending on the liquid and temperature. In the presence of the electric field, some fluids react with water to form a dense conductive carbonaceous flocculent. Certain fluids are catalyzed by certain metals at varying reaction rates. Finally, if any particulate contamination is present, the contamination tends to line up along field lines, forming a bridge between the two plates.

Partial internal discharges occur first at electrode edges where the electric field can become several times larger than the average field. This is especially true when the foil edges are not opposite one another, but are instead out of alignment, such as in extended foiled windings. Such discharges can be detected long before either a measurable change in dissipation factor or actual catastrophic failure occurs. This phenomenon is largely a result of space charge building up in the dielectric close to the electrode. This charge may be in the form of free electrons which have been field-emitted from the metal surface, and ions and electrons which may have been created by collisions with those electrons. The change in electrode potential during a voltage cycle reverses the force on those charges, and the field between the space charges and the electrode surpasses the breakdown strength of the dielectric, resulting in a discharge which does not actually bridge the gap between both electrodes. In the process, heat is generated, molecules are ionized, and bubbles may form. Each voltage surge now incurs another discharge and the bubbles grow larger and larger in volume each time. The damage is permanent; the corona will not disappear, even at greatly reduced voltages. The process

will continue until the damage weakens the insulation enough to permit a total breakdown of the dielectric.

Another form of electrical failure which has been observed in pulse capacitors, where high peak current densities occur in the electrodes and terminations, is that of current flow across holes in metal foils.¹⁸ This results in burning of the insulation and, as in the case of partial discharges, eventual failure. When tabs are used to terminate foils of pulse capacitors, arcs may occur between the tab flag and the electrode, eventually disintegrating the foils.

2.2.2 Thermal Failure

Failures attributable to thermal effects are found most often when power is transferred at very high rates. The physical phenomenon underlying this form of failure is that all dielectrics dissipate some energy when energy is stored in them, and some when it is released. A measure of this dissipation is a bulk material property called dissipation factor or loss tangent (power factor is nearly the same thing, below a value of 0.01). The dissipation factor DF is defined (ASTM D-150) as:

$$DF \approx \tan \delta = \frac{X_p}{R_p} \quad (2-8)$$

where δ is the loss angle, X_p the parallel reactance, and R_p the effective AC parallel resistance. This parameter, different for different materials, varies much with frequency and temperature. As an example, typical curves for three different temperatures for polyvinylidene fluoride (KF film) are shown in Figure 2. The dissipation factor measured for a complete capacitor normally is slightly larger than for a dielectric system alone, as I^2R losses in the foils and leads affect the loss tangent. Additionally, the amount of power dissipated depends on the rate of energy transfer as well as the total energy stored. This rate effect is important.

The failure mechanisms, related either to the temperature rise caused by dissipation of energy in the dielectric or to a thermally-triggered effect, divide roughly into three classes: gross failures caused by thermal runaway;

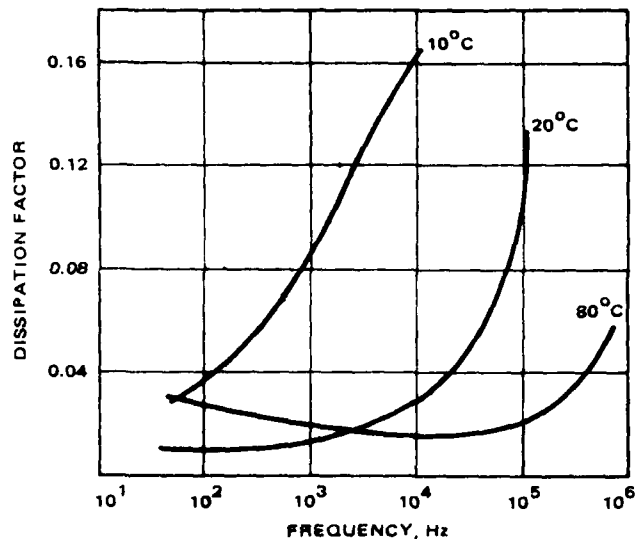


Figure 2. Polyvinylidene film dissipation factor versus frequency.

insulation failures caused by the crease of dielectric strength with increasing temperature; and insulation failures resulting from actual decomposition or change of state of the dielectric.

The first type of thermal failure is often the most spectacular; sometimes the oil-filled metal cases actually explode as the increase temperature causes a large thermal expansion of the oil. A thermal runaway normally requires a material with a dissipation factor versus temperature curve that increases monotonically, as in Figure 3. Most plastic films and papers

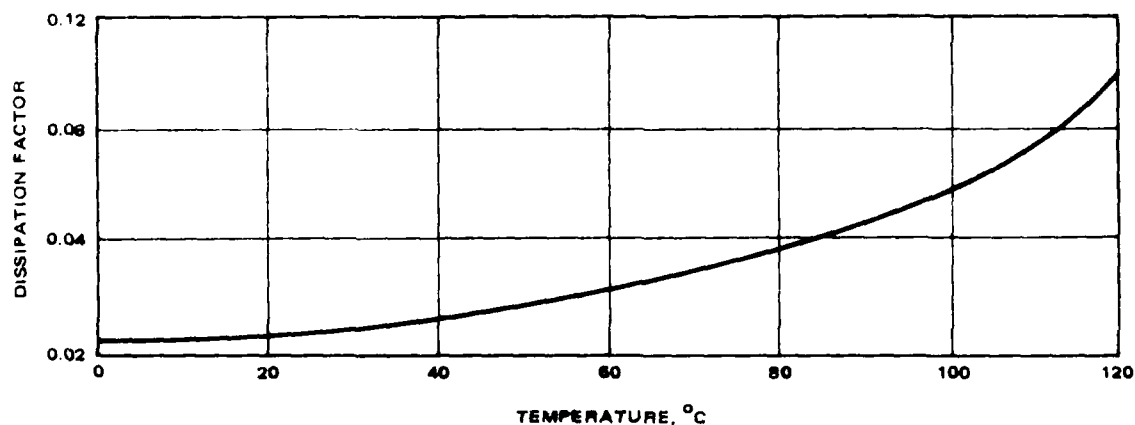


Figure 3. Typical dissipation factor versus temperature.

have curves with that characteristic. The usual sequence of events leading to failure is that the component is run at a high power level and gets warm. As the component warms up, more power is dissipated which further increases the power dissipation until failure occurs. The component container may suddenly rupture if it is not equipped to handle the increasing volume of the gas impregnant. Otherwise, the high dielectric temperature will cause the dielectric to fail electrically by one of the mechanisms discussed below.

Generally the dielectric strength of a material measured using a standard test (ASTM 149-64) decreases monotonically with temperature. Measurements for several materials are shown in Figure 4. This characteristic behavior raises the problem of high temperature electric field stability. While the standard test in no way duplicates actual capacitor operation, the results indicate that, at higher temperatures, lower electric fields must be used in

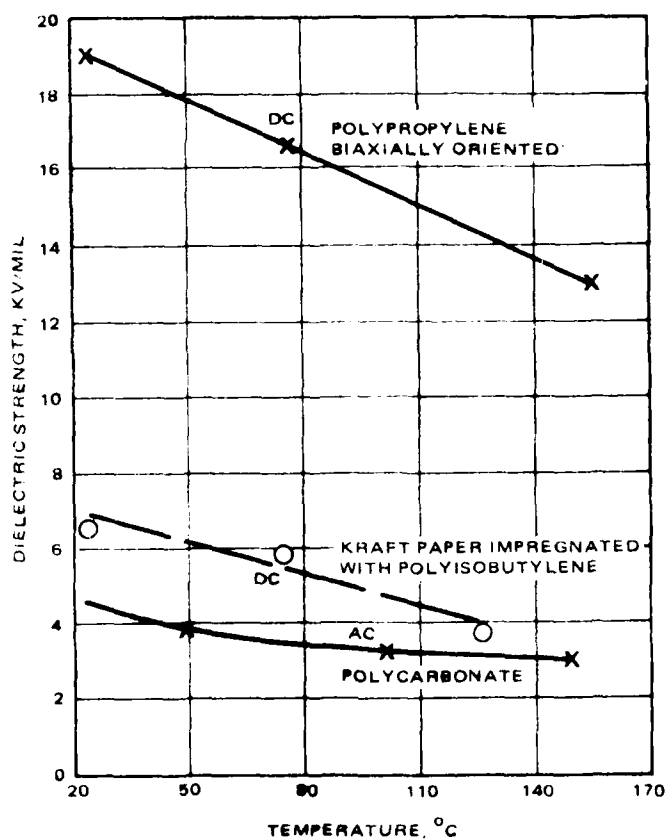


Figure 4. Dielectric strength versus temperature of various capacitor dielectrics.

given material to obtain the same operating safety factor. Experience with standard film capacitors shows an increase in leakage current and a lower average life at higher temperatures. Usually the ultimate failures are caused by excessive corona and breakdown.

Each material used in a dielectric system has, as an intrinsic property, a temperature above which irreversible physical or chemical changes take place. These changes are different for each material and depend on the particular environment. Polyvinylidene fluoride (KF film) in the extruded state shrinks at about 160°C but is chemically stable at 300°C. Cellulose (Kraft paper) gives up bound water at about 150°C. This water may then cause hydration of the impregnant or other effects. In high electric fields, some impregnants produce hydrogen gas at high temperatures. Each material is subject to oxidation above a certain temperature. The operation of a dielectric system above the service temperature of one of its components will lead to failure, the time of failure depending on the mechanism and the temperature. Both the ambient temperatures and the hot-spot temperatures within the capacitor, caused by power dissipation in operation, are of concern here. A component could be thermally stable (no runaway) but could fail electrically because of this combination of ambient temperature and service temperature rise.

Thermal failure is of critical importance in the repetition-rate pulse capacitors, the high frequency AC inverter capacitor, and the 400 Hz filter capacitor (intended to operate in a 125°C ambient environment). In the case of the resonant inverter capacitor, it is in fact the power density, and not the energy density, which is the central design problem. Similarly, the high repetition rate pulse capacitor is a substantially more difficult component than the low repetition rate capacitor, simply due to the increased generation of heat.

2.2.3 Dielectric Flaws

Plastic films may include a number of types of imperfections such as non-uniform crystallinity, gel particles, conducting particles, pinholes, thin spots, cavities, and so on. Many materials contain ionic contaminants which can severely affect the dielectric strength under certain conditions of voltage application. Because they are high resistance insulators, films tend

4.3 PARAMETRIC CHARACTERIZATION

Tests to completely characterize the material may be performed during the development phase but most certainly will be performed at the end of the development phase. The purpose of this battery of tests is to give information to the capacitor designer. Therefore, important properties at the anticipated operating points in actual devices will be measured.

4.4 ACCEPTANCE TESTING

Acceptance tests are performed to make reasonably certain that the insulation material is as ordered, to detect gross defects, and to ensure that the material has been properly packaged and not damaged in shipment. For these reasons, neither complete parametric characterizations nor difficult developmental tests will be performed.

4.5 TEST PROCEDURES

Procedures for testing are organized into separate groups for films, oils, and papers. Each group is divided further into electrical tests, physical properties, chemical properties, packaging, etc. The test procedures for films are summarized in Table 8. Test procedures for oil are summarized in Table 9, and test procedures for papers are summarized in Table 10. As noted in the Test Plan, displayed in Appendix B, the procedure for each test is specified in detail or referred to an ASTM specification.

4.6 REQUIREMENTS

The test requirements are given in tables that give the required test limits and acceptance values for each test. A separate table is given for each test sequence. Not all tests are intended to provide a "go no-go" criterion but rather to provide parametric values of the various material properties of interest to the capacitor designer. For these tests, the word "Report" appears in place of a specific set of limits for acceptance and rejection.

4.0 MATERIAL TEST PLAN

4.1 INTRODUCTION

As described in the SOW, the Material Test Plan presented in its entirety in the Interim Technical Report (Hughes Report No. FR-82-76-799) is intended to perform several different specific functions:

1. To assess the improvement in the materials being developed during the development phase
2. To identify and evaluate parameters of particular interest to the capacitor designer, during and at the end of the material development phase
3. To provide specific acceptance test criteria, to be applied as an incoming inspection to the materials as produced in their final forms

Three specific test sequences are envisioned: developmental testing, parametric characterization, and acceptance testing. These are explained in the remainder of this section.

4.2 DEVELOPMENTAL TESTING

Developmental testing is performed during the work aimed at improving the characteristics of insulating materials. Particularly difficult or delicate tests may be included, tests that normally would not be performed during incoming inspection. Usually complete parametric characterization would not be performed at this stage unless new materials or new chemical compounds were being used.

Developmental tests are performed at the discretion of the development engineer to show improvement. Only the properties expected to improve normally would be tested.

dissipation factors, while the high power throughput argues for a very low dissipation factor. Accordingly, Kraft paper is not used, and a very low loss impregnant is selected.

Total layers dielectric	3
Material/thickness	Polysulfone/8 μ
Foil	Aluminum, 6 μ
Dielectric fluid	Silicone

Estimates are:

Operating voltage per pad	1500 V
Average field	2343 V/mil
Average dielectric constant	3.33
Energy density	0.05 J/g (21.3 J/lb)

Layers Kraft paper	3
Kraft thickness	1-7.6 μ , 2-10.2 μ
Foil	Aluminum, 6 μ
Dielectric fluid	Diocetylphthalate

Estimates are:

Operating voltage per pad	8000 V
Average field	5063 V/mil
Average dielectric constant	4.32
Energy density	0.28 J/g (128.3 J/lb)

3.3.3 DC Capacitor

The ripple in this component is low enough so that the principal failure mechanism will be electric-field-driven rather than thermal. Then polyvinylidene fluoride can be used.

Total layers dielectric	5
Layers PVDF	3
PVDF thickness	9 μ (35 gauge)
Layers Kraft paper	2
Kraft thickness	7.6 μ (0.3 mil)
Foil	Aluminum, 6 μ
Dielectric fluid	Diocetylphthalate

Estimates are:

Operating voltage per pad	8333 V
Average field	4273 V/Mil
Average dielectric constant	7.19
Energy density	0.3375 J/g (152.8 J/lb)

3.3.4 High Frequency AC Capacitor

This component is difficult because of the combination of military temperature range (although no specific temperature specification is given in the SOW) and very large power throughput. The military temperature range rules out materials such as styrene and polyethylene, which have the lowest

field of at least 10 percent would be achieved. Because the energy density goes as the square of the electric field, a 21 percent improvement was projected.

3.3 PRELIMINARY CANDIDATE SYSTEMS AND ESTIMATES

Preliminary pad designs and estimates of average dielectric constant, average stress, and energy density of the pad are given in this subsection. These designs represent minor changes, in most cases, to designs previously developed; therefore, some data, particularly weights, are used from previous designs.

3.3.1 High Repetition Rate Capacitor

This design is similar to that found in AFWAL-TR-80-2037, page 86, labeled design A.

Total layers dielectric	5
Layers polysulfone	2
Polysulfone thickness	6 μ (24 gauge)
Layers kraft paper	3
Kraft thickness	7.6 μ (0.3 mil)
Foil	Aluminum, 6 μ
Dielectric fluid	Diethylphthalate

For this configuration, the following estimates can be obtained:

Operating voltage per pad	7500 V
Average field	5068 V/mil
Average dielectric constant	4.29
Energy density	0.28 J/g (128.6 J/lb)

3.3.2 Low Repetition Rate Capacitor

This design is similar to the above design. The repetition rate is too high to allow the use of polyvinylidene fluoride.

Total layers dielectric	5
Layers polysulfone	2
Polysulfone thickness	6 μ (24 gauge)

at low frequencies and low at high frequencies. The DC resistivity is characteristically low. However, both resistivity and power factor are affected by the chemical purity of the ester. To take maximum advantage of the desirable properties of dioctyl phthalate, the fluid must be highly refined to achieve and maintain a very low acid number and a very low dissolved water content. As a generic class, the organic esters are more vulnerable to hydrolysis by water than are the hydrocarbons and silicones.

3.2 EXPECTED IMPROVEMENTS

Primarily as a result of the expected improvement in the polysulfone film, an expected 21 percent improvement in energy density was originally estimated.

If the number of breakdowns per unit area of a large piece ($\sim 100\text{cm}^2$) of film is measured as a function of applied field, a curve such as that shown in Figure 5 is obtained. The failures in the lower field part of the curve represent the defects that cause the capacitor structure to fail at a field well below the knee of the curve. Initially it was thought that the steps described above would result in the elimination of many of those "defects," causing the curve to be essentially at the zero count level until the knee was reached. It was thought that an improvement of the operating electric

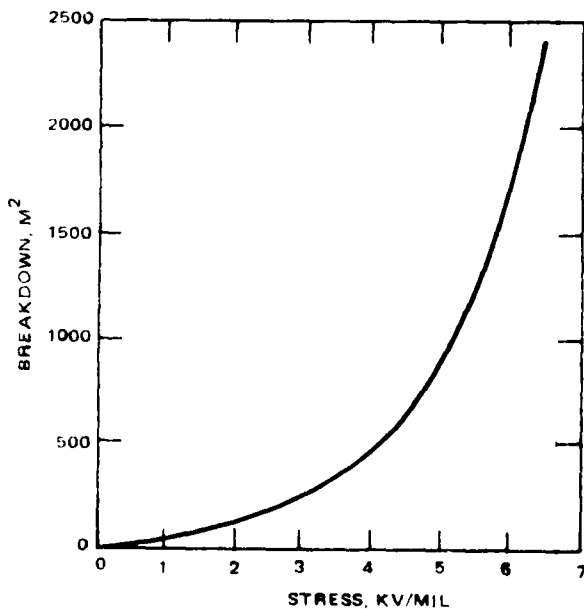


Figure 5. Typical large area breakdown test results.

TABLE 7. PROPERTIES OF IMPREGNANTS

Dielectric liquid	Density g/cm ³	Pour Point, °C	Flash Point, °C	Dielectric Constant (1kHz)	Dissipation Factor (1 kHz)	Volume Resistivity, ohm-cm	Breakdown Strength, Volts/mil	Surface Tension, dyne/cm	Viscosity (25°C), cSt
Diethyl phthalate (BASF PLATINOL)	0.99	-46	218	5.3	10 ⁻³	10 ¹³	403	32.5	83
Castor oil	0.95	-15	290	4.7	10 ⁻³	10 ¹⁴	-	-	-
Phenyl Xylol Ethane (Nisseki-S)	0.99	-50	150	2.6	10 ⁻⁴	10 ¹⁶	-	-	5.1
Silicone oil (Dow Corning-200)	0.96	-60	304	2.7	10 ⁻⁶	10 ¹⁶	430	22.3	20
Mineral oil (Sun Cap oil)	0.91	-46	154	2.2	10 ⁻⁵	10 ¹⁵	400	45	21
Alkylated Benzene (Chevron Alk-21)	0.87	-72	127	2.3	10 ⁻⁶	10 ¹⁶	417	-	6.0
Fluorinated oil (3M FC-40)	1.87	-57	-	1.9	10 ⁻⁴	10 ¹⁵	310	16.0	2.4
Fluorinated oil (HELIX FE-4)	1.76	-94	-	2.5	10 ⁻⁵	10 ¹⁵	450	15.2	2.3
Isopropyl Biphenyl (Wemco?)	0.99	-55	155	2.83	10 ⁻⁴	-	600	-	20

A matte surface can be impressed onto the plastic film easily, at least in principle, since the polysulfone (and most other candidate films except polyvinylidene fluoride) is solution cast. A casting drum would have to be provided with a pattern engraved on the surface, and the pattern would be replicated faithfully on the surface of the film.

3.1.4 Film Lamination

Capacitors are normally made with a multiplicity of layers, to greatly reduce the possibility of failure due to a through hole or conducting flaw in a single film. It is clearly also possible to make a laminated film, in the manner of a flat cable, which would greatly reduce the through holes but that would have the advantage of winding as a single film. This material would have a substantially higher dielectric strength than a single film of the same thickness. It was thought that it might be possible to make a two-layer lamination in about the same thickness presently used (7 to 13 μm).

3.1.5 High Dielectric Constant Impregnants

A number of fluids with dielectric constants exist in the range 6 to 12. Two are well-characterized, and the remainder are either little used or new experimental materials. Fluids with large dielectric constants exist; the most common example is water. In general, however, these fluids are useful only in certain specialized situations and are not applicable for military capacitor service. The properties of some of the possible fluids are summarized in Table 7. The polychlorinated biphenyls (PCBs) have been widely used as capacitor fluids. Formerly available as Arochlor, Pyranol, or Inerteen, they were not considered for this program because their production and use were banned in the United States after 1974.

Diocetyl phthalate was selected as a candidate fluid for its potentially high energy density storage properties. This material was one of four selected for capacitor use in the previous AFAPL program, and extensive contamination and compatibility experiments have been conducted. This organic ester is being used commercially in transformers and capacitors as a replacement for the unavailable PCBs. The ester offers a relatively high dielectric constant and a low density. The power factor of the organic esters is relatively high

of the paper-fluid assembly will increase (if the dielectric constant of the fluid is below 6.3). Also, because there are fewer spaces, the chance for electrically weak spots is reduced; therefore, the average dielectric strength is improved. All of these factors aid in achieving a more favorable field balance -- one in which each material is stressed at the same percentage of its breakdown stress.

Thus, several advantages accrue:

1. Thinner fluid layer (higher dielectric strength)
2. Higher effective dielectric constant
3. Higher dielectric strength (paper)
4. Better field balance (AC and pulse).

5.1.3 Kraft Paper Replacement

As venerable an insulation as it is, Kraft paper has three serious drawbacks:

1. Shrinkage (non-isotropic)
2. Moisture absorption
3. Low decomposition temperature.

Therefore, it might be interesting to investigate a replacement that performs the same functions as Kraft but that does not have as many bad features.

Strictly speaking, the common explanation that Kraft paper acts as a wick or a medium enhancing impregnation is fallacious, since the paper is actually nonporous and nonwicking to any liquid that is not aqueously based. Kraft first functions as an electrical barrier, as any plastic film would, raising the insulation breakdown voltage from 400 V/mil for fluid to about 4500 V/mil. By comparison, fluid filled porous felt, which acts as a wick but not as a barrier, breaks down at about 700 V/mil. Second, the Kraft provides a means for defeating the electrostrictive failures. Any replacement must seek to do both these tasks.

Kraft paper can be replaced in one of two ways: the impression of a matte surface onto a plastic film or the treatment of the film to enhance wettability. The first method was explored extensively.

3.1.2 Denser Kraft Paper

A separate subject in the development of improved dielectrics for high energy density capacitors is the use of a denser, thinner Kraft capacitor paper than currently used. Several advantages can be realized by such an approach. First the entire dielectric pad becomes thinner, and higher capacitance is obtained at equivalent basis weight. Second, a denser paper will produce very thin layers of impregnating liquid. The dielectric strength of liquids, while generally lower than that of dielectric solids, can be very high if the layers are thin enough. Finally, the paper substance, because of its higher dielectric constant, transfers much of the electrical stress to the dielectrically stronger layers of film. Hence, a more dense paper will mean even more stress will be transferred to the film.

One problem encountered in the previous AFAPL program was the optimization of the design of AC and pulse discharge capacitors to obtain the maximum safe energy storage in each dielectrical layer (film, paper, oil). A typical field distribution for a very high energy density component is given in Table 6. The field distribution in an AC or pulse component depends on both dielectric constants and thicknesses of layers, so that the use of a denser, thinner Kraft will shift more stress to the polysulfone.

TABLE 6. FIELD DISTRIBUTION IN PULSE DISCHARGE COMPONENT

Material	Field, V/mil	Breakdown Field, V/mil	Ratio*
Kraft	3430	4500	0.76
Polysulfone	5266	7500	0.70
Oil	2761	4000	0.69
*Operating field/breakdown field			

The dielectric constant of Kraft is somewhat of a volumetric average number. The figure of cellulose is 6.3, while that for dry Kraft is in the range of 3.5 to 5. This is because the Kraft is not smooth; therefore, some of the volume between measuring electrodes fills with air (or, in a capacitor, the oil used for impregnation). A denser paper has more Kraft per unit volume and fewer spaces. Then there will be less fluid, and the dielectric constant

of approaches was included in the proposal, per the requirements of paragraph 4.1.1.1 of the SOW. Only those techniques seriously pursued in the first phase are discussed in this section.

3.1.1 Higher Quality Films

The practical operating stress of film dielectrics, in general, is far below the "intrinsic dielectric strength" of the polymer. But experiments demonstrate that, at least in tests on small areas where the likelihood of encountering an electrical weak spot is slight, breakdown stresses in excess of 15 kV/mil can be attained. In spite of this fact, not much effort has been expended in the production of film with fewer weak spots because historically such films have been used in metallized capacitors in which the weak spots can be eliminated easily by "clearing". Experiments have shown that these electrically weak spots may be the result of conducting particles, voids, pinholes or low basis weight (low mass/area).

The initial goal of the research program was to develop polysulfone film that, by reducing the frequency of electrical imperfections, can operate at electrical stresses significantly above those currently employed. Polysulfone film was chosen for study because it has good dielectric properties over the temperature range of interest, is compatible with a range of dielectric fluids used for impregnating capacitors and, most important, is already of a quality that the goals envisioned for the program were reasonable.

The first step in this program was to identify, by non-destructive testing, the most frequently encountered causes for low electrical strength. These techniques have been used in the past by the Schweitzer Division for identifying causes of breakdown in both films and in paper. Then, improved experimental films were to be made on the casting equipment. Improved techniques for the filtration of casting solution (dope) were explored during this phase in an attempt to reduce the number of conducting particles in the film. Also, filtration of drying air was explored to reduce the number of particles deposited on the film. Large area specimens of these films were tested for electrical breakdown to assess the progress. The final step was scaling up the laboratory developments to production size equipment. The influence of hot stretching on impairing dielectric strength was considered carefully at this point.

3.0 PRELIMINARY MATERIAL/DIELECTRIC SYSTEMS SELECTION

In this first phase of the program, the dielectric materials requirements were determined, candidate materials and improvements were selected, and improved materials were fabricated and tested. This phase was divided into the three tasks discussed in this section. The Schweitzer Division of Kimberly-Clark assisted in the performance of Tasks I and II and performed substantially all of Task III.

The program conducted by Hughes before the present program resulted in the development of lightweight high-repetition-rate pulse discharge capacitors employing polysulfone, kraft paper and dioctylphthalate as a dielectric system. These capacitors, designed to a performance specification similar to that of paragraph 4.3.1 of the Statement of Work (SOW) of the present program, failed by two different mechanisms:

1. Random dielectric failures (RDF)
2. Corona at foil edges.

The first failure causes both infant mortality and wearout, while the second is primarily a wearout mechanism. The problem of corona at foil edges has been discussed in the literature and was addressed during the previous program, although only small foil specimens were actually fabricated and tested. The improvements sought in this task were, therefore, in the reduction of RDF in the dielectric system.

3.1 CANDIDATES FOR IMPROVEMENT

The quality and energy density of a capacitor dielectric system might be improved by several methods. An extensive discussion of a wide variety

Variations in winding tension can also stretch the thin materials and produce wrinkles. These wrinkles are points of field enhancement or stress concentration, and are potential sources of failure.

2.2.5 Mechanical Failure

The rhythmic charge-discharge of pulse capacitor sections can produce mechanical motion at the pulse frequency, particularly if the sections are wound by conventional techniques; the standard technique produces rather loosely packed sections. In severe instances, the capacitors emit clicking noises at each discharge. The mechanical motion causes tabs and connections to fracture and sometimes causes the center of the winding to walk out of the section. This pumping of the dielectric tends to squeeze the impregnant out of the winding in all-film capacitors, resulting in voids when the stress is relaxed. Kraft seems to prevent this by resisting the rapid flow of liquid out of the winding as a result of its complex surface.

to build up surface charges and to collect dust out of the air during winding operations.

Kraft paper has similar problems which are typified by large numbers of pinholes and conducting particles per unit area relative to plastics. Because of its very nature, paper is very difficult to clean up. In addition, the cellulose fibers which comprise the paper become detached and suspended in the impregnant. These fibers may line up and form bridges across the insulating fluid.

The impregnant itself invariably contains some particulate contamination, even after special filtering and refining. Many of these particles will be conductive, or, like the cellulose fibers, will aggregate and severely lower the breakdown voltage of the liquid.

All of these imperfections result in random dielectric failure. These failures are obvious because they occur away from the highest stress region — the foil edge — and are often termed bulk failures. The exact cause of the failure can seldom be identified, due to the damage which results when the stored energy in the capacitor is expended in the breakdown and vaporization or melting of dielectric and foil. Because of the microscopic nature of the actual flaws, even very small amounts of energy can eliminate all traces of them.

2.2.4 Manufacturing Flaws

Due to the stresses involved in achieving high energy densities, the elimination of imperfections is very important. Not only are flaws present in the materials themselves, but they may also be introduced in the process of manufacturing the capacitor. Typically, the steps involved include winding, pressing, assembly, drying, impregnation, and sealing. Insufficient attention to the details of processing the capacitor can result in wrinkles, underlying, inclusions of foreign particles, tearing of the dielectric, unstable capacitance, gas voids, and so on.

A common practice is to wind capacitor pads on cylindrical mandrels and then flatten them to a more rectangular form suitable for packaging. This method generally results in distortion and deep wrinkling after drying.

TABLE 8. TEST PROCEDURES FOR FILMS

ELECTRICAL TESTS	ROLL FORMATION AND CHARACTERISTICS
Dielectric Constant Dissipation Factor Surface and Volume Resistivity Dielectric Strength Gross Flaw Fine Flaw	Cores Roll Quality Width and Diameter Splices Marking
TESTS FOR CONTAMINANTS	PACKAGING
Surface Contamination Residual Solvent Moisture Absorption	Wrapping Outer Package General Requirement
PHYSICAL AND MECHANICAL TESTS	
Film Thickness Film Density Tensile Strength at Break Elongation at Break Shrinkage	

TABLE 9. TEST PROCEDURES FOR OILS

PHYSICAL PROPERTIES	CHEMICAL PROPERTIES
Viscosity Flash and Fire Points Pour Point Specific Gravity Weight per Gallon Interfacial Tension Color Visual Examination	Neutralization Number Water Content Inorganic Chlorides and Sulfates Oxidation Stability Oxidation Inhibitor Constant Gassing
ELECTRICAL PROPERTIES	PARTICULATE CONTAMINATION
Dielectric Constant Dissipation Factor Dielectric Breakdown Voltage Volume Resistivity	

TABLE 10. TEST PROCEDURES FOR PAPERS

ELECTRICAL PROPERTIES	CHEMICAL TESTS
Dielectric Constant Dissipation Factor Dielectric Strength Conducting Paths Fine Flaws	Aqueous Extract Conductivity Soluble Chlorides Acidity-Alkalinity-pH Moisture Content
PHYSICAL TESTS	ROLL CHARACTERISTICS AND PACKAGING
Paper Thickness Apparent Density Holes and Felt Hair Inclusions Tensile Strength and Yield Properties Air Resistance	Cores Roll Workmanship Width Marking Packaging

4.7 USING THE TEST PLAN

The test plan is divided into films, oils, and papers. The test procedures (specifications) are listed according to each group. Most tests are performed per ASTM specifications. Special tests are explained and defined. The test requirements are summarized in the tables according to test sequence; i.e., developmental, parametric characterization, or acceptance tests. To use the test plan, the test sequence must be picked and then the appropriate tests selected from the table of test requirements.

The Material Test Plan is a flexible, comprehensive document. It can be used effectively to:

1. Assess improvement in materials being developed
2. Provide data of interest to the designer during the development phase.

Although the test plan is not organized along the lines of a military specification, it could be used easily to produce a military specification that would furnish in-process controls for manufacturing and provide acceptance tests for production materials.

5.0 MATERIAL FABRICATION AND TESTING¹

5.1 INTRODUCTION

The manufacture of capacitors with high energy density places severe demands on both the dielectric material and the workmanship in the capacitor itself. This latter problem has been addressed in previous work at Hughes. The purpose of the present work was to develop improved dielectric materials. Since the energy density in a capacitor varies with the square of the applied voltage, the most effective way of building high energy density capacitors is to use dielectric materials that will withstand high voltage stress without breakdown.

Previous work at Hughes on a wide variety of available dielectric materials showed that polysulfone film had the necessary combination of properties to make it suitable for further development. These properties included stable dielectric constant over the range of temperatures and frequencies of interest and a low dissipation factor over the same range of temperature and frequency. Therefore the primary goal of this study was to produce a polysulfone film with a significantly higher dielectric breakdown strength than standard commercial film. Further, the technical effort could be redirected toward other materials that may increase the likelihood of achieving increased dielectric performance.

It is fair to ask why commercially available polysulfone dielectric film does not have a dielectric breakdown strength high enough to be useful in high energy density capacitors. The answer is primarily a practical one. By far the largest use of such films is in metallized film capacitors in which defects

¹This work was carried out by E.P. Bullwinkel and A.R. Taylor at Schweitzer Division, Kimberly-Clark Corporation.

in the film are "cleared" when voltage is impressed, leaving a tiny hole in the dielectric and a small area around the hole where the thin metallized layer has been vaporized. This process removes imperfections in the film without harming its dielectric properties. Such a process does not pertain to film/foil constructions as envisioned for high energy density capacitors where any breakdown in the capacitor would result in a short circuit. In addition, typical metallized film constructions are used at significantly lower fields than envisioned for high energy density capacitors. Thus, no commercial reason has been found for providing polysulfone film with high dielectric strength.

The intrinsic dielectric breakdown strength of all dielectrics (polysulfone included) is well above that observed in practical applications; i.e., breakdown stresses of 700 to 800 V/ μ m (18 to 20 kV/mil) can be observed under special conditions and these levels of stress are inherent or "intrinsic" to the dielectric. At the beginning of the present program, it was believed that breakdowns below this level were related to inclusions of conductive particles, grain spots or holes in the dielectric. As shown in this section, while these defects are undoubtedly important in dielectrics, other phenomena are also important, especially at high stress, and remain poorly understood.

The various test apparatus and procedures developed for small and large area destructive breakdown tests, attempts at developing a nondestructive breakdown test, and equipment for measurements of conductivity on various films are described here. Then, the experimental results for large and small area breakdown tests and the conclusions are given. Finally, the recommended dielectric systems are discussed.

5.2 VOLTAGE BREAKDOWN TESTING

At the beginning of this work, a strong belief was that the key to improving the large area dielectric strength properties of polysulfone films would involve lowering the density (number per unit area) of possible defects (Figure 6). Such a belief immediately suggests that it would be extremely valuable to have a method of determining the actual density of these individual defects so that the efficacy of various process modifications could be

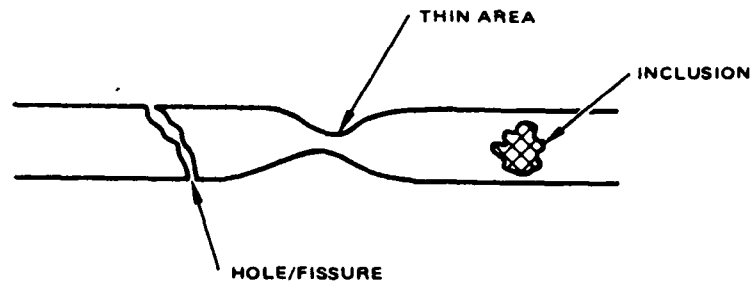


Figure 6. Density of defects in polysulfone films.

directly known and not merely inferred. Accordingly, much effort was expended on developing nondestructive voltage breakdown testing (VBT) methods that would survey large film areas continuously. This work was in two parts. In the first, electrode systems would be developed that would give essentially line contact across a moving film web without causing mechanical damage to the delicate web. (By the provision of indexing markers, portions of film carrying the line locus of breakdown could be removed from the web and subsequently scanned along the line to exactly locate the breakdown site.) The second part was circuit development that would remove or reduce the enormous power dissipation at the breakdown site. (This dissipation is responsible for the destruction of any defect evidence in ordinary VBT.)

While success was achieved in developing suitable electrodes, the second part that involved preservation of the breakdown site proved intractable. Before these matters are discussed, one quick, simple method of large area VBT employed over the years is described. This static method merely involves laying a film sample on a large, polished brass plate, that acts as one electrode. Next, a web of metallized film, metal side down, is carefully placed over the sample to serve as the second electrode.

When voltage is applied across these two electrodes, electrostatic forces in conjunction with the limpness of the two films tend to squeegee out bothersome air interfaces and give very intimate electrode-film contact. Whenever a voltage breakdown occurs in the test sample, the metallized film electrode "clears." This clearing, the result of volatilizing of the metal adjacent to the breakdown site, not only gives a permanent visual record but also automatically disconnects the site from the remaining test area so that the test can be continued without the need for external intervention.

Apart from the slight bother of laying up samples, this test is extremely useful. Indeed, this method was used for most of the large area testing (LAT) reported. Nevertheless, since the method involves volatilizing metal, it certainly is not the basis for nondestructive VBT of polymer films.

Returning now to the development of line contact electrodes suitable for testing moving film webs, the final design evolution is shown in Figure 7.

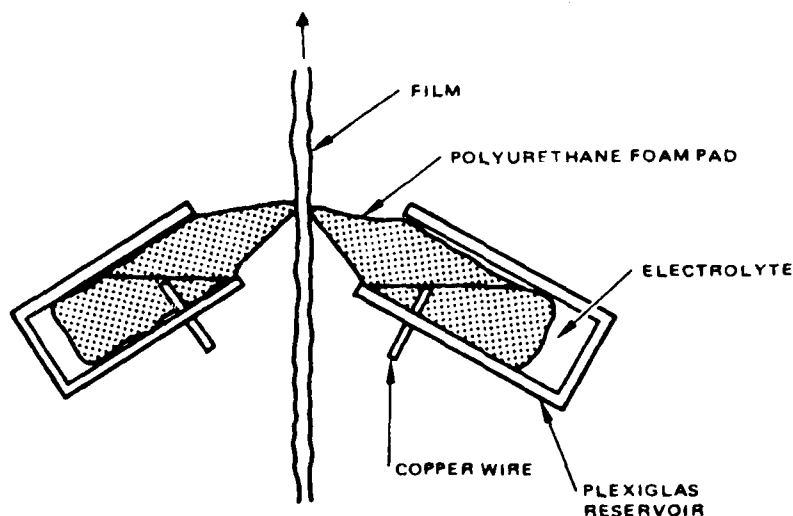


Figure 7. Aqueous line contact electrodes.

In this arrangement, the actual electrical contact to the film is achieved by an aqueous electrolyte solution maintained in situ by various surface tension and electrostatic forces involving this solution, the foam pad wicks, and film under test. While the polysulfone film surface is sufficiently hydrophobic so that a discontinuous (beaded) electrolyte film is deposited on the web as it exits from the line contact, these electrodes must be used carefully to provide sufficient dead time following a breakdown so that false surface flashovers are avoided. In general, this dead time (i.e., voltage removed) should be long enough so that at least 1 cm of film has passed through the electrode system.

The favorite electrolyte has been $0.1\text{F Cu(en)}_2\text{SO}_4$. In contrast to ordinary CuSO_4 solutions, this ethylenediamine complex ion avoids fouling the copper terminals with various copper oxides. Additionally, the strong violet

color of this ion is helpful in aligning the electrodes. Experiment has shown that the bulk conductivity of polysulfone film is not enhanced in the presence of this aqueous electrolyte.

The use of the wedge shaped pads (available in most hardware stores as paint applicators) permits line breadth contacts down to approximately 1 mm so that interelectrode capacitances of only 25 pF per cm of electrode width are achievable with 10 μ m polysulfone film. (The importance of this capacitance will become clear below.) The electrical contact with the film by these conformable liquid electrodes is equivalent to that obtained with evaporated metal electrodes, i.e., no disturbing air gaps are present.

The principles of nondestructive BVT are simply stated - detect the very first beginnings of voltage collapse across the sample and then, as quickly as possible, disable or crowbar any energy sources that can promote any future growth or duration of the breakdown process with the reasonable hope that the sample will be returned to its normal insulating state undamaged. (These energy sources are invariably various stray capacitances that are fully charged to the particular test voltage at the time of breakdown initiation.)

A reasonable circuit for performing these tasks is shown in Figure 8 where a small thyatron crowbar can be triggered into full conduction in

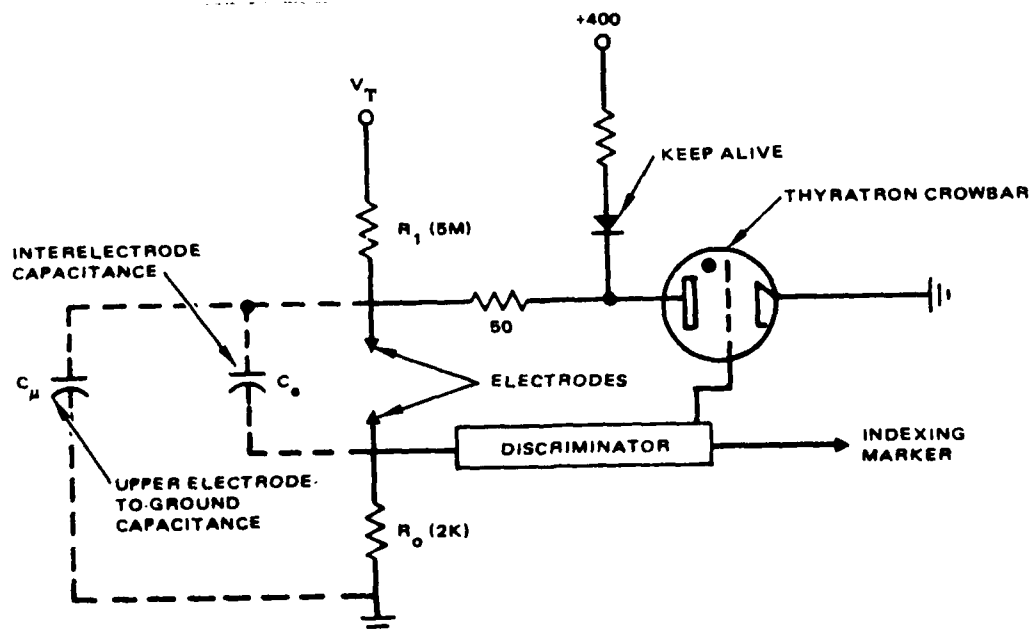


Figure 8. Nondestructive VBT.

approximately 10 to 20 ns by overdriving its grid with a fast discriminator-trigger circuit (avalanche transistors). The discriminator is provided to distinguish a true breakdown event from minor surface discharges that occur when using the aqueous line electrodes described above. The input to this discriminator is generated by current pulses that flow from the lower electrode to ground. (As will be shown, this embodiment leads to serious errors.)

Since the thyatron crowbar is not instantaneous, the success of the circuit in Figure 8 in providing the nondestructive VBT resides in the sample behavior itself. As shown in Figure 9, the question arises, can the sample dissipate the energy stored in the interelectrode capacitance C_e during the wait for the crowbar action without physical harm? (The upper electrode-to-ground capacitance, C_u , usually is negligible compared to C_e .) Initially the answer to this question would have been yes, but further diagnostic examination of films so tested gave such conflicting results that doubts arose as to whether nondestructive VBT was being observed when using the circuit of Figure 8. Indeed, the results obtained had been masked by surface discharges. This masking can best be understood by considering Figure 10, where a surface discharge is simply considered to short out capacitor C'_s . This shorting of capacitor C'_s leads to the waveforms shown in Figure 11.

Of particular interest in Figure 11 is the lower e_o waveform that closely mimics the expected results for a true breakdown, especially when various risetime problems are considered. Unfortunately, this waveform has been used as a measure of breakdown and to trigger the crowbar circuitry. It

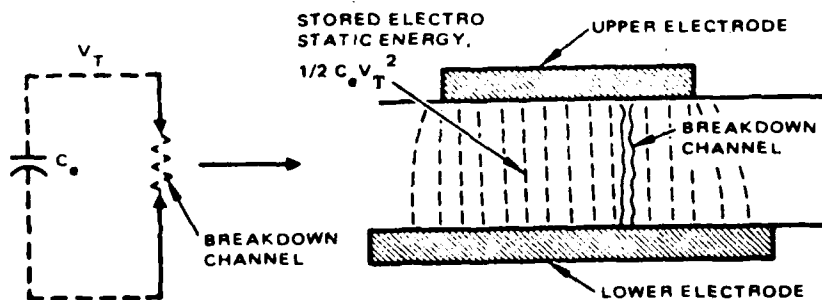


Figure 9. Energy dissipation in sample.

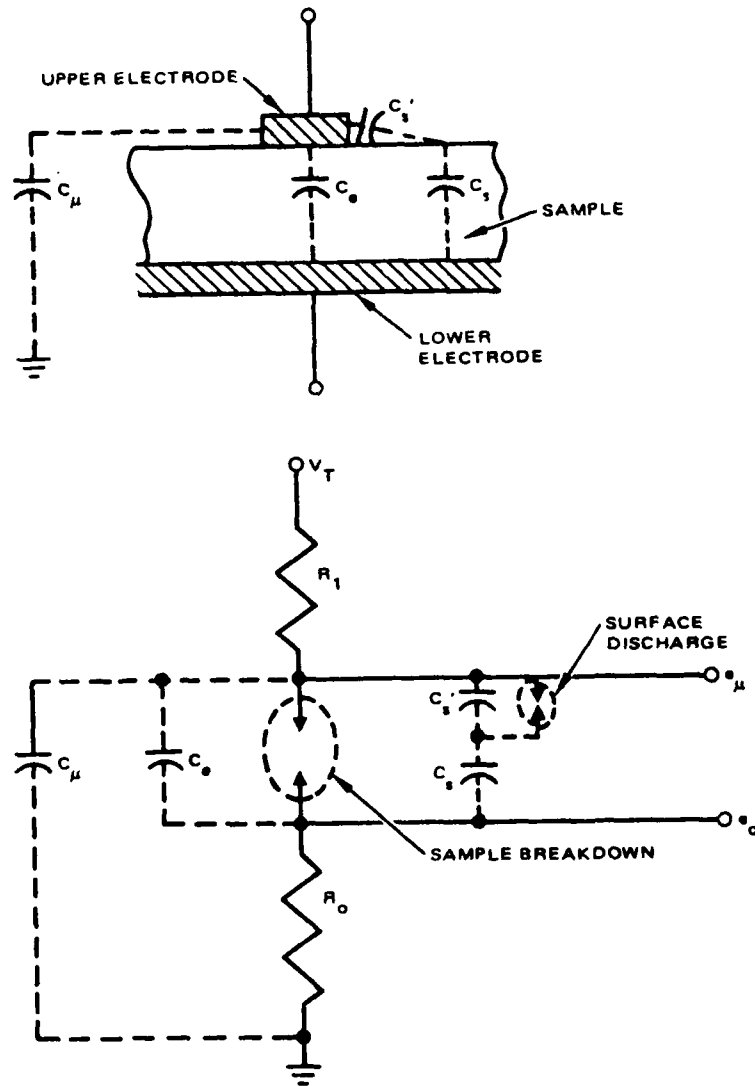


Figure 10. Electrode circuits.

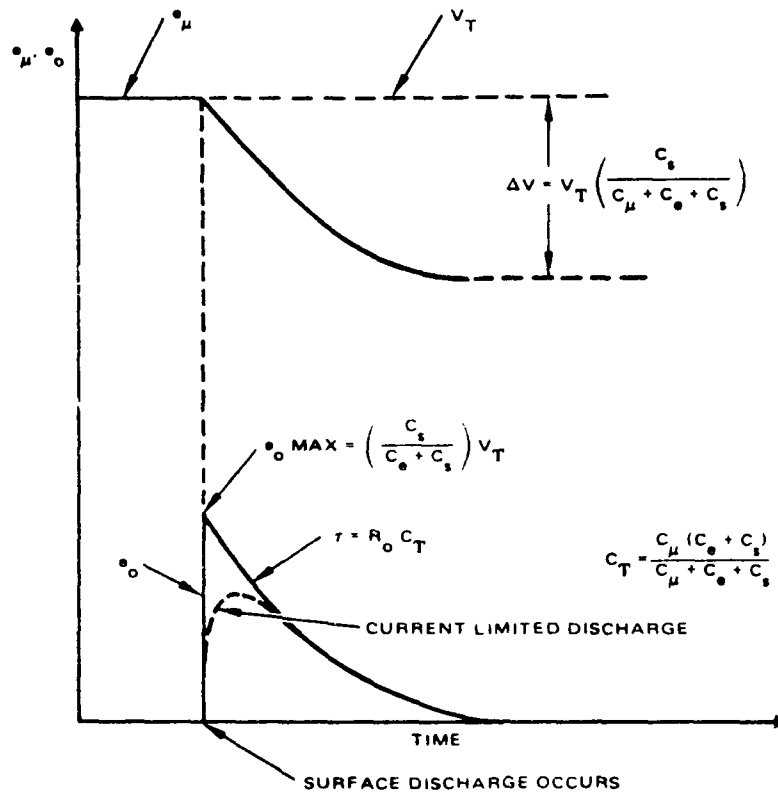


Figure 11. Waveforms.

is obvious from Figure 11 that the true distinction between surface discharge and breakdown is best made by noting that in the former case the voltage e_μ fails to go to zero.

To investigate breakdowns in which these surface discharges are absent, tests were performed with the electrode system shown in Figure 12. Here a fixed sample geometry is used with a conformable mercury electrode surrounded by a pool of mineral oil. This arrangement eventually became the standard small area test (SAT).

To minimize the interelectrode capacitance and thereby give nondestructive testing the best chance, the mercury contact with the sample was restricted to a 1 mm diameter circle ($C_e \sim 5$ pF). This test voltage was applied as a linearly rising ramp of 0.8 kV/second. (Here the desire was not to intentionally overstress the sample test area.) In all cases, the samples failed abruptly, with e_μ collapsing to zero in submicrosecond time. Subsequent examination of

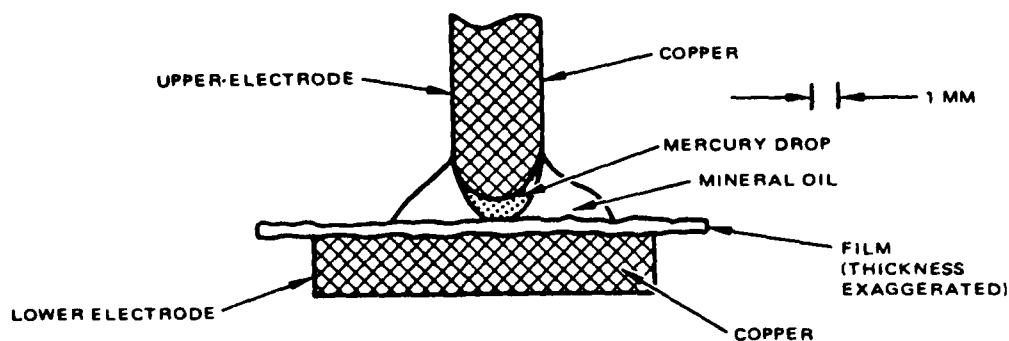


Figure 12. Surface discharge — free electrode system (SAT).

the failed areas invariably showed the presence of 10-60 μm holes. In addition, scanning electron microscopy showed that the borders of the holes were thickened, thus giving the distinct impression that the holes result from melting of the film with subsequent surface tension forces pulling the film into this pattern. Calculations of the electrical energy stored in the interelectrode capacitance of 5 pF show that sufficient energy exists under adiabatic conditions to cause such melting easily. Indeed, the whole breakdown act is so fast (nanoseconds) that no hope exists of performing nondestructive testing with electrodes of any reasonable dimensions.

Several reports in the literature claiming nondestructive VBT of dielectric films also show results that are masked by the problem of surface discharges masquerading as true breakdowns.*

5.3 MEASUREMENT OF IONIC CONTAMINANTS IN POLYMER SOLUTIONS AND SOLVENTS

The dielectric loss of a polar liquid, such as methylene chloride, represents the sum of losses arising from dipole relaxing processes whose time scales intrude on the particular measurement frequency and losses representing DC conductivity. Since all polar liquids of reasonable viscosities have relaxation times of the order of 10^{-12} seconds, it is a very good approximation at low frequencies (10 kHz or lower) to ascribe all the observed loss to

* Riel, et al., "Z fur angew," Phys. 27, p. 261, 1969.

DC conductivity. Thus, if the familiar parallel model definition of dissipation factor is combined with the geometric definitions of capacitance and conductance, this important relationship may be defined:

$$DF = \frac{2 \times 10^{12} g}{f \epsilon'}$$

where:

DF = dissipation factor

f = frequency of measurement, Hz

ϵ' = dielectric constant of the liquid

g = specific conductance (ohm · cm)⁻¹

This relationship indicates that the DC conductivity of a fluid may be measured by measuring its dissipation factor with a capacitance bridge connected to a simple capacitance cell containing the fluid as the dielectric (a small air capacitor submerged in the liquid will do). It is important to note the enormous numerical factor of 2×10^{12} relating DF to specific conductance.

The conductivity of a liquid is solely ascribable to the presence of ions, which can arise from two sources. The first is the intrinsic property of the liquid to autoionize, e.g., $H_2O = H^+ + OH^-$. (As a practical matter, this autoionization is assumed to be negligible.) The second and more interesting source is the presence of adventitious contaminants that can dissociate in the dielectric liquid to yield ions. Here the enormous influence that the dielectric constant of the liquid plays on the extent of this dissociation must be understood. As shown in Figure 13, a few parts per million of a quaternary ammonium salt in mineral oil ($\epsilon' = 2.2$) would exist almost completely in the form of neutral ion pairs, $[R_4N^+NO_3^-]^0$, and as such would make little or no contribution to the liquid's dissipation factor. However, if this same concentration of this salt were present in methylene chloride ($\epsilon' = 9$), its contribution to the liquid's dissipation factor would be enormous because the dissociation constant of the salt has been increased by a factor of 10^{12} ! (It is reasonable to infer that the often observed fact

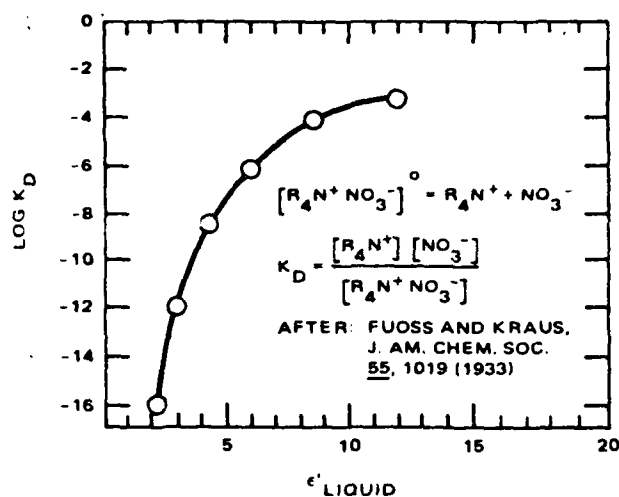


Figure 13. Ion pair dissociation versus liquid dielectric constant.

that liquids of high dielectric constant are always quite lossy arises from this exponential influence of dielectric constant and not on a particularly enhanced concentration of impurities over that present in liquids of lower dielectric constant.)

Thus, the basis is attained of an extremely sensitive and simple testing system for assaying the concentration of ionic contaminants in polysulfone resin, solutions and solvent systems; i.e., known quantities of these materials are dissolved in carefully purified (distillation) methylene chloride and the dissipation factor of resulting solution measured.

5.4 POLYMER FILM CONDUCTIVITY

All measurements were performed with gold sputtered electrodes, which were offset from one another so that limp, aluminum foil electrodes could be attached with Aquadag. The effective area was calculated from capacitance measurements.

5.5 FILTRATION STUDIES

Many experiments were performed to evaluate the effect of filtration of the casting solution on the breakdown properties of polysulfone film. In some cases, before the films were actually cast, the performance of the filter was

ulated by diluting the casting solution with filtered methylene chloride and filtering the solution on Millipore filter pads and counting the number of particles. A typical analysis of this type is presented in Table 11.

TABLE 11. PARTICLE ANALYSES OF FILTERED CASTING SOLUTIONS

Filter Type	Micrometer Rating	Particle Analysis (per gram resin)	
		7-15 μ m	15 μ m
Cox	1	6.1	2.1
Cox	2	5.7	1.0
Cox	5	17.0	5.2
Cuno 10A	10	3.7	1.8

Films prepared from filtered casting solutions were cast on the laboratory caster and the number of breakdowns counted using a large area test (LAT). Breakdown counts per unit area are shown in Figure 14 as a function of stress.

In an attempt to improve the breakdown performance of the laboratory cast films various other procedures were employed to eliminate particulate contamination during the casting operation. These steps included a second stage of filtration for the drying air for the lab caster and enclosing the caster in a tent to reduce airborne contamination. These additional procedures did not affect the occurrence of dielectric breakdown.

As these experiments proceeded, it became increasingly apparent that mere filtration of the casting solution and attention to the details of maintaining a particle-free film were not the whole reason for breakdown at the voltages of interest. This fact is noted by considering the particle counts presented in Table 11 and the breakdown results in Figure 14. Consideration, for example, of the particle counts for the 1 μ m Cox filter shows that there are a total of 140 particles greater than 7 μ m in a square meter of film such as that presented in the breakdown results of Figure 14. Since the film is about 4 μ m thick, there are not nearly enough particles to account for the large number of breakdowns observed.

5.9 TEXTURED FILM

At the outset of this work, one stated goal of the program was to develop a technique for providing a film with a textured surface. It was thought that such a material might provide a capacitor winding that could be impregnated and thus avoid the necessity of using Kraft capacitor tissue with its inherent moisture absorption. To fulfill this need, UltemTM polyetherimide film was prepared on a sandblasted laboratory casting drum. Scanning electron micrographs of this film and a comparative micrograph of film cast on a polished casting drum show that, while the exact extent and nature of the roughness introduced in this experiment may not be optimum, casting on roughened drums does seem to be a viable technique for producing textured film.

TABLE 14. PROPERTIES OF ULTEM[®] AND POLYSULFONE RESIN

Property	Polysulfone	Ultem [®]
Glass Transition Temperature, °C	190	217
Ultimate Tensile Strength, psi	15,000	26,000
Oxygen Index (bulk resin)	30	47
Dielectric Constant 23°C, 60 Hz	3.07	3.0
Dissipation Factor 23°C, 60 Hz	0.0008	0.0012

Accordingly, film was cast from this material, stretched in the fashion as for polysulfone (although at a higher temperature) and slit into bobbins. The breakdown characteristics of the film were determined using both the aqueous electrode and the metallized film electrode systems. The results of these tests are shown in Figure 25. When this curve is compared with those for polysulfone, considerable improvement in breakdown characteristic is noted over polysulfone. Therefore, this material was selected for further study and evaluation.

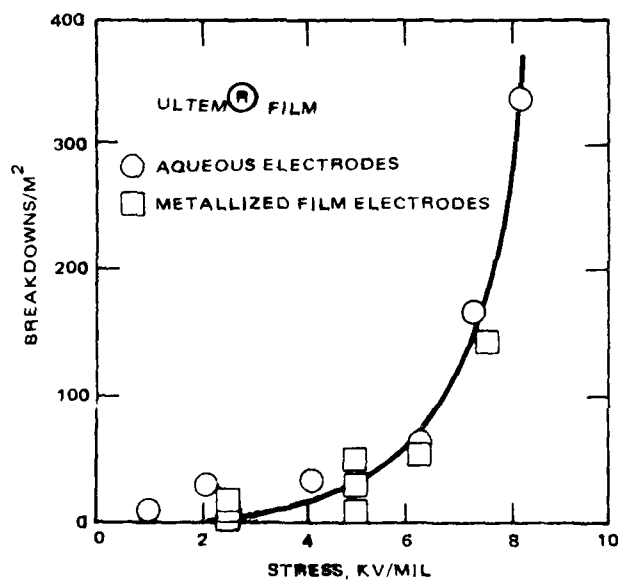


Figure 25. Large area breakdown counts/meter² versus voltage stress Ultem[®] film.

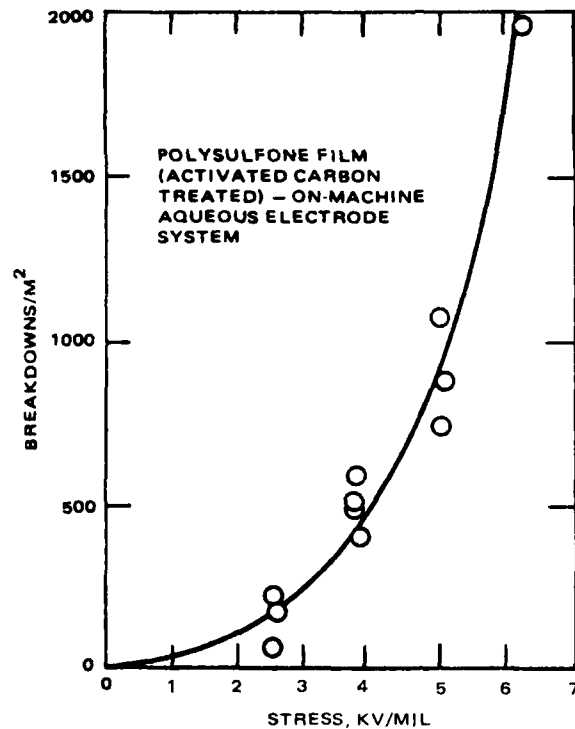


Figure 24. Large area breakdown versus voltage stress.

sides, in addition to large area breakdown tests using the brass plate/metallized film electrodes. These extra precautions were taken to avoid any potential problems with air gaps between the sample and electrodes.

5.8 POLYETHERIMIDE FILM

During this work, a new polyetherimide resin was commercialized by the General Electric Company. This new material, with the trade name of Ultem[®] has many properties to recommend it for high energy density capacitors such as proposed in this study. The relevant thermal, mechanical and dielectric properties of both polysulfone and Ultem[®] are given in Table 14.

From these properties, the permissible operating temperature of capacitors made from Ultem[®] film is assumed to be higher than for polysulfone. In addition, because of its superior strength, fabrication of capacitors may be easier. Finally, because of the very high oxygen index for this material, the flammability of capacitors is considerably reduced.

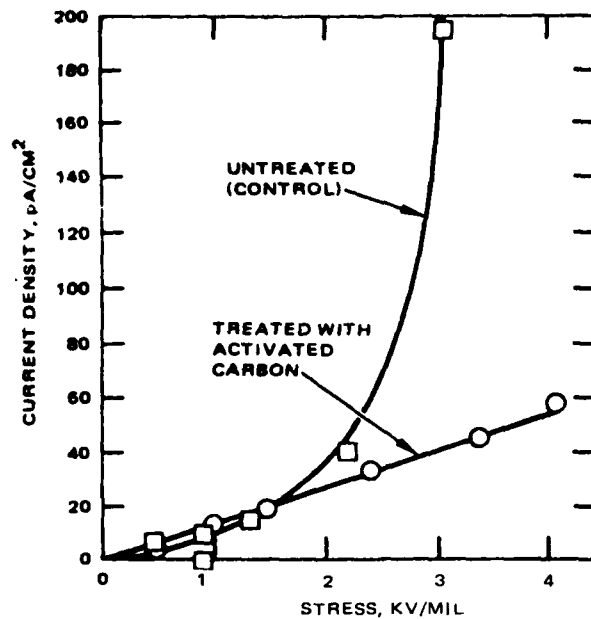


Figure 23. Current density versus voltage stress for treated and untreated film.

While experiments measuring the ionic contamination in the casting solution, small area tests, and film conductivity all show some improvement in film properties, these improvements were a result of decontamination procedures and were not carried through to large area breakdown tests or time-dependent breakdown. To evaluate the dielectric strength properties of films without the necessity of handling or further contaminating the film, the laboratory casting machine was fitted with an aqueous line contact electrode system as described in Section 5.2.

A polysulfone solution was treated with activated carbon and filtered through a composite filter medium consisting of a 5 and 0.65 μm filter. The dissipation factor of the solution thus prepared was 43 percent in a 7 percent polymer solution. The breakdown counts using the aqueous electrode system are shown in Figure 24. Comparison of this figure with Figure 14 shows that very little improvement has been gained in large area testing.

Films cast from treated solutions also exhibit time-dependent breakdown. For these experiments, a number of breakdown tests were performed using film samples of approximately 6 cm diameter that were sputtered with gold on both

TABLE 12. DISSIPATION FACTOR MEASUREMENTS FOR VARIOUS SOLUTIONS

Test	Sample Designation	Percent Resin Weight	Percent DF, (1 kHz)
1	Technical Grade Methylene Chloride	0	>100
2	Polysulfone Resin (as received)	0.65	>100
3	Distilled Methylene Chloride	0	5-8
4	Commercial Polysulfone Film Sample - good SAT	1	38
5	Commercial Polysulfone Film medium SAT	1	58
6	Polysulfone Solution Treated with Activated Carbon (50 percent of resin weight)	7	20-40
7	Polysulfone Solution Treated with Cellulose	1	73

TABLE 13. SAT BREAKDOWN FOR TREATED FILMS

Test	Treatment	Mean Breakdown Voltage, kV/mil	Standard Deviation, kV/mil
1	No Treatment - Lab Cast Film	10.2-11.4	2.5-3.8
2	Cellulose	15.5	1.4
3	Water Extraction	13.2	2.1
4	Activated Carbon	15.7	2.3
5	Diatomaceous Earth	14.0	1.5

Results of conductivity measurements on treated and untreated films show that some reduction in conductivity can be obtained. The curves in Figure 13 show current density versus voltage stress for two films with the same thermal treatment before testing. The untreated film was cast from a solution that went through the same procedure as the treated solution except that the activated carbon was omitted. The results show that not only is the conductivity generally lower with the treated film but also more nearly ohmic.

the polymer solution. The results must be interpreted carefully, however, since, regardless of the nature of the ionic impurity, they all behave as weak electrolytes when in a solvent with a low dielectric constant such as methylene chloride. The extent of the dissociation of the ion pairs is then a function of the concentration of the electrolyte and follows the classical Ostwald dilution law. Unfortunately, the concentration of the impurities is not known; therefore, the dissipation factor results only can be compared at equal polymer concentration. The relative extent of the ionic contamination can be determined because of the ability of the polymer to dissolve in a convenient solvent. Such determinations would be much more difficult in a polymer such as polypropylene since it does not have a convenient solvent.

From the tests and procedures described above it was apparent that sorption of the ionic contaminants was most effectively done with activated carbon. Several determinations of dissipation factor for various samples are compiled in Table 12. From tests 1 and 2 in Table 12, it is clear that both the technical grade methylene chloride normally used to make casting solution and the polysulfone resin are replete with ionic contaminants. Test 3 indicates that distillation does a reasonable job of removing ionic contaminants. Commercial polysulfone film samples showed a considerable reduction in ionic contamination relative to the resin as shown in tests 4 and 5 but not nearly as great a reduction as achieved when the polymer solution was treated with activated carbon (test 6). The reduced amount of ionic contamination in the commercial films compared to the resin may be caused by sorption by the filtration medium normally used for filtering casting solutions. These filters are typically cellulosic in nature, and cellulose has been shown to provide some reduction in ionic content (test 7).

Many films prepared from casting solutions treated to remove ionic contaminants were tested using the SAT described previously. Since the data from these determinations contained considerable scatter, at least 10 separate readings were made for each film and the standard deviation computed. A number of these determinations are given in Table 13 with the various treatments applied to the casting solutions. From these data and others not listed, the treatments seem to have some influence on the small area test results. However, the scatter in the data make such comparisons difficult.

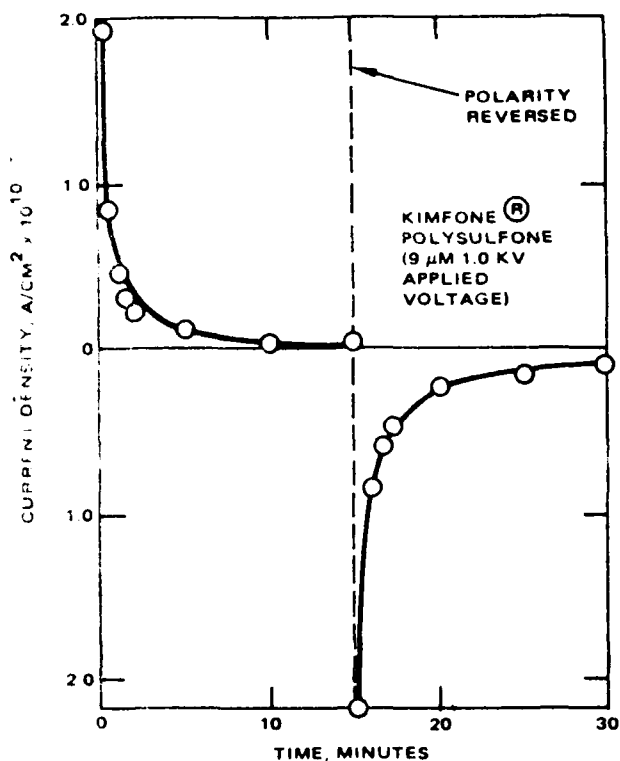


Figure 21. Current density versus time for commercial polysulfone film.

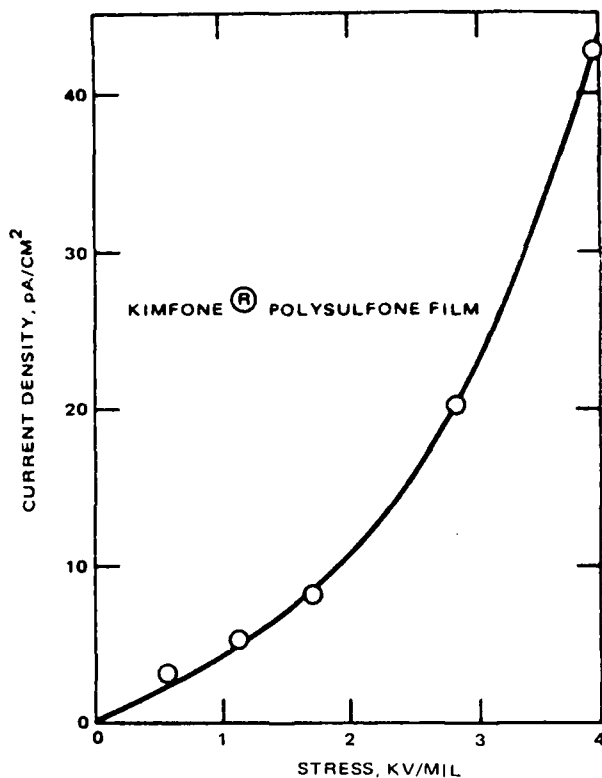


Figure 22. Current density versus voltage stress for commercial polysulfone film.

or chemically pure cellulose fibers such as used for manufacture of Kraft capacitor tissue. Still further purification was attempted by exhaustively extracting contaminants from the cast film with methanol in a Soxhlet extractor.

The procedure used in purification was to first dilute the normally very viscous casting solution with distilled methylene chloride to provide a viscosity low enough to get good mixing of the absorbent and the polymer solution. Then the absorbent was added to the solution, usually at a level of about 50 percent of the resin weight, and shaken for 16 hours. The slurry was then filtered to remove the absorbent and concentrated by evaporation of methylene chloride using a rotary evaporator.

The technique for evaluating the effectiveness of the decontamination procedure was to measure the dissipation factor of a dilute methylene chloride solution of the polymer. This procedure (described more fully in Section 5.3) is performed rather simply by dipping a clean air capacitor into

5.6.3 Film Conductivity

To assess the changes in conductivity of the film samples because of the movement of charge carriers, a cell was constructed to measure film conductivity at various voltages, temperatures and times. The time-dependence of these measurements is particularly interesting in light of the results discussed above concerning time-dependence of dielectric breakdown. Current density versus time is shown in Figure 21 for a commercial sample of polysulfone film with an applied voltage of 1000 volts. From these data it is clear that the current is initially high but decreases with time, presumably as the mobile charge carriers accumulate near the electrodes. After 15 minutes the polarity was reversed, and the current was observed again to be initially high but to decrease with time and at approximately the same rate as initially. In these experiments, current density rather than a computed resistivity has been plotted as a function of time because of the non-ohmic nature of the conductivity. This behavior is best illustrated in Figure 22 in which current density is plotted as a function of voltage stress for the same sample as in Figure 21. In both figures, the sample area used to determine the current density was determined from capacitance measurements. (In calculating the current density, the current is assumed to be flowing uniformly through the sample which may not be the case.)

5.7 DECONTAMINATION PROCEDURES

From the experiments discussed above, it is clear that some procedure must be developed to remove or ameliorate the effect of the ionic impurities present in the film. Further, some test must be available to assess the efficacy of the decontamination procedure. Accordingly, many procedures were tried for decontaminating the casting solutions. Since the composition of the contaminants was unknown, the procedures selected generally were applicable for a wide variety of organic and inorganic materials. The evaluation included absorption with activated carbon, extraction with deionized water, absorption with silica gel, activated alumina, talc, and diatomaceous earth. Another procedure employed was filtration of the polymer solution through a thick pad

breakdown counts increase indefinitely with time. In fact, such experiments have been continued for as long as 30 minutes with no sign of stopping. In such a test, it is reasonable to ask why one spot breaks down before another when the same voltage is applied to the entire sample. Evidently, the mobile carriers do not build up uniformly at the electrodes due to slight differences in carrier concentration or mobility.

Some interesting comparative experiments were performed with other dielectric films to determine if they also exhibit time-dependent breakdown. Using the same metallized film/brass plate electrode arrangement as above, both polyethylene terephthalate (Mylar) and polypropylene films were tested. At the modest voltages available with this equipment, no time-dependent breakdowns were observed in the polypropylene samples but were observed in the Mylar samples as indicated in Figure 20. Thus, while the breakdown voltages may not be the same, time-dependent breakdowns are not restricted to polysulfone films.

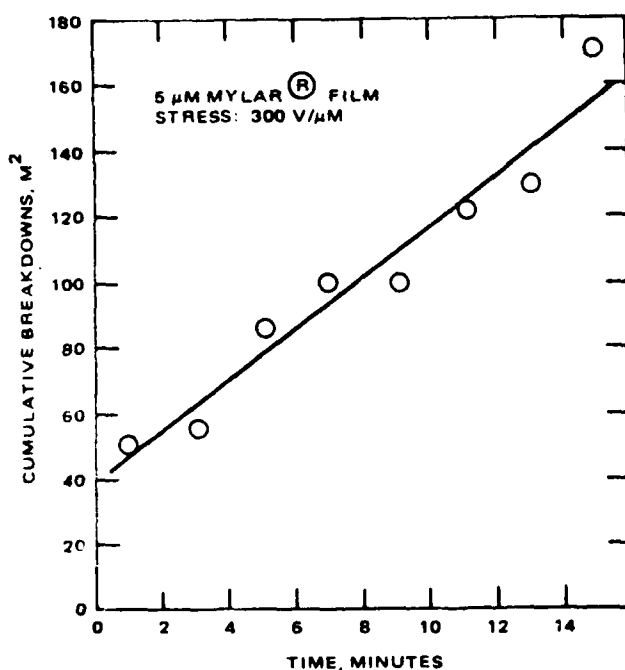


Figure 20. Cumulative breakdowns versus time of application of voltage.

These results show that as the DC voltage is reduced to some value less than the high-ramp rate breakdown voltage, breakdown still occurs but at increasingly longer times. These results can be interpreted as indicating that a critical field distortion pattern can be created by the mobile charge carriers. Thus, it can be argued that the field is much enhanced near the electrodes but over dimensions such that the sample fails first near the electrodes and then in the interior of the dielectric. The progression in time of the voltage within the sample is illustrated in Figure 18.

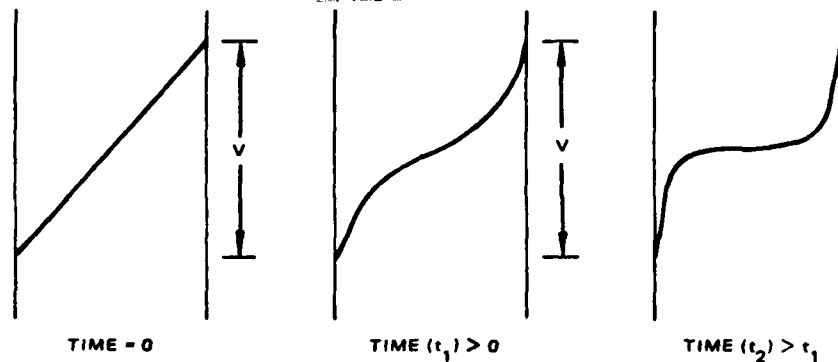


Figure 18. Field distortion versus time.

In another experiment, in which time dependent breakdown was observed, a constant DC voltage was applied to a large area of commercial polysulfone film using the metallized film/brass plate electrode arrangement. The results of this experiment are presented in Figure 19. As shown, the cumulative

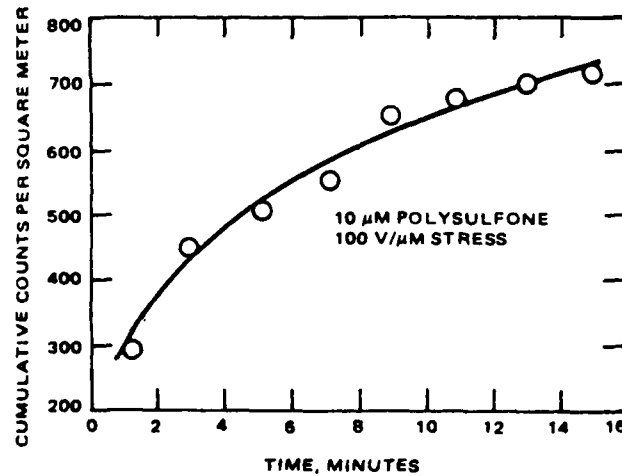


Figure 19. Time-dependent breakdown cumulative counts/meter³ versus time of application of voltage.

very large in a very thin region adjacent to the electrodes. It is well known for most dielectrics that very thin layers of insulating material display extremely high dielectric strength. Furthermore, an intermediate condition might exist wherein the field would be high near the electrodes but not in a layer thin enough to display high breakdown voltage. Such a situation is discussed in the next section.

5.6.2 Time-Dependent Breakdown

In a typical breakdown experiment, when voltage is applied to a sample, the dielectric weak spots are expected to fail and thereafter breakdowns will cease. Application of a higher voltage will cause more weak spots to fail and so on. Such is not the case with many of the films tested in this work; instead breakdowns continue as voltage is left on the sample.

A revealing experiment was conducted with polysulfone film using the small area breakdown testing apparatus discussed in the previous subsection. In this experiment, the average breakdown voltage under high ramp rate conditions was determined for the sample. Then, using the same setup, a percentage of that voltage was applied under DC conditions until breakdown occurred. The results are shown in Figure 17.

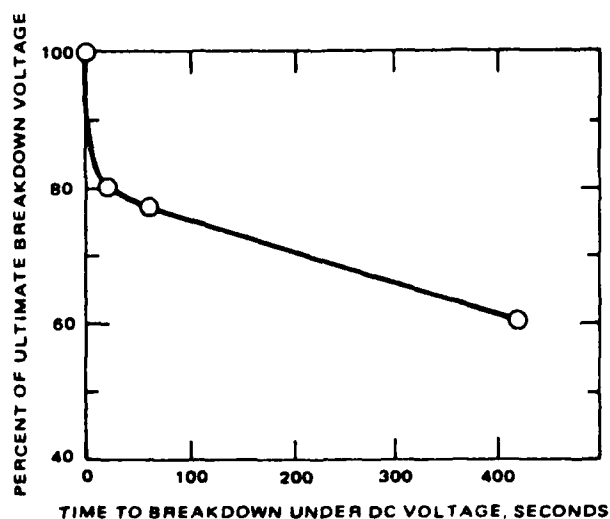


Figure 17. Percent of ultimate breakdown voltage under ramp conditions versus time of application of DC voltage small area test.

Moreover, in these tests if the bias is removed for a time equal to its application before the ramp is started, the breakdown voltage returns to its original value. From these experiments, it is evident that some migration of charge carriers within the dielectric must be occurring to account for the difference in breakdown voltage. This idea is especially cogent since films such as polypropylene, which have an initially high breakdown voltage by this test, do not display a higher voltage when "polarized" as described above. This observation suggests that when a few mobile charge carriers are present, application of a bias voltage will have little effect on the breakdown voltage.

While the interpretation of these results is somewhat speculative, a possible explanation exists in the field distortion illustrated in Figure 16. In Figure 16a, the sample is completely non-polarized, and the charge carriers are uniformly distributed throughout the dielectric. In Figure 16b, a polarizing voltage has been applied for some time causing a field distortion because of the presence of charge carriers adjacent to the electrodes. When a ramp voltage is applied to the electrodes, the electric field (the slope of the curve in Figure 16b) will be small in the bulk of the sample but

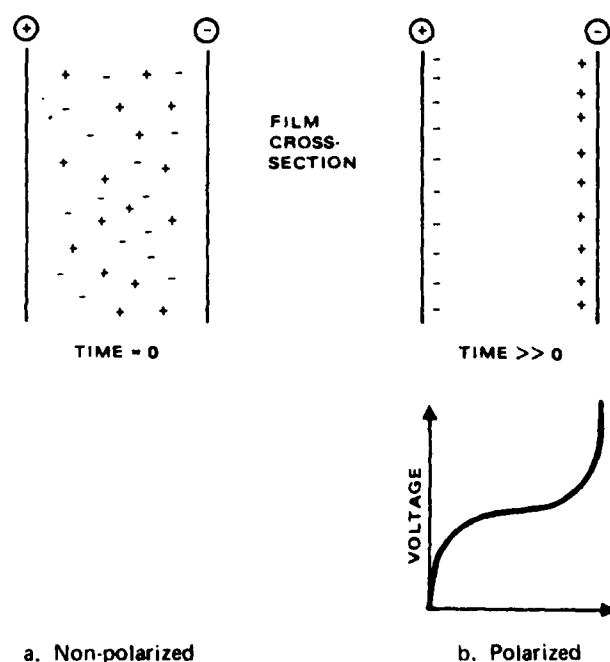


Figure 16. Charge distribution within "polarized" dielectric.

In light of the above experiments, other mechanisms for dielectric breakdown were considered. In a series of experiments that are discussed in the next section, the film samples were found to contain mobile charge carriers, probably dissolved ionic impurities, which move through the dielectric when voltage is applied and cause distortion and enhancement of the electric field.

5.6 CHARGE MOBILITY EXPERIMENTS

5.6.1 Small Area Tests

To avoid the influence of conducting particles on dielectric breakdown, the small area test (SAT) was employed. This device examines only a few square millimeters of film and is described more fully in the Test Development Section of this report. In this test, a ramp of voltage (5 kV/sec) is applied to the sample until breakdown occurs. A storage oscilloscope records the voltage.

In a crucial experiment, a bias voltage of 1000 V (a fraction of the ultimate breakdown voltage) was applied to the film for various times before starting the voltage ramp. The results as shown in Figure 15, show that the longer the bias voltage is applied, the higher the ultimate breakdown voltage.

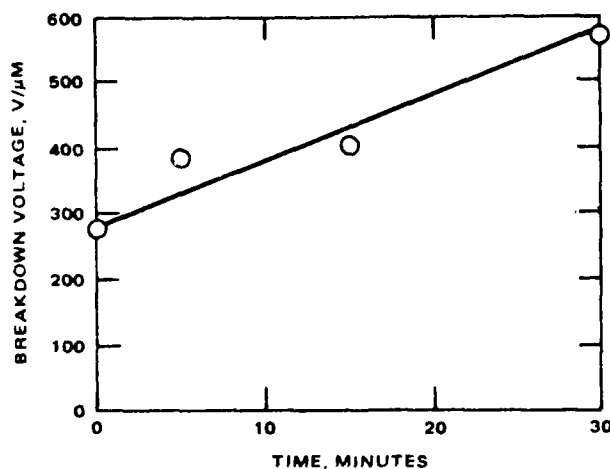


Figure 15. Breakdown voltage stress versus time of applied bias voltage.

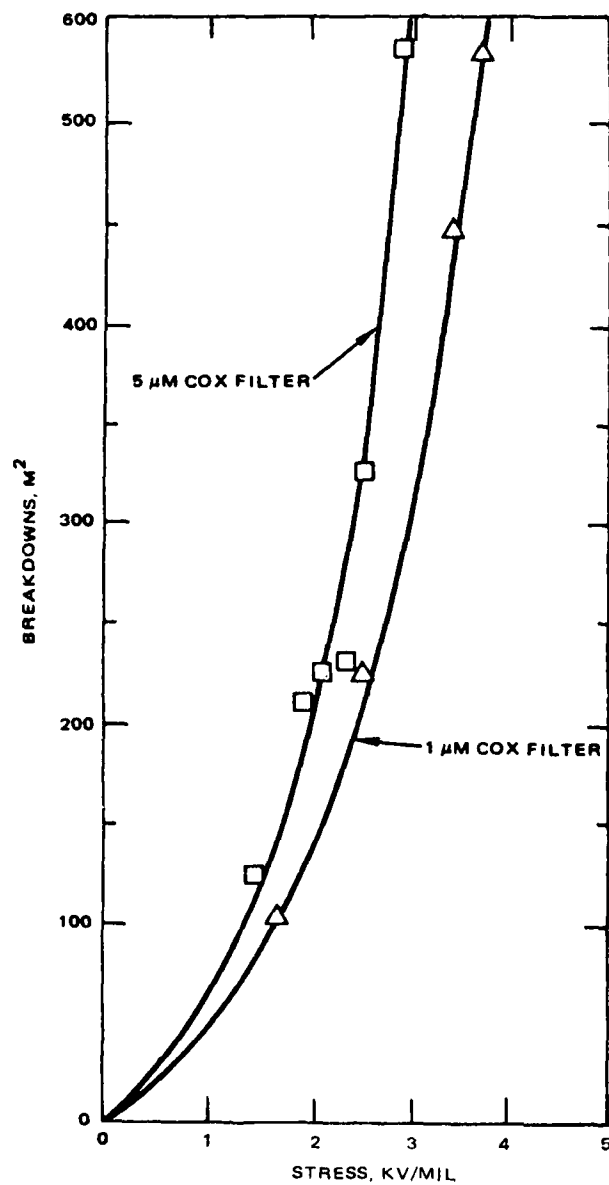


Figure 14. Breakdowns versus voltage stress.

6.0 FINAL SELECTION

6.1 RECOMMENDED DIELECTRIC SYSTEMS AND REVISED ESTIMATES

Based on the results of the work of Schweitzer, the dielectric systems were revised to include Ultem[®] polyetherimide in cases where it shows an advantage over polysulfone. Because the development resulted in a material of higher temperature capacity rather than of improved dielectric strength, the capacitors in general would be expected to have the same or slightly better energy density, but they could be operated at higher cold-plate temperature or higher duty cycle. Thus, the overall system weight would be lower even if the energy density measured in the laboratory shows limited improvement.

6.1.1 High Repetition Rate Capacitor

In this design (similar to design B on page 86 of AFWAL-TR-80-2037) the operating field has been reduced slightly. However, the parts should have better life and better power throughput than the components made from polysulfone:

Number of dielectric layers	5
Ultem [®] layers	2.6 μm (24 gauge)
Kraft layers	3/10 μm (0.4 mil)
Foil	Aluminum/6 μm
Dielectric fluid	Diethylphthalate

Estimates are:

Average electric field	4464 V/mil
Average dielectric constant	4.302
Energy density	22 J/g (99.8 J/lb)

6.1.2 Low Repetition Rate Capacitor

This component has the same pad design as the high rate component, but a slightly higher operating field.

Number of dielectric layers	5
Ultem® layers	2/6 μm
Kraft layers	3/10.1 μm
Foil	Aluminum, 6 μm
Dielectric fluid	Diethylphthalate

Estimates are:

Average electric field	4762 V/mil
Average dielectric constant	4.302
Energy density	0.25 J/g (113.6 J/lb)

6.1.3 DC Filter Capacitor

For this design, either the design for the pulse capacitor as above or the previously cited design using PVDF could be used.

6.1.4 High Frequency AC Capacitor

The Ultem® polyetherimide material has particular application here, as this component will unavoidably get very warm.

Number of dielectric layers	2
Ultem® thickness	6 μ (0.24 mil)
Foil	Aluminum, 6 μ
Dielectric fluid	Silicone

Estimates for these components are:

Average electric field	3125 V/mil
Dielectric constant	3.2
Energy density	0.08 J/g (37 J/lb)

7.0 MATERIAL CHARACTERIZATION

Subsequent to the developmental efforts in Phase I, parametric tests were carried out to characterize the materials used or proposed for use in the capacitor dielectrics. These tests were carried out according to the Material Test Plan described in Section 4.0. In many instances, data on the materials was available from the literature or manufacturer's data sheets. This information was considered sufficient for design purposes and measurement was not necessary for characterization purposes. This data and its source are listed in this section. Some tests were not carried out and no values were available from other sources. These tests were not considered to be critical for the design of the capacitors.

7.1 TESTS ON PLASTIC FILMS

Four plastic film materials were used in the course of this program in various dielectrics. These were:

1. Ultem® polyetherimide
2. Kimfone polysulfone
3. Bollowe polypropylene
4. Fluorofilm-C polytetrafluoroethylene

In addition, a sample of textured Ultem® film was prepared for testing the wetting properties of textured versus plain films. This work was considered important for the eventual elimination of Kraft paper in oil-impregnated high voltage capacitors.

7.1.1 Ultem Polyetherimide

This material was cast by Schweitzer on a laboratory caster from resin manufactured by General Electric. Three gauges of plain film were supplied to Hughes — 0.20 mil (5 μ m), 0.24 mil (6 μ m), and 0.36 mil (9 μ m) — as well as 0.24 mil metallized film. The plain film was slit to 4.50 inch width, while the metallized material was slit to 2.00 inch width and had 0.040 inch wide margins. A single roll of 0.32 mil (8 μ m) textured film of 4.50 inch width was also supplied. This was later slit by Component Research Company, Inc. to make windings. The slit width was 2.00 inch.

The tests described in the approved test plan are listed in Table 15 along with the values obtained in tests performed by Hughes, Schweitzer, and General Electric. In the latter case, tests were performed on the bulk material and not on the films cast by Schweitzer.

Dielectric constant and dissipation factor measurements were made over the range of 50 to 10^6 Hz and 20 to 140°C. Measurements are plotted in Figures 15 and 16.

The dielectric strength of the plain and textured films was measured using ASTM Method D149-75. This was a short-time test with a 1000 V/sec rate-of-rise employing the Type 3 electrode arrangement. Six measurements were made on each gauge. The data is presented in Table 16. It appears that the dielectric strength of the textured film has not been impaired to a degree measurable in this way. The absolute values of these measurements are low compared to what was expected based on the large area breakdown tests performed by Schweitzer and shown in Figure 25. This was probably due to different measurement conditions.

The insulation resistance of the various film thicknesses was also measured and is reported in Table 17. Test voltages of 10 and 500 volts were used. At 500 volts, nearly half the samples broke down. The overall mean of all measurements made at 10 V was 4.6×10^{16} ohm-cm. General Electric reports a typical insulation resistance of 6.7×10^{17} ohm-cm for a 0.0625 inch thick sample.

TABLE 26. ULTEM 24GA PROPERTIES

Paragraph	Description	Method (ASTM)	Value	Unit	Source
3.1.1	Dielectric Constant	D150	3.17	—	Hughes
3.1.2	Dissipation Factor	D150	0.0014	—	Hughes
3.1.3	Surface Resistivity	D257		MΩ	
3.1.4	Volume Resistivity, 50% RH	D257	4.8×10^{16}	ohm-cm	Hughes
3.1.5	Dielectric Strength, Air	D149, D2305	2813	V/mil	Hughes
3.1.6	Gross Flaw	Hughes		m ⁻²	Hughes
3.2.1	Fine Flaw	Hughes	See Figure 5-20	—	Schweitzer
3.2.2	Surface Contamination	D202			Hughes
3.2.3	Residual Solvent	Hughes	1.6	%	Hughes
3.2.3	Moisture Absorption, 24h	D570	0.25	%	GE
3.3.1	Film Thickness	D374 (A or C)		mils	Hughes
3.3.2	Film Density	D1505	1.24	g/cm ³	Hughes
3.3.3	Tensile Strength at Break	D882(A)	15,200	psi	GE
3.3.4	Elongation at Break	D882(A)	60	%	GE
3.3.5	Shrinkage, M.D.	Hughes		%	Hughes
3.4.1	Cores	Hughes	OK	—	Hughes
3.4.2.1	Telescoping	Hughes	OK	—	Hughes
3.4.3	Width and Diameter	Hughes	OK	—	Hughes
3.4.4	Splices	Hughes	OK	—	Hughes
3.4.5	Marking	Hughes	OK	—	Hughes
3.5.1	Wrapping	Hughes	OK	—	Hughes
3.5.2	Outer Package	Hughes	OK	—	Hughes
3.5.3	General Requirement	Hughes	OK	—	Hughes

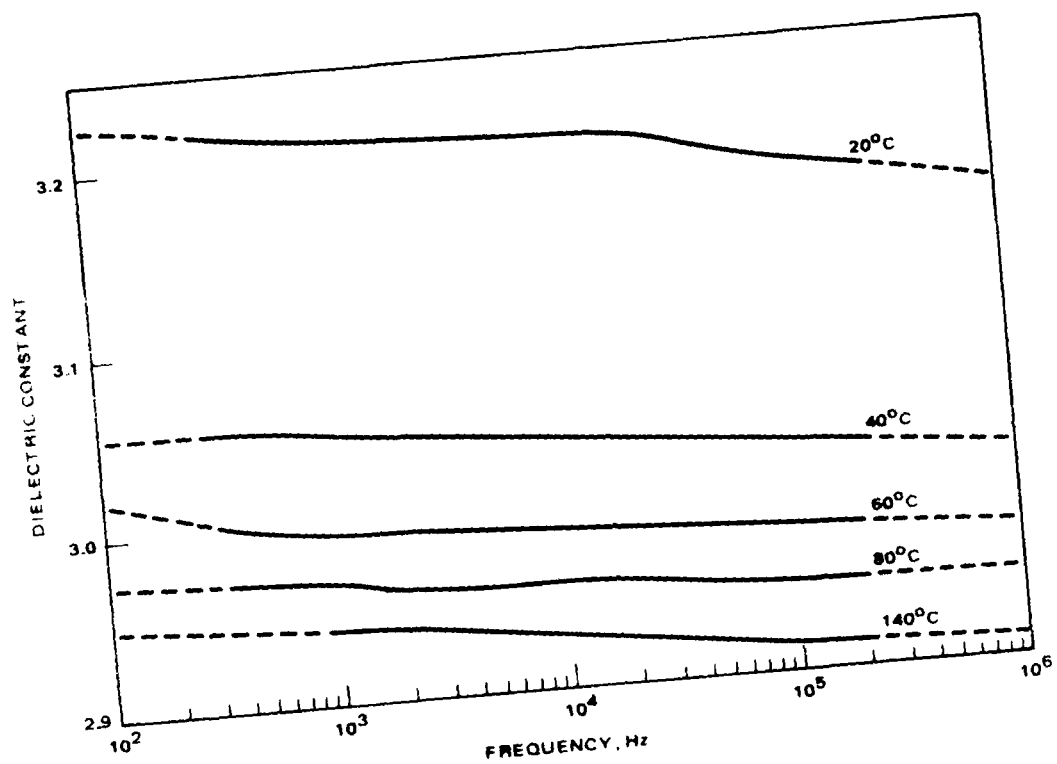


Figure 26. Ultem dielectric constant.

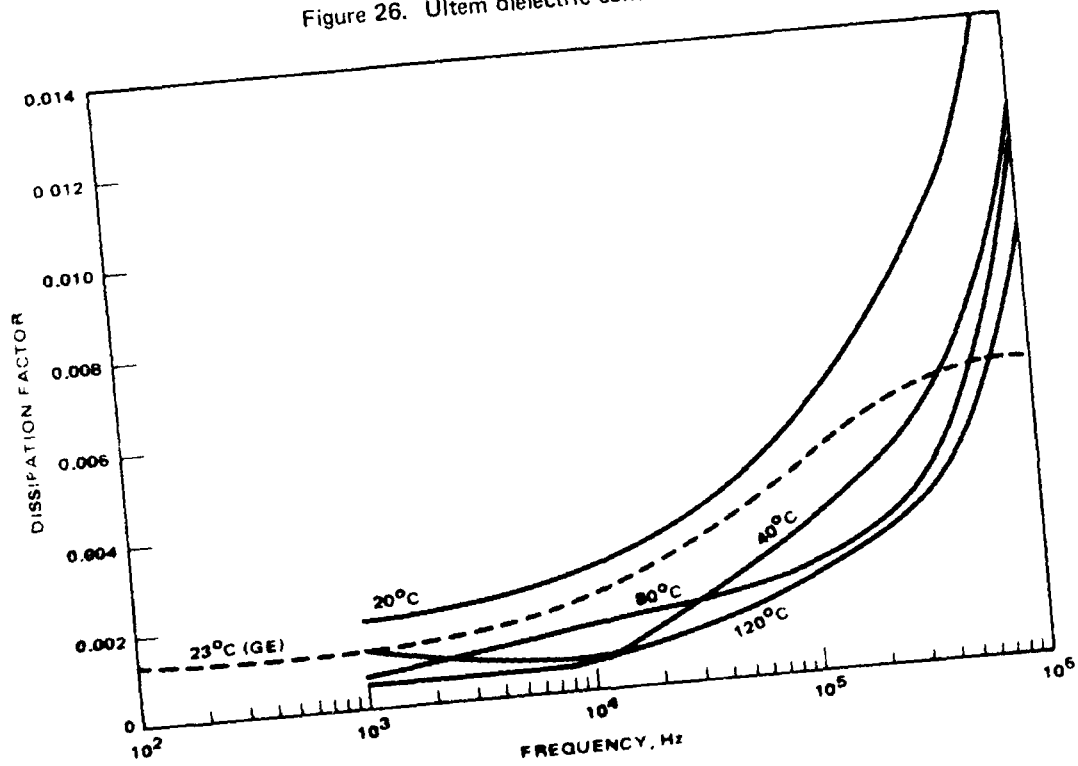


Figure 27. Ultem dissipation factor.

TABLE 16. BREAKDOWN STRENGTH OF ULTEM

Thickness, mils	Breakdown Voltage, volts	Breakdown Field, volts/mil
0.24 (plain)	500	2083
	500	2083
	500	2083
	600	2500
	750	3125
	1200	5000
Mean \pm Std. Dev.	675 \pm 251	2812 \pm 1047
0.32 (textured)	450	1406
	500	1563
	500	1563
	750	2344
	750	2344
	1250	3906
Mean \pm Std. Dev.	700 \pm 274	2188 \pm 856
0.36 (plain)	500	1389
	500	1389
	500	1389
	600	1667
	1000	2778
	1800	5000
Mean \pm Std. Dev.	817 \pm 474	2269 \pm 1317

TABLE 17. INSULATION RESISTANCE OF ULTEM

Thickness, mils	Test Voltage, volts	Resistance, m Ω	IR, ohm-cm
0.24	10	$3.8 \cdot 10^6$	$2.5 \cdot 10^{16}$
	10	$1.0 \cdot 10^7$	$6.6 \cdot 10^{16}$
	10	$5.0 \cdot 10^6$	$3.3 \cdot 10^{16}$
	10	$6.0 \cdot 10^6$	$4.0 \cdot 10^{16}$
Mean	10	$6.2 \cdot 10^6$	$4.1 \cdot 10^{16}$
0.24	500	$3.5 \cdot 10^6$	$2.3 \cdot 10^{16}$
	500	Short	—
	500	$4.0 \cdot 10^6$	$2.6 \cdot 10^{16}$
	500	Short	—
Mean	500	$3.8 \cdot 10^6$	$2.5 \cdot 10^{16}$
0.32	10	$9.0 \cdot 10^6$	$5.9 \cdot 10^{16}$
	10	$9.0 \cdot 10^6$	$5.9 \cdot 10^{16}$
	10	$8.0 \cdot 10^6$	$5.3 \cdot 10^{16}$
	10	$8.0 \cdot 10^6$	$5.3 \cdot 10^{16}$
Mean	10	$8.5 \cdot 10^6$	$5.6 \cdot 10^{16}$
0.32	500	$1.5 \cdot 10^6$	$9.9 \cdot 10^{15}$
	500	Short	—
	500	$1.8 \cdot 10^6$	$1.1 \cdot 10^{16}$
	500	$2.0 \cdot 10^6$	$1.3 \cdot 10^{16}$
Mean	500	$1.8 \cdot 10^6$	$1.1 \cdot 10^{16}$
0.36	10	$6.0 \cdot 10^6$	$3.9 \cdot 10^{16}$
	10	$6.0 \cdot 10^6$	$3.9 \cdot 10^{16}$
	10	$7.0 \cdot 10^6$	$4.5 \cdot 10^{16}$
	10	$7.0 \cdot 10^6$	$4.5 \cdot 10^{16}$
Mean	10	$6.5 \cdot 10^6$	$4.2 \cdot 10^{16}$
0.36	500	Short	—
	500	$8.0 \cdot 10^5$	$5.3 \cdot 10^{15}$
	500	$1.5 \cdot 10^6$	$9.9 \cdot 10^{15}$
	500	Short	—
Mean	500	$1.2 \cdot 10^6$	$7.6 \cdot 10^{15}$

7.1.2 Kimfone Polysulfone

Polysulfone film was used in the 400 Hz AC filter capacitor for comparison to the polyetherimide. The same film thickness, 0.24 mil (6 μ m), was used in each design with 2.00 inch width and 0.040 inch margins. Because this material has been commercially available for some time and has been well characterized, no additional testing was performed at Hughes. Typical test values are listed in Table 18.

7.1.3 Bollore Biaxially Oriented Polypropylene

No data sheet was available on this film from the vendor, so data have been taken from other sources on the same generic type of film (Toray T-2400, for example). A thickness of 0.24 mil (6 μ m) in 3.00 inch width was procured for use in a 10 kHz AC inverter capacitor design. Data on this film is presented in Table 19.

7.1.4 Fluorofilm-C Polytetrafluoroethylene

This film is a unique multilaminar cast film made by the Dielectrix Division of Fluorocarbon Company. A 0.25 mil (6 μ m) thickness film of 3.00 inch width was procured for use in a 10 kHz AC inverter capacitor design. Test results on this film are presented in Table 20.

7.2 TESTS ON DIELECTRIC LIQUIDS

Three dielectric liquids were used in the various designs developed for this program:

1. BASF Platinol[®] Dioctyl Phthalate (DOP)
2. Dow Corning DC-200 Poly-dimethyl siloxane
3. Helix FE-4 Poly-1,2-Epoxyhexafluoropropane Ether

No additives were used in preparing these oils for use. Improved lifetime has been achieved in DOP impregnated capacitors through the use of epoxides which neutralize phthalic acid formed by hydrolysis of the ester. Rather than introduce such additives, efforts were made to minimize the moisture content of the oil and capacitors.

TABLE 15. PROPERTIES OF POLYKUNTFONE POLYSULFONE

Paragraph	Description	Method (ASTM)	Value	Unit	Source
3.1.1	Dielectric Constant, 1 kHz	D150	3.07	—	Schweitzer
3.1.2	Dissipation Factor, 1 kHz	D150	0.0008	—	Schweitzer
3.1.3	Surface Resistivity	D257		M Ω	
3.1.4	Volume Resistivity, Dry	D257	5×10^{16}	ohm-cm	Schweitzer
3.1.5	Dielectric Strength, Air	D149, D2305	7500	V/mil	Schweitzer
3.1.6	Gross Flaw	Hughes		m ⁻²	Hughes
3.2.1	Fine Flaw	Hughes	See Figure 5-9	—	Schweitzer
3.2.2	Surface Contamination	D202		—	Hughes
3.2.3	Residual Solvent	Hughes	0.3	%	Hughes
3.3.1	Moisture Absorption, 24h	D570	0.22	%	Schweitzer
3.3.2	Film Thickness	D374 (A or C)	0.24	mils	Schweitzer
3.3.3	Film Density	D1505	1.24	g/cm ³	Hughes
3.3.4	Tensile Strength at Break	D882(A)	10,000	psi	Schweitzer
3.3.5	Elongation at Break	D882(A)	50	%	Schweitzer
3.4.1	Shrinkage, M.D.	Hughes	1-3	%	Schweitzer
3.4.2.1	Coresh	Hughes	OK	—	
3.4.3	Telescoping	Hughes	OK	—	
3.4.4	Width and Diameter	Hughes	OK	—	
3.4.5	Splices	Hughes	OK	—	
3.5.1	Marking	Hughes	OK	—	
3.5.2	Wrapping	Hughes	OK	—	
3.5.3	Outer Package	Hughes	OK	—	
	General Requirement	Hughes	OK	—	

TABLE 19. PROPERTIES OF POLYPROPYLENE FILM

Paragraph	Description	Method (ASTM)	Value	Unit	Source
3.1.1	Dielectric Constant, 1 kHz	D150	2.2	—	Toray
3.1.2	Dissipation Factor, 1 kHz	D150	0.0001	—	Toray
3.1.3	Surface Resistivity	D257		MΩ	
	Volume Resistivity	D257	8×10^{18}	ohm-cm	Toray
3.1.4	Dielectric Strength, Air	D149, D2305	9600	V/mil	Toray
3.1.5	Gross Flaw	Hughes		m ⁻²	
3.1.6	Fine Flaw	Hughes			
3.2.1	Surface Contamination	D202			
3.2.2	Residual Solvent	Hughes	0.5	%	Hughes
3.2.3	Moisture Absorption, 24h	D570	<0.5	%	82MPE
3.3.1	Film Thickness	D374 (A or C)		mils	—
3.3.2	Film Density	D1505	0.907	g/cm ³	Toray
3.3.3	Tensile Strength at Break	D882(A)	26,000	psi	Toray
3.3.4	Elongation at Break	D882(A)	130	%	Toray
3.3.5	Shrinkage, M.D.	Toray	7.5	%	Toray
3.4.1	Cores	Hughes	OK	—	Hughes
3.4.2.1	Telescoping	Hughes	OK	—	Hughes
3.4.3	Width and Diameter	Hughes	OK	—	Hughes
3.4.4	Splices	Hughes	OK	—	Hughes
3.4.5	Marking	Hughes	OK	—	Hughes
3.5.1	Wrapping	Hughes	OK	—	Hughes
3.5.2	Outer Package	Hughes	OK	—	Hughes
3.5.3	General Requirement	Hughes	OK	—	Hughes

TABLE 20. PROPERTIES OF FGA FLUOROFILM-C

Paragraph	Description	Method (ASTM)	Value	Unit	Source
3.1.1.1	Dielectric Constant, 1 kHz	D150	2.0	—	DIL
3.1.1.2	Dissipation Factor, 1 kHz	D150	<0.0003	—	DIL
3.1.1.3	Surface Resistivity, 100% RH	D257	3.6×10^6	MΩ	DIL
3.1.1.4	Volume Resistivity	D257	$>10^{15}$	ohm-cm	DIL
3.1.1.5	Dielectric Strength, Air	D149, D2305	4200	V/mil	DIL
3.1.1.6	Gross Flaw	Hughes		m ⁻²	
3.1.1.7	Fine Flaw	Hughes			
3.2.1	Surface Contamination	D202			Hughes
3.2.2	Residual Solvent	Hughes	0.0	%	Hughes
3.2.3	Moisture Absorption, 24h	D470	0.00	%	DIL
3.3.1	Film Thickness	D374 (A or C)		mils	
3.3.2	Film Density	D1505	2.1 - 2.2	g/cm ³	DIL
3.3.3	Tensile Strength at Break	D882(A)	4300	psi	DIL
3.3.4	Elongation at Break	D882(A)	400	%	DIL
3.3.5	Shrinkage, M.D.	Hughes	(NEG)	%	Hughes
3.4.1	Cores	Hughes	OK	—	Hughes
3.4.2.1	Telescoping	Hughes	OK	—	Hughes
3.4.3	Width and Diameter	Hughes	OK	—	Hughes
3.4.4	Splices	Hughes	OK	—	Hughes
3.4.5	Marking	Hughes	OK	—	Hughes
3.5.1	Wrapping	Hughes	OK	—	Hughes
3.5.2	Outer Package	Hughes	OK	—	Hughes
3.5.3	General Requirement	Hughes	OK	—	Hughes

In addition to characterization tests and measurements, quality control tests were performed on the oils and are reported in Section 9.0.

7.2.1 BASF Platinol DOP

This is a plasticizer-grade dioctyl phthalate liquid supplied in 55 gallon drums. The as-received material quality has been found by Hughes to be comparable to reagent grade liquid in terms of volume resistivity and dielectric strength. Filtration methods used on this program have typically achieved water contents of 30 ppm and volume resistivities as high as 1.5×10^{12} ohm-cm.

Data on the as-received material is given in Table 21.

7.2.2 Dow Corning DC-200 Silicone

This material is frequently used in both capacitors and transformers and is well-characterized in the literature. A significant problem with polydimethyl siloxanes is its gassing tendency and decomposition products in the presence of partial discharges. Test results on the as-received material, which is electrical grade and requires minimal processing, are given in Table 22.

7.2.3 Helix FE-4 Fluoropropane Ether

This dielectric liquid was considered as a possible improvement over the 3M Fluorinert[®] fluids for the capacitor application. A significant difference between the two is the increased dielectric constant of this liquid, which is useful for achieving higher energy densities. Many of the useful physical properties of the Fluorinert liquids, such as low viscosity, low surface tension, and wide operating temperature range, are preserved in the FE-4.

Data on the material as supplied are given in Table 23.

7.3 KRAFT PAPERS

The Schweitzer Division of Kimberly-Clarke manufactured the two grades of capacitor paper used for this program. One of the grades, EIB Kraft, is no longer produced. This was a high dielectric strength paper. The other grade, Norden (normal density) Kraft, is still available. Data on this grade are given in Table 24.

TABLE 21. PROPERTIES OF BASF PLATINOL DOP

Designation	Description	Method (ASTM)	Value	Unit	Source
Q-1.1	Viscosity, 20°C	D-88	83	CSU	BASF
Q-1.2	Flash Point	D-92	78	°C	BASF
	Fire Point	D-92		°C	
Q-1.3	Pour Point	D-97	-36	°C	BASF
Q-1.4	Specific Gravity	D-153	0.982 - 0.986	gm/cm ³	BASF
Q-1.5	Weight per Gallon, 20°C		8.23	lbs	BASF
Q-1.6	Interfacial Tension	D-971	32.5	dync/cm	Hughes
Q-1.7	Color	D-1500	35	APHA	BASF
Q-1.8	Visual Examination	D-1544			
Q-2.1	Dielectric Constant	D-924	2.25		Hughes
Q-2.2	Absorption Factor	D-924	0.0014		Hughes
Q-2.3	Dielectric Breakdown Voltage	D-877 or D-1816	503	V/ml	Hughes
Q-2.4	Volume Resistivity		1.1×10^{10}	ohm-cm	Hughes
Q-2.5	Neutralization Number	D974	0.034	mg KOH/g	Hughes
Q-2.6	Water Content	D1315 or D1533	222	ppm	Hughes
Q-2.7	Inorganic Chlorides and Sulfates	D878	NFC		Hughes
Q-2.8	Oxidation Stability	D2112, D2440			
Q-2.9	Oxidation Inhibitor Content	D2668	NA		
Q-2.10	Cracking	D2300			
Q-3	Particulates	Hughes		per 100 ml	Hughes
	5-10 µ		1522		
	10-20 µ		391		
	20-50 µ		143		
	50-100 µ		52		
	100 µ		12		

AD-A151 709

ADVANCED CAPACITORS(U) HUGHES AIRCRAFT CO EL SEGUNDO CA

2/3

ELECTRO-OPTICAL AND DATA SYSTEMS GROUP

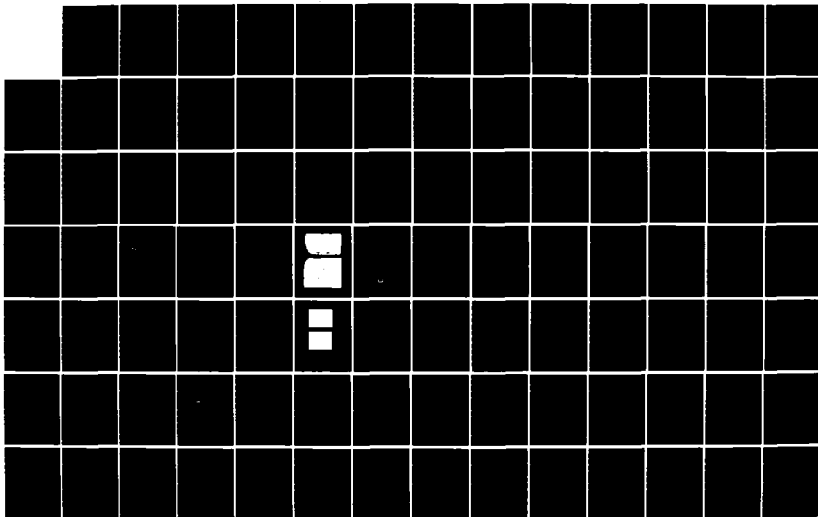
J B ENNIS ET AL. OCT 84 HAC-FR84-76-621

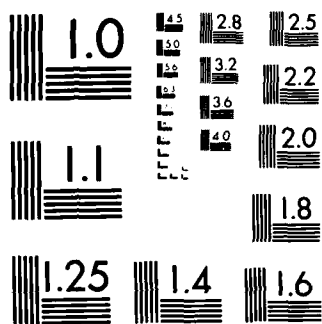
UNCLASSIFIED

AFWAL-TR-84-2058 F33615-79-C-2081

F/G 9/1

NL





MICROCOPY RESOLUTION TEST CHART
NATIONAL BUREAU OF STANDARDS-1963-A

TABLE 22. PROPERTIES OF DC-200

Paragraph	Description	Method (ASTM)	Value	Unit	Source
4.1.1	Viscosity	D-88	20.0	CST	DC
4.1.2	Flash Point	D-92	232	°C	DC
	Fire Point	D-92	DNA	°C	DC
4.1.3	Pour Point	D-97	-60	°C	DC
4.1.4	Specific Gravity	D-1898	0.955	gm/cm ³	DC
4.1.5	Weight per Gallon		8.00	lbs	DC
4.1.6	Interfacial Tension	D-971	22.3	dyne/cm	Hughes
4.1.7	Color	D-1500	1	Gardner	Hughes
4.1.8	Visual Examination	D-1524			
4.2.1	Dielectric Constant	D-924	2.72	-	DC
4.2.2	Dissipation Factor	D-924	5.4×10^{-6}	-	DC
4.2.3	Dielectric Breakdown Voltage	D-877 or D-1816	430	V/ml	Hughes
4.2.4	Volume Resistivity		1.0×10^{14}	ohm-cm	DC
4.3.1	Neutralization Number	D974	0.01	mg KOH/g	Hughes
4.3.2	Water Content	D1315 or D1533	270	ppm	LIT
4.3.3	Inorganic Chlorides and Sulfates	D878	NEG	-	Hughes
4.3.4	Oxidation Stability	D2112, D2440			
4.3.5	Oxidation Inhibitor Content	D2668	NA		
4.3.6	Gassing	D2300			
4.4	Particulates	Hughes		per 100 ml	Hughes
	5-10 μ m		714		
	10-25		415		
	25-50		90		
	50-100		43		
	>100		27		

TABLE 23. PROPERTIES OF HELIX FE-4 FLUOROPROPANE ETHER

Paragraph	Description	Method (ASTM)	Value	Unit	Source
4.1.1	Viscosity, 25°C	D-88	2.3	CST	HEL
4.1.2	Flash Point	D-92		°C	
	Fire Point	D-92	500	°C	HEL
4.1.3	Pour Point	D-97	-94.4	°C	HEL
4.1.4	Specific Gravity	D-1898	1.768	gm/cm ³	HEL
4.1.5	Weight per Gallon		11.71	lbs	HEL
4.1.6	Interfacial Tension	D-971	14.4	dyne/cm	Hughes
4.1.7	Color	D-1500	1	Gardner	Hughes
4.1.8	Visual Examination	D-1524		-	
4.2.1	Dielectric Constant	D-924	2.50	-	HEL
4.2.2	Dissipation Factor	D-924	0.00006	-	HEL
4.2.3	Dielectric Breakdown Voltage	D-1816	324	V/mil	Hughes
4.2.4	Volume Resistivity		1.1×10^{13}	ohm-cm	Hughes
4.3.1	Neutralization Number	D974	0.1	mg KOH/g	Hughes
4.3.2	Water Content	D1315 or D1533	68	ppm (wt)	HEL
4.3.3	Inorganic Chlorides and Sulfates	D878	NEG	-	Hughes
4.3.4	Oxidation Stability	D2112, D2440	NA		
4.3.5	Oxidation Inhibitor Content	D2668	NA		
4.3.6	Gassing	D2300			
4.4	Particulates	Hughes		per 100 ml	Hughes
	5-10 μ m		700		
	10-25		190		
	25-50		98		
	50-100		58		
	100		14		

TABLE 24. NORDEN KRAFT 30 GA PROPERTIES

Paragraph	Description	Method (ASTM)	Value	Unit	Source
5.1.1	Dielectric Constant	D150	2.30	—	Schweitzer
5.1.2	Dissipation Factor, 40°C	D150	<0.00175	—	Schweitzer
5.1.3	Dielectric Strength	D149	>1850	V/mil	Schweitzer
5.1.4	Conducting Paths	D202	<7.0	ft ⁻²	Schweitzer
5.1.5	Fine Flaws (Stain)	D202	<400	ft ⁻²	Schweitzer
5.2.1	Paper Thickness	D374	0.28 - 0.32	mils	Schweitzer
5.2.2	Apparent Density	D202(A)	0.95 - 1.05	g/cm ³	Schweitzer
5.2.3	Holes	D202		per 10 ft ²	
	and Felt Hair Inclusions	D202		per 10 ft ²	
5.2.4	Tensile Strength	D202, D76		psi	
	and Yield	D202, D76		psi	
5.2.5	Air Resistance	D726(C)			
5.3.1	Aqueous Extract Conductivity	D202	3.3	μS/cm	Schweitzer
5.3.2	Soluble Chlorides	D202	<4	ppm	Schweitzer
5.3.3	Acidity-Alkalinity-pH	D202, E70	6.2 - 7.4	pH	Schweitzer
5.3.4	Moisture Content	D202, D644	4.0 - 7.5	%	Schweitzer
5.4.1	Cores	Hughes	OK	—	Hughes
5.4.2	Roll Workmanship	D1930	OK	—	Hughes
5.4.3	Width	Hughes	OK	—	Hughes
5.4.4	Marking	D1930	OK	—	Hughes
5.4.5	Packaging	D1930	OK	—	Hughes

7.4 WETTING STUDY

Impregnation of a plastic film capacitor not containing Kraft paper has been found to be relatively difficult. Recent advances in this area have utilized low surface tension liquids and large space factors (low winding tension). The basic problem is to achieve wetting between the liquid and the film which physically prevents the formation of voids between liquid and solid surfaces. If this can be achieved with the proper selection of film and liquid, Kraft paper can therefore be eliminated from the dielectric. As a result, dissipation factors can be reduced by about an order of magnitude, the dielectric strength of a given total thickness of dielectric can be increased, and the distribution of stress in the dielectric can be greatly simplified. With the proper material selections, the temperature range of the dielectric can also be widened, since the limitations of Kraft paper have been removed.

The 10 kHz AC inverter capacitor development effort on this program required the elimination of Kraft paper to minimize dissipation losses and dielectric heating. For this reason, efforts were made to characterize the wetting properties of various films and dielectric liquids as part of the material selection process. In addition, a textured Ultem® film was cast by Schweitzer using a sandblasted laboratory casting drum. The wetting properties of this material were to be compared to the wetting properties of the plain film. If a textured film could be made which would have the surface properties of Kraft paper, then impregnation problems would be greatly simplified.

The first step in the analysis was the measurement of liquid-vapor surface tensions for the impregnants. These numbers provide information about the wetting properties of the liquid alone. A high-wetting liquid will have a low surface tension. Liquid-vapor surface tension (γ_{LV}) measurements were carried out using a Fischer surface tensiometer (platinum-iridium DuNouy ring) at 25°C. The experimental results ranged from 1.7 to 6.1 dynes/cm greater than values published in the literature. Eight standard test liquids and three dielectric fluids were measured. The results obtained (averages of four measurements) and published values are presented in Table 25.

TABLE 25. LIQUID-VAPOR SURFACE TENSION OF LIQUIDS (γ_{LV})

Test Liquid	Measured Surface Tension, (25°C) dyne/cm	Literature Value (20°C) dyne/cm
1. Water	75.2 \pm 0.05	72.8
2. Glycerol (99+%)	69.0 \pm 0.13	64.0
3. Formamide	61.9 \pm 0.22	58.3
4. Ethylene Glycol	50.9 \pm 0.00	48.3
5. 1-Bromonaphthalene	46.6 \pm 0.04	44.6
6. Polyglycol E200	48.9 \pm 0.00	43.5
7. Polyglycol 15-200	38.3 \pm 0.07	36.6
8. Polyol P1200	37.4 \pm 0.04	31.3
9. FE-4 Polyfluoroether	14.4 \pm 0.04	15.2
10. DC-200 Silicone	22.3 \pm 0.04	
11. Platinol DOP	32.5 \pm 0.07	

Sources of error in these measurements include tipping of the ring from its horizontal plane, size of the test vessel, liquid surface wave motion, purity of the test liquid, evaporation of the test liquid, and temperature.

The next step was to measure the contact angle between the edge of a drop of test liquid and surfaces of the films of interest. The smaller this angle is, the lower the surface free energy of the film, and the greater the surface tension of the impregnant may be and still wet the film. If wetting occurs, the contact angle is so small it is quite difficult to measure.

Advancing contact angle measurements were performed at 25°C in the environmental chamber of the NRL-goniometer (Rame-Hart, Inc., Mountain Lake, NJ) apparatus. Measurements were repeated five times using each liquid on each of the four test films. The films were:

1. 32GA Kimfone Polysulfone
2. 20GA Bollore Biaxially Oriented Polypropylene
3. 24GA Ultem Polyetherimide
4. 25GA Fluorofilm C Polytetrafluoroethylene.

Tests on the Kimfone and Ultem films were performed on the smooth side. The data are presented in Table 26.

From these data, the nominal work of adhesion, W_a , and the solid-vapor surface tension, γ_{SV} , were calculated using the following analysis.¹⁹ The work of adhesion is calculated by:

$$W_a = \gamma_{LV} \cdot (1 + \cos \theta) \quad (7-1)$$

where the measured values of γ_{LV} were used. Based on the equations

$$\gamma_{LV} = \alpha_L^2 + \beta_L^2 \quad (7-2)$$

$$\gamma_{SV} = \alpha_S^2 + \beta_S^2 \quad (7-3)$$

$$W_a = 2[\alpha_L \alpha_S + \beta_L \beta_S] \quad (7-4)$$

TABLE 26. CONTACT ANGLE (θ) MEASUREMENTS

Test Liquid	Contact Angle, degrees (25°C)			
	Kimfone	Bollore	Ultem	Fluorofilm
Water	67.5 ± 0.5	81.0 ± 0.0	70.4 ± 0.4	89.5 ± 0.5
Glycerol (99+%)	59.4 ± 0.4	77.0 ± 1.0	58.4 ± 0.4	83.5 ± 0.3
Formamide	49.6 ± 0.5	76.5 ± 0.5	52.8 ± 0.4	79.8 ± 0.4
Ethylene Glycol	48.5 ± 0.0	64.0 ± 0.0	45.4 ± 0.5	75.6 ± 0.4
1-Bromonaphthalene	<5	36.1 ± 0.5	<5	58.8 ± 0.3
Polyglycol E-200	20.7 ± 0.5	61.0 ± 0.0	27.7 ± 1.0	75.0 ± 0.5
Polyglycol 15-200	14.8 ± 0.8	39.5 ± 0.0	25.8 ± 0.8	76.3 ± 0.3
Polyol P1200	8.8 ± 0.3	18.8 ± 0.3	8.3 ± 0.3	52.8 ± 0.6
FE-4	<5	<5	<5	<5
DC-200	<5	<5	<5	37.6 ± 0.7
DOP	<5	7.7 ± 0.4	<5	58.2 ± 0.3

where α_L , β_L are the square roots of the separate dispersion and polar contributions to the liquid-vapor surface tension, and α_S , β_S are the corresponding parts of the solid-vapor surface tension, we obtain:

$$W_a/2\alpha_L = \alpha_S + \beta_S (\beta_L/\alpha_L) \quad (7-5)$$

The values of $2\alpha_L$ and β_L/α_L are taken from the literature.²⁰ The last equation is solved by least-squares fit to the points β_L/α_L , $W_a/2\alpha_L$. The values actually used and computed are listed in Table 27.

As can be seen from the contact angle measurements in Table 26, only the fluoroether was suitable for wetting the cast PTFE film, while only FE-4 or the silicone oil would wet the polypropylene. The dioctyl phthalate would wet only the polysulfone and polyetherimide films. This information was used in the selection of film-liquid combinations used in the various pad designs described in Section 8.0, and was especially important for the high frequency inverter capacitor designs.

7.5 TEXTURED FILM STUDY

The surface profile of the 32 gauge textured Ultem[®] film was measured using a profilometer and compared to profiles of 36 and 24 gauge plain Ultem film measured on the "dull" or rough side of the film. While the textured material was significantly rougher than the thicker plain film, the thinner gauge film was comparable in roughness to the textured material. This was unexpected. Samples of the profile recordings are plotted in Figure 28.

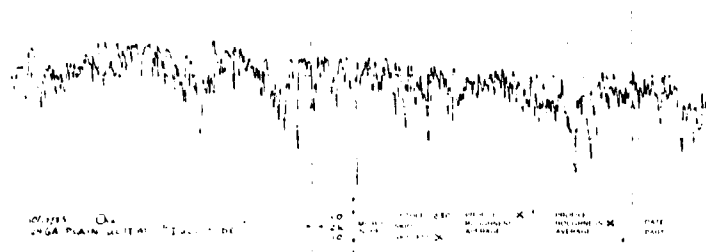
A test of wettability was conducted using windings of both the textured film and metallized 24 gauge Ultem film. For this test, the single roll of textured film was slit into two 2.0-inch wide rolls. For each material, double layers of film were tightly wound on an epoxy glass mandrel with a 1.125 inch outside diameter. Ten turns were wound, and the end taped. Each sample was vacuum impregnated with dodecyl benzene dyed with indigo after an 85°C bakeout overnight. After filling, the samples were allowed to stand overnight at one atmosphere under dry nitrogen. When the samples were

TABLE 27. SOLID-VAPOR SURFACE TENSION OF LIQUIDS (γ_{SV})

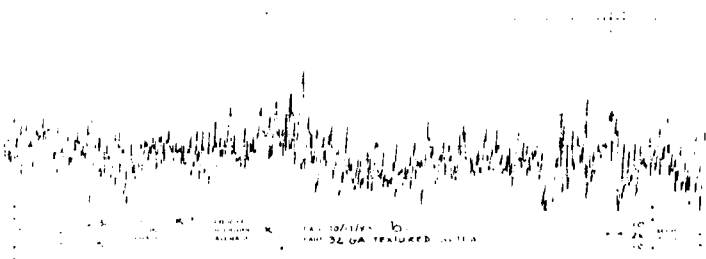
Test Liquid	$2\alpha_L$ (dyne/cm) ^{1/2}	ϵ_L/α_L	$W_a/2\alpha_L$ (dyne/cm) ^{1/2}			
			Kimfone	Bollore	Ultem	Fluorofilm
Water	9.34	1.53	11.13	9.31	10.74	8.12
Glycerol	11.66	0.94	8.92	7.27	9.01	6.59
Formamide	11.37	0.90	8.98	6.72	8.74	6.39
Ethylene Glycol	10.83	0.81	7.81	6.76	8.00	5.88
1-Bromonaphthalene	13.36	0.00	6.97	6.31	6.97	5.28
PGE 200	10.62	0.74	8.90	6.84	8.67	5.80
PG 15-200	10.20	0.64	7.38	6.65	7.13	4.63
PG P-1200	9.90	0.53	7.51	7.35	7.52	6.05
Least Squares Fit						
β_S (dyne/cm) ^{1/2}			2.824	1.753	2.612	1.927
α_S (dyne/cm) ^{1/2}			6.300	5.816	6.359	4.626
Correlation			0.9077	0.8062	0.9117	0.8064
γ_{SV} (dyne/cm)			47.7	36.9	47.3	25.1

TABLE 28. SURFACE TENSION OF SELECTED POLYMERS

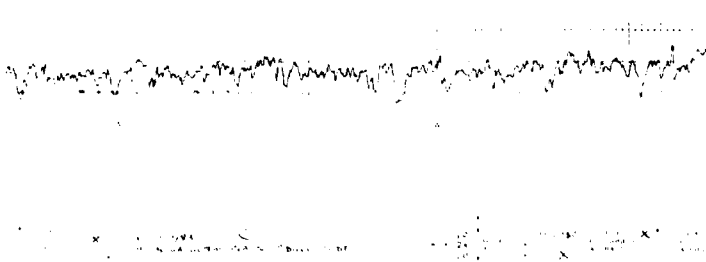
Polymer	γ_{SV} (dyne/cm)
Hexafluoropropylene	12.4
Tetrafluoroethylene	15.5
Trifluoroethylene	24.8
Vinylidene fluoride	32.3
Ethylene	32.4
Vinyl fluoride	36.6
Ethylene terephthalate	39.5
Vinyl chloride	39.6
Styrene	40.6
Vinylidene chloride	41.3
Nylon 6,6	41.3
Nylon 2	51.9



a. 24 gauge plain film.



b. 32 gauge textured film.



c. 36 gauge plain film.

Figure 28. Profilometer profile measurements of Ultem films.

unwound and examined, it was difficult to see the dye in such a thin liquid layer. By feeling the film, it seemed that both the plain and textured film windings had been wet and penetrated by the oil. It was observed that the textured side of the film felt wet, while the smooth side felt dry. This is a subjective observation and quite qualitative, but it does imply that the textured surface does wet better than the smooth surface, and the desired effect is accomplished.

Film texturing may be useful in obtaining complete impregnation of film capacitor windings which contain no paper wick. However, the interaction between film and liquid at the microscopic interface is more critical for electrical performance. Therefore it is always necessary to use a liquid which wets the film.

8.0 CAPACITOR PAD DESIGNS

During the second phase of the program, the materials and techniques developed in Phase I were applied to capacitor designs that were manufactured and then tested under electrical conditions matching those of actual service. Rather than construct large, multiple element components for this purpose, model capacitors consisting of single pads or windings were evaluated. Whenever possible, existing test fixtures were used to reduce costs.

The basic design philosophy for each of the capacitors is discussed in this section. The problems faced by the designer, as well as the solutions used are also described.

8.1 CAPACITOR PAD TEST PLAN

At the beginning of Phase II of this program, a test plan was written for the evaluation of capacitor pads of each type in life tests. This test plan is included as an Appendix. The Capacitor Pad Test Plan provided the direction for the remainder of the technical work. Its philosophy was clearly to life test each design under a single set of conditions corresponding to the operating parameters described in the Statement of Work. This approach provided a clear set of data about the usefulness of each design in an actual system.

Another approach to testing capacitor designs would have been to evaluate each over a range of conditions similar to and including those in the actual application. This approach would have provided more information about the cause of failure and the deficiencies of the design. Because of the number of different capacitor types which were to be evaluated, this more intensive research approach was not economically feasible. It was hoped that a second design iteration of each type of capacitor might be possible to build and test, but in some cases even this was not possible.

8.4 CAPACITOR SECTION SIZE

Before continuing in the dielectric design process, the selection voltage and capacitance had to be selected. This determines the series-parallel arrangement of elemental units within each capacitor package. No "floating foil" elements were to be used unless the number of series units grew very large, since better volume efficiency can be attained using individual windings in this case.

For the high repetition rate unit, the windings were originally 2.2 μF , 7.5 kV units arranged as shown in Figure 29. When the testing of these units using the available equipment was found to be impossible due to power supply limitations, the capacitance of each pad was dropped to 1.1 μF . This meant that the complete capacitor would now consist of four parallel strings, as shown in Figure 30. A total of eight pads was required. The 2.2 μF pad design was more efficient, but there are benefits from using the smaller pads in solving the problem of heat removal. Peak currents in each pad would be 5 kA instead of 10 kA.

The low repetition rate pulse capacitor had an operating voltage of 40 kV at a capacitance of 2.2 μF . In this case, the layout called for five parallel strings of five series 2.2 μF pads. A total of 40 windings would be required per capacitor. In this case, parallel floating foils might be used in a later design. For the purposes of this program, single section windings were used for testing. Each pad was to be rated at 8.0 kV. Peak current in each pad would be 10.5 kA.

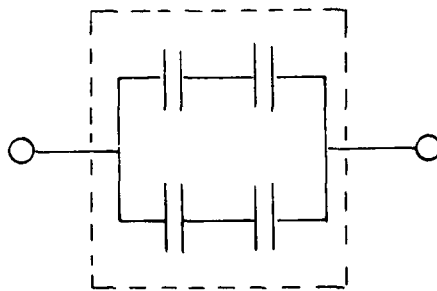


Figure 29. Original high repetition rate pulse capacitor for 2.2 μF pad arrangement.

To accomplish complete impregnation, liquids were considered which have low viscosity and low surface tension. These include the fluorocarbon liquids, such as 3 M's Fluorinert® series. In fact, another fluorocarbon, poly-1,2-epoxyhexafluoropropane ether, sold by Helix Associates, Inc., appears to have some properties superior to the Fluoroinerts for this application. A lower dissipation factor, and higher dielectric constant make these liquids more attractive, and resulted in the selection of FE-4 for use here, based on its higher boiling point than the FE-2 grade.

Silicone oil, monoisopropyl biphenyl, phenyl xylyl ethane, and branched dodecyl benzene were also considered to be possible candidates, but none had the wetting properties of the FE-4. Those properties would be especially important in the case of the Fluorofilm-C pad design, since PTFE is extremely difficult to wet.

The choice of electrode material here was more difficult because of the extremely important consideration of thermal and electrical conductivity out of the pad interior and across the termination. Extended foil was considered a must, and the problem of connecting to an aluminum foil was cause for concern. Consideration was given to the use of copper foil in 0.25 mil (6 μ m) or 0.15 mil (4 μ m) gauges available from Arnold Engineering, Marengo, Illinois. Unfortunately, costs were simply too large to justify the use of this foil. Therefore, Alloy 1145 aluminum foil was also selected for use here.

Termination was to be made using a system very similar to that developed by G.H. Mauldin at Sandia National Laboratories. A chemically etched copper grid, with a flexible strap leading to the terminal, would be made as a single piece. This would be bonded to the foil ends using Ablebond 36-2 silver loaded conductive epoxy.

4.3.4 AC Filter Capacitor

The material selections for this capacitor were as described above, polysulfone and polyetherimide metallized films with 0.040 inch margins.

Aluminum foil was selected for the electrodes, as this material has the best conductivity-to-weight ratio and is available in gauges down to 0.17 mil. The exact type used was Republic Foil (Div. of National Steel Corp.) Alloy 1145, Electro-Dry II.

8.3.2 Low Repetition Rate Pulse Capacitor

Based upon very similar considerations to those which applied to the 300 Hz component, the same material selections and basic layout were used for this component. Ultem film, EIB Kraft paper, dioctyl phthalate, and Alloy 1145 aluminum foil were selected.

8.3.3 High Frequency AC Capacitor

A careful look at the polysulfone and polyetherimide film designs proposed during Phase I for this application indicated that the predicted temperature rise was unacceptable due to the dissipation factors of these films. In order to obtain the very low losses which were required, other films had to be considered.

In the end, Dilectrix Fluorofilm-C polytetrafluoroethylene and Toray T-2400 polypropylene were selected for each of two different designs. These films were available in gauges at least as thin as 0.25 mil (6 μ m). The Fluorofilm-C is a multilaminar, solution cast (rather than skived) film, which is relatively new on the market, and is of interest due to its low dissipation factor and high temperature capability. It should be noted, however, that due to the various transitions of PTFE at temperatures below the melting point, the actual high end to the temperature range might be lower than in other applications.

The polypropylene has much less temperature range than PTFE, but it has the advantage of a higher dielectric strength across a wide portion of that range than most other materials. The DF is comparable to that of PTFEs.

No Kraft would be used in the dielectric due to its high dissipation factor. As a result, the impregnant would have to be able to penetrate the winding and wet the film surfaces without the aid of paper.

TABLE 32. COMPARISON OF POLYSULFONE AND POLYETHERIMIDE FILMS

	Filtered Resin Polysulfone	Uitem 1000 Polyetherimide
Dielectric Constant (25°C, 1 kHz)	3.07	3.17
DF		
(1 kHz, 25°C)	0.0008	0.0013
(1 MHz, 25°C)	0.0067	0.015
(1 kHz, 85°C)	0.0003	0.0009
(1 MHz, 85°C)	0.0022	0.011
Volume Resistivity 25°C	$5 \cdot 10^{16}$	$>1 \cdot 10^{16}$ ohm-cm
Breakdown Strength	7500 V/mil	-
Large Area Breakdowns		
100 V/ μ m (2540 V/mil)	180	5 m^{-2}
200 V/ μ m (5080 V/mil)	930	36 m^{-2}
Density	1.24	1.27 g/cm^3
Tensile Strength, MD	10,000	15,200 psi
Ultimate Elongation, MD	50	60%
Modulus of Elasticity, MD	360,000	430,000 psi
Melting Point	315°C	-
Maximum Operating Temp	149	176°C
Minimum Operating Temp	-50°C	-
Glass Transition Temp	190	216°C

The oil selected was dioctyl phthalate, an ester. Usually this material is combined with stabilizing additives, but pure material was used in these capacitors. The selection was based on the high permittivity of the oil, wide temperature range, and moderate breakdown strength. This oil is slightly gas absorbing. Other high permittivity oils, such as castor oil, did not have the required temperature range. Castor oil is widely used as an impregnant for pulse capacitors because of its gas absorbing nature and benign decomposition products, which result in greatly increased lifetimes as compared to mineral oil or PCB impregnants.

Without describing why all the other films were rejected, the most interesting films for this application were Kapton-H, Kimfone, Ultem 1000, and T-2400 polypropylene. DuPont has had some difficulty in the past providing consistent quality thin Kapton films, although several workers have reported successes in developing Kapton capacitors despite this. The higher dissipation factor of this film over the others was cause for rejection, because the other dielectric materials (paper, oil) would not have the Kapton's high temperature capability. Polypropylene from various manufacturers is now enjoying widespread use in pulse capacitors due to its high dielectric strength. However, it was felt that the temperature rise which would occur, on top of the ambient, was simply too much for this material. Polysulfone and polyetherimide films were able to meet the criteria for low dissipation factor, high dielectric strength, and high temperature rating. In addition, the dielectric constants of these films were moderate, so that the potential energy storage capability was higher than for the Teflons, for example.

A comparison of these two films is given in Table 32. The high end temperature limit of the Ultem is higher by 27°C, while the dissipation factor has also increased by 50%. The large area breakdown test results reported in Section 5.0 do indicate a significant improvement in the number of flaws in Ultem over filtered-resin polysulfone. It was expected that the breakdown strength of either film in oil would be much greater than these numbers would seem to indicate.

The Ultem film was selected for testing on this program as it appeared that the breakdown characteristics might have been improved and the temperature range increased. The dissipation factor, however, was a drawback, as 50 percent greater losses in the film meant a significant rise in the heat generated and the total temperature rise in the capacitor.

The remaining films were selected to increase the permittivity of the total dielectric system. The originally selected paper grade was EIB Kraft, a hard-core paper with slightly higher permittivity and higher dielectric strength than normal density paper. This paper was purchased and used on the previous AFWAL program. Later, the Norden Kraft grade was used when failure analyses on the 50 Hz pulse capacitor pointed to possible embrittlement of the paper during storage.

TABLE 30. POLYMER FILMS CONSIDERED

Liquid	Dielectric Constant (25°C, 1 kHz)	Volume Resistivity (ohm-cm)	Breakdown Strength (V/mil)	Melting Point (°C)	Glass Transition (°C)	Surface Tension (dyne/cm)	Density (g/cm ³)
Carbon - EP	10.7	0.0159	4100	180	-40	21-28	1.125
Carbon - G	3.5	0.0015	7000	None	360-410	25.0	1.125
Nylar - G	3.25	0.0050	7500	250	67-125	20	1.02
Ketone	3.0	0.0008	7500	315	100	10.3	0.8
Ultem 1000	3.0	0.0013	6.10 ¹⁵	-	216	15.2	-
Mylarol ES	2.8	0.0008	1.10 ¹⁵	270	147	32-41	1.02
100-00	2.2	0.0002	8.10 ¹⁸	176	-	26	0.98
Teflon TFE	2.1	0.0001	10 ¹⁵	327	127	21.5-6.0	1.125
Fluoroteflon	2.0	0.0001	10 ¹⁵	327	127	4.5	1.125
Teflon FEP	2.0	0.0001	10 ¹⁶	275	-	27-41	1.125

TABLE 31. DIELECTRIC LIQUIDS CONSIDERED

Liquid	Dielectric Constant (25°C, 1 kHz)	Dissipation Factor (25°C, 1 kHz)	Volume Resistivity (ohm-cm)	Breakdown Strength (V/mil)	Pour Point (°C)	Boiling Point (°C)	Viscosity (25°C), cSt	Surface Tension (dyne/cm)	Density (g/cm ³)
Cyanomethyl Sucrose	25.0	10 ⁻¹	1 · 10 ¹²	200	+30	-	10	-	1.25
Diethyl malonate	5.25	10 ⁻³	1 · 10 ¹³	400	-46	230	83	-	0.96
Caster oil	4.7	-	2 · 10 ¹⁴	350	-	-	-	-	0.96
Monoisobutyl Biphennyl	2.83	-	-	600	-55	295	30	-	0.79
Fluoroether FE-2	2.75	10 ⁻⁵	4 · 10 ¹⁴	340	-123	104	0.6	15.9	1.66
DC-100 Silicone	2.71	10 ⁻⁶	1 · 10 ¹⁶	430	-60	-	20	-	0.96
Phenyl Xylyl Ethane	2.7	10 ⁻⁴	1 · 10 ¹⁶	-	-50	260	10	-	0.88
Fluoroether FE-4	2.50	10 ⁻⁵	4 · 10 ¹⁴	450	-94	194	2.4	15.2	1.76
Branched Dodecyl Benzene	2.28	10 ⁻⁶	1 · 10 ¹⁶	420	-72	277	6.6	-	-
Mineral oil	2.25	10 ⁻⁵	5 · 10 ¹⁵	400	-45	-	16-21	-	0.85
Fluoroether FC-40	1.80	10 ⁻⁴	4 · 10 ¹⁵	400	-57	153	3.4	24.0	1.25
Fluoroether FC-70	1.80	10 ⁻⁴	2 · 10 ¹⁵	400	-110	97	0.5	5.0	1.25

8.3 MATERIAL SELECTION

Probably the single most important step in the capacitor design process is the selection of materials for the particular application. When the energy density, power density, and/or temperature range are being pushed beyond the state-of-the-art, this must be done with extreme care. As we have seen, all of these stresses were being increased on this program.

Part of the material selection process was carried out early in the program, with the selection of polysulfone film for improvement efforts. Later, when polyetherimide was selected as an alternative to polysulfone, its evaluation became the aim of the program. In one case, the inverter capacitor, neither film was really suitable due to high loss factors, and in this case alternative materials had to be considered during Phase II. In addition, the results of failure analyses of failed capacitors later in the program resulted in other changes to the designs presented in Section 6.0.

The selection of the film materials used on the various capacitors was made from the list shown in Table 30. All of these films are available in gauges at least as thin as 0.50 mil (12 μ m).

Kraft paper was selected from the capacitor grades (Loden, Norden, and ElB), manufactured by Schweitzer in the United States. None of the denser grades manufactured in Europe or Japan were considered.

Dielectric liquids were selected from the list given in Table 31, although other materials were suggested in the first phase of the program as being of possible interest. Most of these materials have been used in capacitors with success in various applications, and are well characterized.

8.3.1 High Repetition Rate Pulse Capacitor

The basic design concept for this capacitor was film/paper/oil/foil. Although it can be argued that an extended foil termination system should have been used, inserted tabs in pressure contact were used to make connection to the foils. This would permit a direct comparison with designs built on the previous AFWAL contract, and would reduce the total weight and volume of these units.

For the purposes of this development effort, a direct comparison between the polysulfone and the new polyetherimide films was to be made. Attention was focused on the pads themselves. It was decided to have one of the original vendors of the capacitor wind both polysulfone and polyetherimide pads and apply the flame sprayed termination, so that these processes were similar to those in the original design.

The failure mechanisms seen in the previous parts were extensive "clearing" at the metallization edge, resulting in low insulation resistance or catastrophic shorting, and similar "clearing" in the bulk of the winding, resulting in reduced insulation resistance below the specified value. Clearing refers to the process of localized electrical breakdown of the film, and the subsequent self-healing process whereby the metallization vaporizes due to high current density in the region of the short. If incomplete clearing occurs, there will be surface discharges and leakage causing localized heating and further damage, and the damaged area will spread in area simultaneously, melting adjacent layers of film.

Several causes may contribute to this process. The electrode resistivity has been found to be a major factor, as this will determine the area of metallization which is removed by a given amount of energy passing through the breakdown arc. The oxygen content of the insulation material and the ratio of carbon to hydrogen atoms has been found to influence the self-healing property. The applied voltage and the pressure between film layers are also important.

It has been found that an electrode resistivity of 3-4 ohms per square is preferable for the self-healing effect, but that capacitance loss due to aluminum corrosion may become critical at this point. High oxygen content and a low C/H ratio are desirable, as this will reduce the tendency to form elemental carbon in an arc, which would cause a short.

The principal problem with this application has been the high ambient temperature, which significantly reduces the breakdown strength of the film. The current carried per pad is small, and the losses also relatively small, being about 0.1 watt for a dissipation factor of 0.001. The 400 Hz frequency does not pose much of a problem either.

TABLE 29. POWER DISSIPATED VERSUS DF

Dissipation Factor	Power Dissipated
0.0001	56.5 W
0.0002	113.0 W
0.0008	451.8 W
0.0012	677.7 W

difficult. It is, in fact, impossible to achieve using the polysulfone or polyetherimide films originally considered. The best values obtainable in those materials are 0.0008 and 0.0012, respectively. This corresponds to 251 W/lb for polysulfone and 376 W/lb for polyetherimide.

As a result of the high current, the conductors in this capacitor must be robust, and the electrodes and their terminations very conductive. Thermal conductivity is important as well, as the electrical conductors provide the lowest thermal impedance path out of the capacitor interior. A thermally conductive impregnant may help to carry off some of the heat, or at least to distribute it within the winding.

8.2.5 AC Filter Capacitor

The high ambient temperature extreme of 125°C for this application is really the major constraint in selecting materials. The original design for this component used 0.25 mil (6 μ m) polysulfone film, metallized. Forty-two pads in parallel made up the total 120 μ F capacitance; each pad was 2.86 μ F, between 0.60-0.65 inches in diameter and approximately 1.2 inches long. The stress in the film was about 825 V/mil.

Termination was made by flame spraying the ends of the capacitor and soldering a tinned copper strap across each end. The capacitors were not impregnated, but the total unit was potted in a flexible material and the case hermetically sealed.

or difficult to handle. As this unit stores 125 Joules at a goal energy density of 100 J/lb, this heat is distributed through about 1.25 pounds of capacitor. The equilibrium temperature rise will depend upon the case surface area and the surrounding medium and its ambient temperature. If a typical ambient range of -65° to $+85^{\circ}\text{C}$ is assumed, the expected temperature rise will not be as critical as the upper ambient extreme will be for the capacitor life.

The dissipation factor requirement is not difficult to meet. However, the achievement of energy density goals was considered of primary importance in the selection of materials.

For the purposes of testing, a period of 1000 hours was selected. Longer lifetimes are preferred, of course, but may be difficult to achieve at this energy density in the near future.

8.2.4 High Frequency AC Capacitor

The inverter capacitor actually stores and transfers the greatest amount of energy of any of the components considered on this program, and it does this continuously -- not in bursts. At an RMS voltage of 1060V, the 8 μF capacitor will see an RMS current of 532.8 amps. The reactive power in this capacitor is therefore a tremendous $5.65 \cdot 10^5$ VAR. It is quite obvious that an extremely low dissipation factor will be necessary for such a component to work. At an energy density of 50 J/lb, this component would weigh 0.18 pounds. This is not a feasible energy density for a self-contained component of this type using any conceivable construction. For purposes of calculating the equilibrium temperature rise, a packaged energy density of 5 J/lb was assumed, giving the component a weight of 1.8 pounds. These numbers are based upon the assumption that a cooling air flow is available for heat removal from the capacitor. If this is not feasible, and heat transfer must be accomplished in still air by convection, the capacitor size will largely be dictated by the surface area required to cool the capacitor in this manner. It can be seen from Table 29 that the heat generated in a 1.8 pound capacitor with an effective DF of 0.0001 amounts to about 31.4 W/lb. Achieving this DF will be

8.2.3 DC Filter Capacitor

This application is the most benign of the four high voltage components because it does not involve the transfer of large amounts of energy during normal operation. The energy density goal is reasonable and can be attained, although without real improvement in the materials, the gains are achieved by trading lifetime for electrical stress.

Capacitors of this generic type and rating are commercially available which have energy densities of about 30 J/lb, lifetimes of 50,000 hours (90% survival point) at 50°C, and dielectrics consisting of paper and polypropylene impregnated with dioctyl phthalate. If the acceptable life can be reduced to 10,000 hours, the energy density of such a capacitor can be substantially improved, depending on the exponent of the life/stress equation for the particular dielectric.

The life limiting factor in such capacitors is the DC stress, coupled with the localized heating of the dielectric by the ripple signal. Visible damage due to corona is not expected here, unlike the pulse capacitors. Failures will occur at dielectric flaws, wrinkles, or locations where mechanical stressing of the dielectric has occurred. This component is probably the best test of the plastic film in the dielectric, since this material has the highest resistivity and therefore carries the major portion of the electric field in the DC or static field case.

The specifications given in the Statement of Work for this capacitor are not self-consistent. The ripple current at 21V RMS will be 1.06A, and not 5.3A. To get 5.3A, the ripple voltage would be 105V. We will consider both situations here; the capacitor was designed to handle the higher voltage and current, but was actually tested at the lower values, per the approved test plan.

The heat generated by the AC signal is

$$P = I_{\text{RMS}}^2 \cdot \text{ESR} \quad (8-4)$$

and for the specified dissipation factor of 0.002, the ESR is 0.0398 ohm. At 5.3A RMS, the power dissipated is 1.12 watts, which is certainly not very large

8.2.2 Low Repetition Rate Pulse Capacitor

The energy density goal for this capacitor, namely 500 J/lb, is actually beyond the ultimate energy density of many of the plastic films considered for use in its dielectric. In other words, under ideal conditions, these materials do not have the capacity to store this density of electromagnetic energy for as long as one minute. Although the so-called "intrinsic" dielectric strengths of these polymers are much greater, so far this has little practical value in achieving the goal in a packaged, mil-spec capacitor capable of storing hundreds of Joules.

To increase the energy density of the capacitor, a greater electric field and greater permittivity dielectric must be used. The same life/stress law rules here as in the high repetition rate pulse capacitor, and again, an exponential decrease in life results from the increased stress, unless the breakdown characteristics of the dielectric have been substantially improved.

The lifetime goal of 10^6 shots is normally not a problem, but when the energy density in the dielectric is pushed too far, the lifetime will be reduced. Further reduction in life will result because the heat generated per unit mass will be correspondingly increased, accelerating chemical degradation.

The total energy stored and discharged during the one minute burst period is $5.3 \cdot 10^6$ Joules. If we model the current pulses similar to the model used above, except making the peak current 52,600 amps, the RMS current is 832 amps, which is greater than the current in the high repetition rate component. The dissipation factor will be approximately the same, and the total heat generated is therefore 15% greater. If the energy density goal of 500 J/lb was attained, 227 watts per pound of capacitor would be dissipated, and a temperature rise of 30°C expected.

The considerations indicate the desirability of using lower loss materials and achieving very low values of ESR in these PFN capacitors to minimize the temperature rise. In any case, the use of moderate to high temperature materials is necessary to accommodate the combined temperature rise and ambient temperature extreme. The conductors and terminal must obviously be robust enough to handle the high peak currents.

Assuming an energy density of 200 J/lb, this equates to 348 watts per pound of capacitor. A temperature rise of 40°C is quite likely under these conditions, since the capacitor can be assumed to heat adiabatically during the burst. Combine this with the upper ambient temperature limit of 72°C, and it is quite obvious that a dielectric temperature rating of 170°C would not be too conservative.

Reducing the dissipation factor and the equivalent series resistance is a considerable problem. A large part of the losses are in the dielectric itself, but some losses do occur in the foil electrodes and terminations. Removal of the heat from the pad interior is basically limited by the electrode thermal conductivity, thickness, and width as well as the thermal conductivity of the terminations and conductors and the temperature of the capacitor terminal and case. Unless quite substantial cooling is provided, the capacitor behaves adiabatically, and essentially no heat is removed from the dielectric during the burst.

The energy density goal is as much as 100% greater than could possibly be attained in this type of capacitor at the start of the program. It is going to be quite difficult to meet this goal without addressing a range of failure mechanisms simultaneously. This program addressed the problem of material defects such as inclusions and contaminants but this did not succeed in improving the breakdown characteristics of polysulfone film. The polyetherimide film has slightly better breakdown characteristics and an increased temperature capability (up to 176°C from 149°C) than the polysulfone, but a substantially greater dissipation factor.

The designs developed were attempts to achieve large energy density by simultaneously increasing the permittivity and the electric field in the dielectric relative to the previous design. It should be realized that the greater electric stress on the capacitor insulation system substantially reduces its operating life. Because of the exponential relationship between life and stress, the lifetime obtained was considerably smaller than the program goal, despite only a small increase in energy density relative to the stated goals.

8.2 DESIGN CONSIDERATIONS

Each of the five capacitor applications which were considered on this program is really a unique design problem. In this section, we will examine each application and identify the crucial considerations from the component design standpoint.

8.2.1 High Repetition Rate Pulse Capacitor

During its 1 minute long operating period, this capacitor transfers a large amount of energy to the PFN inductor and the load. During this burst, a total of $4.5 \cdot 10^6$ Joules (or watt-seconds) is stored and discharged. Because of the very high peak currents, the losses and resulting temperature rise will be quite large. If we model the individual capacitor current pulses in the PFN as having a peak value of 20,000 amps, a pulsewidth of 5 μ sec, repetition rate of 300 pps, and their shape half-sinusoidal, the RMS current is

$$I_{\text{RMS}} = I_p \left(\frac{\tau}{2T} \right)^{1/2} \quad (8-1)$$

$$= 20,000 (5 \cdot 10^{-6} \times 300/2)^{1/2}$$

$$= 548 \text{ A RMS}$$

The energy dissipated in the capacitor, assuming a typical value of dissipation factor of 0.002 across the frequency spectrum is,

$$P = (I_{\text{RMS}})^2 \cdot \text{ESR} \quad (8-2)$$

where ESR is the equivalent series resistance and $\text{DF} = \text{ESR} / \frac{1}{\omega C}$.
Then

$$P = (I_{\text{RMS}})^2 \cdot \text{DF} / \omega C \quad (8-3)$$

$$= 435 \text{ watts}$$

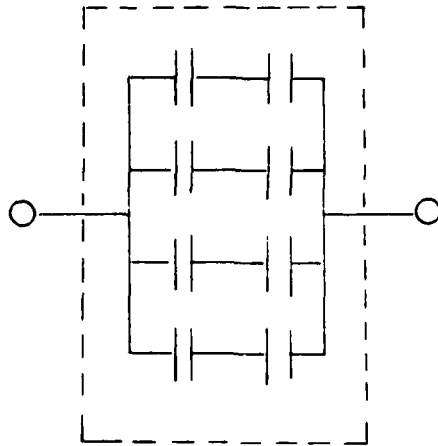


Figure 30. High repetition rate pulse capacitor 1.1 μF pad arrangement.

The DC filter capacitor layout called for three 1.2 μF , 8.3 kV sections in series, to obtain the 0.4 μF , 25 kV total capacitor. The worst case ripple voltage would be 35 V RMS on each pad, assuming equal capacitances.

The high frequency AC capacitors had a number of different arrangements of parallel windings at various phases of the design. The original designs were for 4 μF and 2 μF pads, while later a 1 μF design was considered. In the end, a 2 μF unit, rated at the full 1060 V RMS, was selected which would be used in a four-parallel pad layout to obtain the full 8 μF capacitance. Each pad would carry 133 amps.

In the case of the AC filter capacitor, the original design consisted of 42 parallel 2.85 μF pads. The pads tested were 3.00 μF , and 40 would have been used to obtain the full 120 μF capacitance required. Each pad would carry 0.88 amps and see the full 140 V RMS.

8.5 DIELECTRIC DESIGNS

Once the section parameters were defined and the dielectric materials selected, the next step was to choose gauges of the solid materials and their arrangement in each multilayer dielectric. The thicknesses of each material were limited to those normally available, and the total number of layers in the dielectric stack was restrained to five by the available winding equipment. (There is not expected to be any benefit from using more than five layers.)

The design process is really a matter of predicting what configuration will achieve the energy density and life requirement. In dealing with the new polyetherimide film, without prior experience in its life/stress characteristics, it was assumed that these characteristics would be similar to that observed in paper/polysulfone capacitors tested on the previous AFWAL program. In fact, it was not possible, making this assumption, to achieve both the energy density and life goals on the pulse capacitors. An increase in energy density was designed in, with the hope that the breakdown characteristics observed at the end of Phase I would translate to the same or longer life than had been achieved at lower stresses.

The design process involves calculation of the total dielectric thickness the effective permittivity, and the stress in each layer under transient and/or steady state conditions. Detailed analysis of the effective dissipation factor and density per unit area may also be carried out. A basic design is considered, analyzed, and then refined to achieve the required parameters.

The model used during Phase II of the program considered the layers of paper impregnated with oil to have properties dependent on both the paper and the oil. The total dielectric would consist of discrete layers of film, oil, and this "paper-plus-oil" (when used). The dielectric constant of the "paper-plus-oil," when not measured experimentally, was calculated based upon a series model with thicknesses translated from the apparent density of the paper and the actual density of cellulose.

The space factor in the paper, s , is calculated from the apparent paper density, d_p , and the actual density of cellulose, d_c , which is 1.55 gm/cm^3 :

$$s = \frac{d_p}{d_c} = \frac{d_p}{1.55} \quad (8-5)$$

The space factor is used to calculate the relative thickness of layers of oil and cellulose in a series model of the impregnated paper.

$$t_c = s t_p \quad (8-6)$$

The relative volumes of pure cellulose and oil are then defined, and the dielectric constant of the "paper-plus-oil" calculated using a simple series model:

$$\epsilon_p = \frac{\epsilon_c \epsilon_f \tau_p}{\epsilon_c \tau_f + \epsilon_f \tau_c} \quad (8-7)$$

where the subscripts c, f, and p refer to cellulose, fluid, and the paper system. This model agrees well with measurements made with impregnants having $2.0 < \epsilon_f < 8.0$. The dielectric constant of cellulose is between 6.0 and 6.3, and τ_p is between 0.95 and 1.05 for the papers used on this program.

The stress in this paper-oil system can be calculated and compared to the estimated breakdown strength. The breakdown stress, E_B , for Norden Kraft paper was assumed to obey the equations:

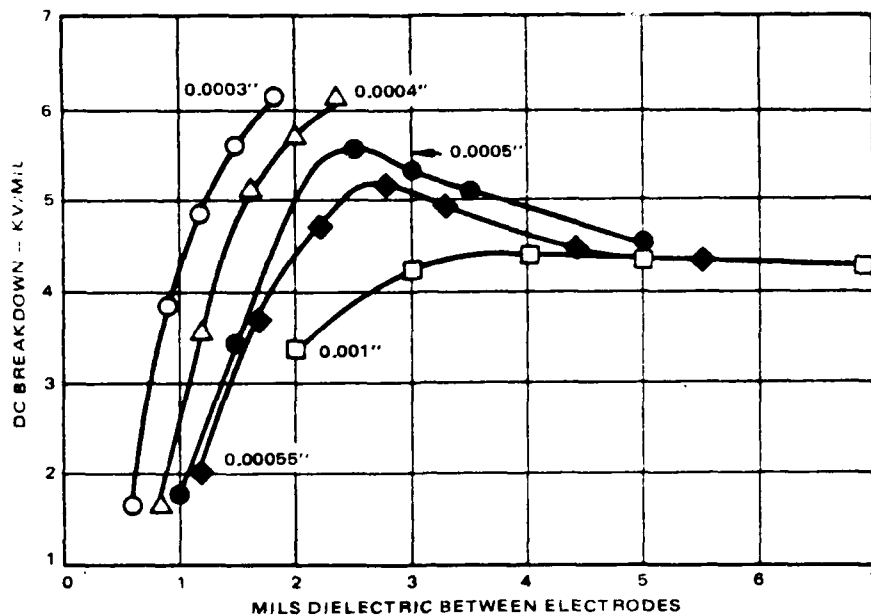
$$\begin{aligned} E_B &= 908 \tau_p^{-0.59} \quad (\text{air}) \\ &= 6048 (n-1.5)^{0.30} \tau_p^{-0.50} \quad (\text{oil}) \end{aligned} \quad (8-8)$$

while the Loden Kraft was assumed to obey:

$$\begin{aligned} E_B &= 757 \tau_p^{-0.63} \quad (\text{air}) \\ &= 4838 (n-1.5)^{0.30} \tau_p^{-0.50} \quad (\text{oil}) \end{aligned} \quad (8-9)$$

where n and τ_p are the number of layers and the total thickness of paper. Similar behavior is illustrated in Figure 31.

In the case of polymer film breakdown strength, a much smaller effect due to the number of layers is expected because of the relative absence of flaws and impurities relative to paper. There is essentially no difference

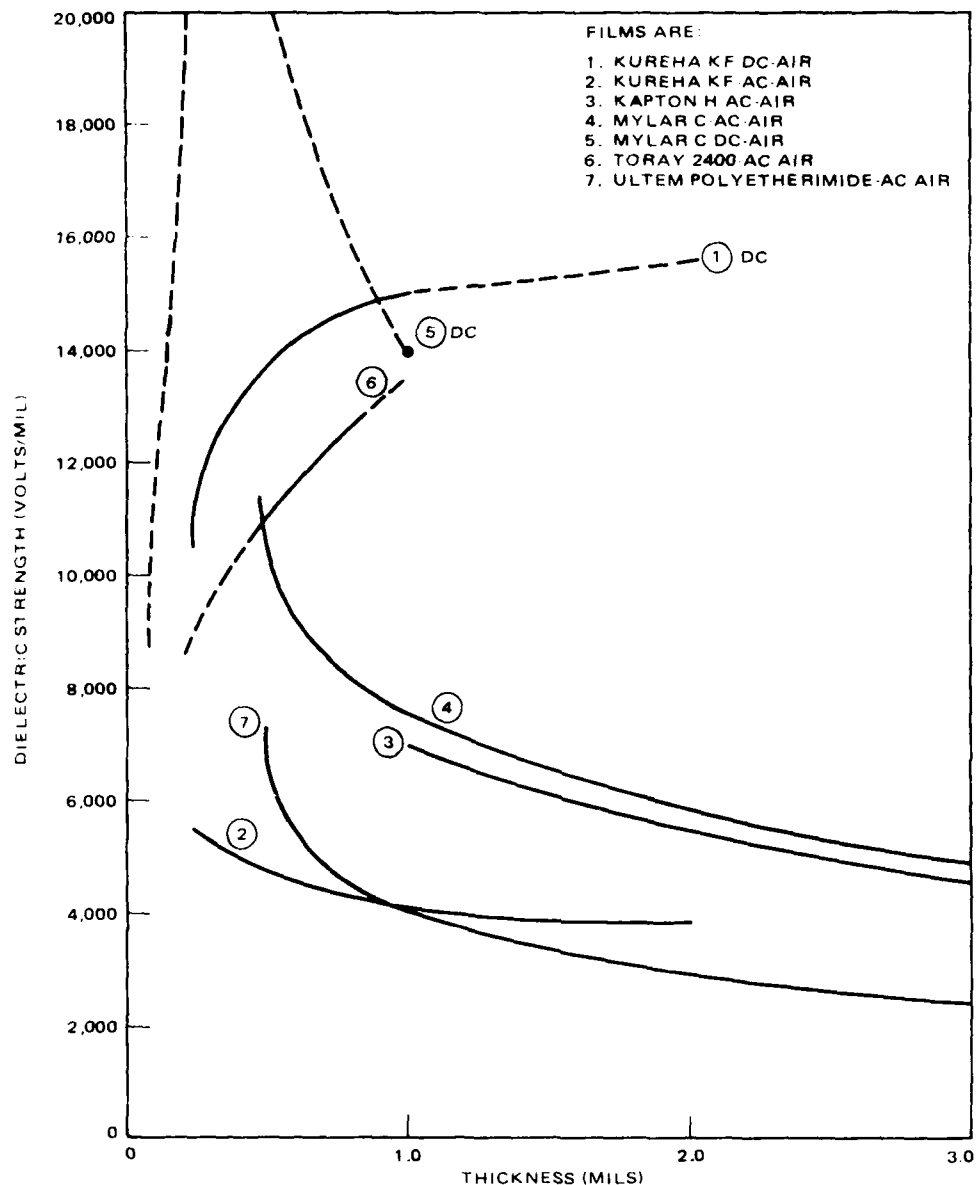


REFERENCE: R. J. HOPKINS, ET AL. "DEVELOPMENT OF CORONA MEASUREMENTS AND THEIR RELATION TO THE DIELECTRIC STRENGTH OF CAPACITORS." AIEE TRANS. VOL 70, PART II, 1951, pp. 1643-1651.

Figure 31. Average direct voltage breakdown strength for typical capacitor dielectric pads built up with five different capacitor paper thicknesses showing effects of varying number of paper sheets between electrodes.

between the small area breakdown strength of one layer of film or two layers of film having the same total thickness. In larger area, of course, multiple layers are preferable because there is a nonzero surface density of flaws such as pinholes in the film. Due to geometric effects, the dielectric strength of two layers of a given film is lower than one layer of that film of the same individual gauge, but differences between gauges may be substantial. Variation of dielectric strength with film thickness for several materials is illustrated in Figure 32, showing the wide differences in behavior between films and due to different stress conditions acting on the same film.

The dielectric strength of oils in very thin layers is substantially higher than that indicated by the standard ASTM test, performed with a 100 mil gap spacing. In the presence of cellulose fibers from the paper, however, this "ideal" value is far greater than the actual value in the capacitor dielectric. This is especially true in the case where there is a substantial amount of water dissolved in the oil.



REFERENCES:

- KUREHA: KUREHA KF FILM -- APPLICATION TO CAPACITORS, KUREHA CHEM IND CO, LTD., PUB 72-6 2000S, TOKYO, JAPAN.
- KAPTON: "KAPTON PROPERTIES," DUPONT PUBLICATION E 42727, DUPONT DE NEMOURS, INC., POLYMER PRODUCTS DEPT., JUNE 1981.
- MYLAR: 4 G. H. MAULDIN, "THE HIGH ENERGY DENSITY CAPACITOR PROGRAM AT SAUDIA NATIONAL LABORATORIES," NAS CONF ON ELECT. INSUL. AND DIEL. PHENOM., 1980.
5 EXTRAPOLATED FROM: SPECIFICATIONS FOR TYPE C MYLAR POLYESTER FILM FOR USE AS A CAPACITOR DIELECTRIC, DUPONT FILM DEPT., PUB NO. A-86586, p. 4, USING 14,000 V/MIL DC DIELECTRIC STRENGTH FIGURE GIVEN IN DUPONT BULLETIN M 4D FOR 1 MIL FILM.
- TORAY: 6 "TORAY TORAY FANT 2400 INFORMATION," TORAY IND., INC., TOKYO, JAPAN.
- ULTEM: 7 "AN INTRODUCTION TO MATERIAL PROPERTIES AND PROCESSING: ULTEM POLYETHERIMIDE RESIN" GENERAL ELECTRIC COMPANY PUB. ULT-301A.

Figure 32. The dielectric strength of several films versus thickness.

The effective dielectric constant of a design, ϵ_{eff} , was calculated using the series model and the model of paper presented above. The thickness of oil layers depended upon the design and winding tension used.

$$\epsilon_{\text{eff}} = \frac{\epsilon_1 \epsilon_2 \epsilon_3 (\tau_1 + \tau_2 + \tau_3)}{\epsilon_2 \epsilon_3 \tau_1 + \epsilon_1 \epsilon_3 \tau_2 + \epsilon_1 \epsilon_2 \tau_3} \quad (8-10)$$

The stress in each material was calculated using equations 2-5 and 2-6. The dissipation factor of the total dielectric was calculated by ignoring interfacial effects and using the series model.

$$(\text{DF})_{\text{eff}} = \frac{\epsilon_2 \epsilon_3 (\text{DF})_1 \tau_1 + \epsilon_1 \epsilon_3 (\text{DF})_2 \tau_2 + \epsilon_1 \epsilon_2 (\text{DF})_3 \tau_3}{\epsilon_2 \epsilon_3 \tau_1 + \epsilon_1 \epsilon_3 \tau_2 + \epsilon_1 \epsilon_2 \tau_3} \quad (8-11)$$

The designs for each capacitor application are summarized in the following paragraphs.

8.5.1 High Repetition Rate Pulse Capacitor

The "time-on" DC charge of this capacitor is sufficiently short that, in the steady state condition in which the film carries most of the voltage stress, the film can be pushed to very low strength/stress ratios. During the actual transient discharge, the distribution of fields in the materials should be nearly proportional to their dielectric strengths. In addition, it is desirable to maximize the permittivity of the dielectric system in order to increase the energy density for a given dielectric thickness.

Table 33 summarizes the parameters of the various designs proposed for this capacitor. All were film/paper/oil. Estimated packaged energy densities are included in this table. Design 864047 was a three-film-layer, two-paper-layer design which had film/foil interfaces, while the other designs all had paper/foil interfaces. This might affect the resistance to partial discharges.

8.5.2 Low Repetition Rate Pulse Capacitor

The dielectric designs for this capacitor are summarized in Table 34. The design considerations for this dielectric are very similar to those in the

TABLE VI. HIGH REPELL ION RATE PULSED CAPACITOR DIELECTRIC SYSTEMS

Calculated Parameters	Phase I		Phase II		Phase III		Units
	Preliminary Design	Final Design	Option A	Option B	Option C		
	864041	864045	864046	864047			
Capacitance	2.2	2.2	1.1	1.1	1.1	1.1	μF
Film	Poly sulfone	Polyetherimide	Polyetherimide	Polyetherimide	Polyetherimide	Polyetherimide	
Gauge x Layers	24 x 2	24 x 2	24 x 2	30 x 2	24 x 3	24 x 3	0.01 mils
Paper	Norden	Flb	Norden	Norden	Norden	Norden	
Gauge x Layers	30 x 3	40 x 3	40 x 3	30 x 3	40 x 2	40 x 2	0.01 mils
Oil	DOP	DOP	DOP	DOP	DOP	DOP	
Foil Gauge	25	25	25	25	25	25	0.01 mils
Dielectric Thickness	1.53	1.83	1.83	1.77	1.67	1.67	mils
Permittivity	4.53	4.76	4.76	4.20	4.13	4.13	
Dissipation Factor	0.0016	0.0018	0.0018	0.0016	0.0016	0.0016	ohm-cm ²
Insulation Resistance	6.1012	6.1012	6.1012	9.1012	9.1012	9.1012	gm/cm ²
Surface Density	1.28	1.31	1.31	1.29	1.28	1.28	
Film Stress							
-AC	7.28	11273	11273	5607	5844	5844	V/mil
-DC	15625	15625	15625	10417	10417	10417	V/mil
Paper Stress							
-AC	3774	6077	6077	3023	3151	3151	V/mil
-DC	0	0	0	0	0	0	V/mil
Oil Stress							
-AC	4227	6807	6807	3386	3529	3529	V/mil
-DC	0	0	0	0	0	0	V/mil
Average Stress	4902	4098	4098	4237	4491	4491	V/mil
Est. Energy Density	129	94.2	94.2	89.9	99.3	99.3	J/lb

TABLE 34. LOW REPETITION RATE PULSE CAPACITOR DIELECTRIC SYSTEMS

Calculated Parameters	Phase I Preliminary Design	Phase I Final Design 864042	Units
Capacitance	2.2	2.2	μF
Film	Polysulfone	Polyetherimide	
Gauges x Layers	24 x 2	24 x 2	0.1 mil
Paper	Norden	EIB	
Gauge x Layers	30 x 1 40 x 2	40 x 3	0.01 mil 0.01 mil
Oil	DOP	DOP	
Foil Gauge	25	25	0.1 mil
Dielectric Thickness	1.73	1.83	mil
Permittivity	4.65	4.76	
Dissipation Factor	0.0018	0.0018	
Insulation Resistance	$6 \cdot 10^{12}$	$6 \cdot 10^{12}$	ohm-cm^2
Surface Density	1.30	1.30	gm/cm^2
Film Stress			
-AC	6784	6571	V/mil
-DC	16667	16667	V/mil
Paper Stress			
-AC	3657	3542	V/mil
-DC	0	0	V/mil
Oil Stress			
-AC	4096	3968	V/mil
-DC	0	0	V/mil
Average Stress	4624	4372	V/mil
Est. Energy Density	128	114	J/lb

above case, which accounts for the fact that the designs used here are basically the same as those given previously. If anything were to be different, a greater thickness of film would allow for the longer time on dc charge which this capacitor experiences due to the lower repetition rate.

8.5.3 DC Filter Capacitor

In this application, the major part of the stress appears across the film, since this material has a much larger volume resistivity than the other materials. The high frequency ripple, as a voltage stress, is very small, and can be neglected. The importance of this ripple, however, is in its heating effect. For these reasons, it is preferable to reduce the amount of paper in the dielectric to a minimum and maximize the amount of film.

While PVDF was considered for this capacitor during Phase I, several arguments against it resulted in its elimination from the selection process early in Phase II. The change in permittivity at low temperatures and the very high dissipation factor were unacceptable.

Three different polyetherimide film, paper, and dioctyl phthalate designs were proposed during Phase II (see Table 35). The third design, 864051, was only arrived at after attempts to wind the 864048 design failed, due to imperfect roll formation in the 36 gauge film. The 864048 design would have been preferred, as the stress in the film was greatly reduced. Lifetime had to suffer due to this change in the design.

Several of these designs utilize three film layers and two paper layers interleaved to eliminate film-film interfaces. This helped to achieve a high film/paper thickness ratio. The DC field distributions in the latter two designs are far better than the 864043 design for this reason.

Energy densities in complete capacitors were estimated to be greater than 100 J/lb in all cases.

8.5.4 High Frequency AC Capacitor

When the original calculations for the power loss in the polysulfone design were checked during Phase II, it was felt that the polysulfone and polyetherimide could be bettered in this application. Subsequently, polypropylene

TABLE 35. DC FILTER CAPACITOR DIELECTRIC SYSTEMS

Calculated Parameters	Phase I Preliminary Design	Phase I Final Design 864043	Phase II Option A 864048	Phase II Option B 864051	Units
Capacitance	1.20	1.20	1.20	1.20	μF
Film	PVDF	Polyetherimide	Polyetherimide	Polyetherimide	
Gauge x Layers	35 x 3	24 x 2	36 x 3	24 x 2 36 x 1	0.01 mil 0.01 mil
Paper	Norden	EIB	Norden	Norden	
Gauge x Layers	30 x 2	40 x 3	30 x 2	30 x 2	0.01 mil
Oil	DOP	DOP	DOP	DOP	
Foil Gauge	25	25	25	25	0.01 mil
Dielectric Thickness	1.80	1.83	1.83	1.59	mil
Permittivity	7.81	4.76	3.88	4.02	
Dissipation Factor	0.0008	0.0018	0.0017	0.0018	
Insulation Resistance	$3 \cdot 10^{12}$	$6 \cdot 10^{12}$	$1.4 \cdot 10^{13}$	$1.1 \cdot 10^{13}$	ohm-cm ²
Surface Density	1.58	1.30	1.27	1.27	g/cm ²
Film Stress					
-AC	3441	6845	5577	6645	V/mil
-DC	7936	17360	7716	9920	V/mil
Paper Stress					
-AC	6145	3689	3007	3582	V/mil
-DC	0	0	0	0	V/mil
Oil Stress					
-AC	6883	4133	3368	4012	V/mil
-DC	0	0	0	0	V/mil
Average Stress	4629	4554	4554	5241	V/mil
Est. Energy Density	153	124	104	124	J/lb

and polytetrafluoroethylene were selected as films for three designs. One of these used silicone oil, while the other two used FE-4 fluoroether for impregnation. A greater space factor was designed into the silicone oil component to permit better penetration of this oil, or else it would have had the greatest energy density of the three Phase II designs.

The power dissipated will probably be greater than the amount indicated in Table 36, since conductor losses have not been included. These numbers are indicative of the smallest amount of heat generation which can be hoped for with these materials.

The energy densities were expected to be several times smaller than the goal set for this program. Because of the considerations which have been outlined previously, these numbers are still optimistic. It must be realized, however, that even a 1 J/lb energy density in this capacitor is a significant improvement in the state-of-the-art.

8.5.5 AC Filter Capacitor

The designs for this dielectric are quite simple, consisting of a single layer of metallized film and a space factor which is minimized to whatever extent is possible in the winding process. As shown in Table 37, polysulfone and polyetherimide films of equal thickness were to be used in the two designs tested. The pads were wound to capacitance.

8.6 PAD DESIGNS

Once the dielectric has been selected and the total thickness and effective dielectric constant defined, the capacitor section, or pad, can be designed. The pad design involves selection of the material widths and margin width, calculation of the active foil length required, selection of start and end leader lengths or number of turns, positioning and sizing of the tabs, and estimation of the final dimensions of the winding.

The margins used on this program on all the high repetition rate and low repetition rate pulse and the DC filter capacitor designs were a standard 0.25 inch. These pads all had operating voltages of 7.5 to 8.3 kV. The high frequency AC inverter capacitor designs used margins of 0.125 inch, with a

TABLE 36. HIGH FREQUENCY AC CAPACITOR DIELECTRIC SYSTEMS

Calculated Parameters	Phase I Preliminary Design	Phase I Final Design	Phase II Option A 864044	Phase II Option B 864049	Phase II Option C 864050	Units
Capacitance	-	-	1	2	2	μF
Film	Polyethylene	Polyetherimide	Polypropylene	PTFE	Polypropylene	
Gauge x Layers	12 x 2	24 x 2	20 x 2	25 x 2	20 x 2	0.01 mil
Oil	DC-200	DC-200	DC-200	FE-4	FE-4	
Foil Gauge	25	25	25	25	25	0.01 mil
Dielectric Thickness	1.06	0.58	0.50	0.575	0.475	mil
Permittivity	3.03	3.08	2.29	2.05	2.24	
Dissipation Factor	0.0007	0.0010	0.0002	0.0001	0.0002	
Power Loss (8 μF)	396	565	113	56.5	113	watts
Insulation Resistance	1.10 ¹⁴	6.10 ¹²	8.10 ¹⁵	1.10 ¹²	8.10 ¹⁵	ohm-cm ²
Surface Density	1.21	1.22	0.90	2.10	1.03	gm/cm ²
Film Stress						
-AC	1398	2513	3117	1540	1529	V/mil
-DC	1415	2586	3750	3000	3750	V/mil
Oil Stress						
-AC	1583	2939	2531	1232	1345	V/mil
-DC	1415	2586	0	0	0	V/mil
Average Stress						
(pk)	1415	2586	3000	2609	3158	V/mil
(RMS)	1001	1829	2121	1845	2233	V/mil
Est. Energy Density	21.3	7.12	7.23	2.59	7.33	J/lb

TABLE 37. AC FILTER CAPACITOR DIELECTRIC SYSTEMS

Parameters	Polysulfone	Polyetherimide	Units
Capacitance	3.00	3.00	μF
Film Thickness	0.24	0.24	mil
Permittivity	3.07	3.17	
Dissipation Factor	0.0008	0.0012	
Insulation Resistance	$3 \cdot 10^{13}$	$3 \cdot 10^{12}$	ohm-cm^2
Surface Density	0.30	0.30	gm/cm^2
Film Stress			
- (pk)	825	825	V/mil
- (RMS)	583	583	V/mil

0.125 inch foil extension beyond the edges of the dielectric at each end. This capacitor had an operating voltage of 1500 V peak. The 400 Hz AC filter capacitors, which operate at only 200 V peak, had a margin of 0.040 inch. The original design for these capacitors had a somewhat larger margin width than this, but no problems were encountered using this width.

The width of the material was dictated, in many cases, by the dimensions of the reusable test vessels. Those units using the vessels had a total pad length of 4.50 inches (+0.10-0.00) and thus a foil width of 4.00 inches. The inverter capacitor width was smaller in order to reduce the length of the thermal path from the center of the pad. A width of 3.00 inches was selected in this case, although this could probably have been reduced even further. The material used on the low voltage filter pads was 2.00 inches wide, while the original design had been considerably narrower. The active widths for these two capacitors were 2.75 and 1.02 inches, respectively.

The active foil length, ℓ , was calculated using the basic equation:

$$\ell = \frac{C \cdot t}{448 \cdot k \cdot W_A} \quad (8-10)$$

where C is the capacitance in picofarads, k is the dielectric constant, t is the dielectric thickness in mils, and W_A is the active width in inches.

Start and end leaders on the pulse and DC filter capacitors were selected to be 5 and 3 turns long, while on the inverter capacitor designs 864049 and 864050, 6 and 3 turns were used. These leaders provide insulation and protection from the outside environment, as well as a radius on the mandrel during winding. An outer wrap of Kraft paper is used in addition to the end leader.

In those designs using tabs, each of two tabs was placed at about the 1/4 and 3/4 points of the active foil length. Tabs for the two foils were separated by a half turn of the winding mandrel, so that they were on opposite sides of the mandrel, as well as projecting out opposite ends of the pad. The tabs used were made by H. H. Hilton Industries, Sarasota, Florida, and were size F010, with flags 2.25 by 1.00 inch nominal, and size F013, with flags 3.50 by 2.00 inch nominal.

The final dimensions of the winding were estimated using equations based upon the known winding geometry. These equations have been found to be fairly accurate, but the results of these calculations were not critical for this program. The volume of each pad can be estimated from the thickness, X, the width, Y, and the length, Z (which corresponds to the total width of the materials as they are arranged in the pad) using

$$\text{Volume} = [X(Y-X) + \pi \left(\frac{X}{2}\right)^2]Z \quad (8-11)$$

which assumes the radius or fold of the pad is a half circle of diameter X. For a multiple-pad can, the volume is more nearly approximated by assuming the pad is a rectangular shape with

$$\text{Volume} = X \cdot Y \cdot Z \quad (8-12)$$

since the can required will not conform to the radius of each pad.

The relatively large deviations in capacitance from the design value for the 864051 was caused by an error in the calculation of the active electrode area for this capacitor. This affects the lifetime to a small degree, but not enough to warrant scrapping the parts.

Dissipation factor measurements indicated that there was a problem in meeting the low loss values needed for a cool running capacitor in the pulse capacitors, and the dissipation factor goal of ≤ 0.002 for the dc filter capacitor was also not met. The cause of the problem was most likely moisture in the paper and/or dioctyl phthalate. The increase in dissipation factor with impregnation on the 864041 and 864042 lots indicates the presence of moisture in the oil, despite the purification processing which was carried out and verified by testing. Another major contribution to the DF and ESR was probably the termination resistance.

10.1.2 Equivalent Series Resistance

The equivalent series resistance, defined by

$$ESR = \frac{DF}{\omega C} \quad (10-1)$$

for a capacitor of value C at an angular frequency $\omega = 2\pi f$, was measured using a Clarke-Hess Model 273A ESR Meter. The frequency of measurement was 100 kHz. Unfortunately, this meter was not available for use when the 864046 and 864051 units were fabricated. The test results are presented in Table 41.

The ESR, when measured at the self-resonant frequency, is a good measure of the contribution of termination resistance to the dissipation factor. At higher frequencies, the ESR has a contribution due to the inductive impedance of the capacitor electrodes, terminations, conductors and terminal.

10.1.3 Insulation Resistance

The insulation resistance (IR) was calculated from the measured leakage current using the equation:

$$IR = \frac{V}{I} \cdot C \cdot 10^6 \quad \Omega\text{-}\mu\text{F} \quad (10-2)$$

TABLE 40. DISSIPATION FACTOR MEASUREMENTS

Dwg No.	S/N	1 kHz		10 kHz		120 Hz	
		Pre	Post	Pre	Post	Pre	Post
864041	3	0.005	0.005	0.020	0.030	0.003	0.004
	5	0.005	0.005	0.029	0.0295	0.003	0.004
	6	0.005	0.005	0.020	0.029	0.003	0.004
	7	0.005	0.005	0.021	0.031	0.003	0.004
864042	5	0.005	0.005	0.0195	0.027	0.003	0.005
	7	0.005	0.005	0.020	0.027	0.003	0.005
	8	0.005	0.005	0.019	0.028	0.003	0.005
864043	9	0.0035	0.004	0.013	0.0205	0.002	0.0025
	10	0.004	0.004	0.015	0.0195	0.003	0.0025
	11	0.004	0.004	0.020	0.022	0.0025	0.003
	12	0.004	0.005	0.014	0.025	0.0025	0.002
864046	1	-	0.0035	-	0.0145	-	0.003
	2	-	0.003	-	0.0135	-	0.003
	3	-	0.003	-	0.014	-	0.004
	4	-	0.004	-	0.014	-	0.004
	5	-	0.004	-	0.015	-	0.004
	6	-	0.003	-	0.014	-	0.003
864051	1	0.003	0.004	0.010	0.015	-	-
	2	0.003	0.004	0.011	0.014	-	-
	3	0.003	0.0035	0.010	0.0135	-	-
	4	0.003	0.003	0.010	0.013	-	-
	5	0.003	0.003	0.010	0.013	-	-
	6	0.003	0.0035	0.010	0.0135	-	-

TABLE 39. CAPACITANCE MEASUREMENTS

Dwg No.	S/N	Capacitance, μF						Design Value	Percent Dev.
		1 kHz		10 kHz		120 Hz			
		Pre	Post	Pre	Post	Pre	Post		
864041	3	1.305	2.34	1.309	2.36	1.312	2.35	2.2	+6.4
	5	1.323	2.34	1.328	2.36	1.329	2.35	2.2	+6.4
	6	1.327	2.34	1.331	2.36	1.332	2.35	2.2	+6.4
	7	1.330	2.35	1.333	2.37	1.334	2.36	2.2	+6.8
864042	5	1.250	2.19	1.2535	2.21	1.255	2.20	2.2	-0.5
	7	1.268	2.20	1.272	2.22	1.274	2.21	2.2	0
	8	1.2625	2.16	1.266	2.18	1.268	2.17	2.2	-1.8
864043	9	0.7575	1.267	0.758	1.2725	0.761	1.271	1.2	+5.6
	10	0.8035	1.296	0.804	1.302	0.807	1.300	1.2	+8.0
	11	0.799	1.320	0.799	1.327	0.802	1.325	1.2	+10.0
	12	0.8015	1.302	0.801	1.3085	0.804	1.307	1.2	+8.5
864046	1	-	1.007	-	1.011	-	1.011	1.1	-8.5
	2	-	1.013	-	1.017	-	1.017	1.1	-7.9
	3	-	1.003	-	1.007	-	1.007	1.1	-8.8
	4	-	1.035	-	1.039	-	1.038	1.1	-5.9
	5	-	1.020	-	1.024	-	1.023	1.1	-8.0
	6	-	0.996	-	1.000	-	1.000	1.1	-9.5
864051	1	0.656	1.065	0.657	1.070	-	-	1.2	-11.3
	2	0.681	1.074	0.682	1.079	-	-	1.2	-10.5
	3	0.642	1.034	0.643	1.039	-	-	1.2	-13.8
	4	0.637	1.041	0.638	1.046	-	-	1.2	-13.3
	5	0.638	1.043	0.539	1.048	-	-	1.2	-13.1
	6	0.639	1.052	0.640	1.056	-	-	1.2	-12.3

10.0 CAPACITOR PAD TESTING

During the design and fabrication portions of Phase II, the development of life test fixtures was carried out for the DC filter, high frequency AC, and AC filter capacitors. These fixtures would supply the required electrical stresses to match those expected in normal service. In addition, the pulse test stand built on the previous AFWAL program at Hughes was modified for testing the 300 Hz unit.

After fabrication was completed, each capacitor pad was subjected to a number of measurements and test prior to actual life testing. Subsequent to the actual end-of-life for each sample, a failure analysis was performed to determine the location of the puncture and contributing factors, such as wrinkling, corona degradation, or impregnant decomposition.

10.1 PARAMETRIC MEASUREMENTS

Parametric measurements were made on packaged pads and pads after impregnation and sealing. Capacitance and dissipation factor measurements were at a temperature of approximately 22°C. Measurements made by Component Research Company, Inc., on the AC filter capacitors were made at 25°C.

10.1.1 Capacitance and Dissipation Factor

At Hughes, these measurements were made using a Hewlett-Packard 4262A LCR Meter at frequencies of 120, 1000, and 10,000 Hz. Readings were taken after assembly (prior to bake out and vacuum impregnation) and after sealing in most cases. Data are presented in Tables 39 and 40.

The capacitors themselves were baked under vacuum at 85°C for at least 72 hours prior to the actual filling operation. The pressure was typically 30 microns of Hg, while 50 microns of Hg was the maximum permitted pressure at the end of this step.

With the side loader sealed off and the main chamber under <50 microns of Hg pressure, DOP was dripped into the 500 ml sample bottle first in order to clear the line of any old oil or particulates. Subsequently each capacitor was filled alternately for a period of about 20 minutes at a rapid drip rate. This process was continued for about four hours and then the filling stopped until the next working day. The process was then continued and the capacitors topped off. The heat on the side loader oil reservoir was shut off at that point. After another 24 hours under vacuum, the capacitors would be topped off once more using room temperature oil. The vacuum line was then valved off and the main chamber backfilled to atmospheric pressure with dry nitrogen gas.

The sealing operation took place after each capacitor vessel was removed from the main chamber. A copper washer was inserted and then a threaded plug was torqued down to provide the seal. The parts were carefully agitated under the oil in the "funnel" to prevent any bubble entrapment.

Finally, the capacitor cans were cleaned off with trichlorofluoroethylene III and vapor degreased. The units were then delivered to the laboratory for final acceptance tests. These tests are described in Section 10.1, and results are included there.

9.7 CONCLUSIONS

The pressing and impregnation processes differ from that used on the previous AFWAL program in that a drying temperature of 85°C was used. This probably accounts for the wrinkles observed in the parts dissected. A lower temperature bake out, for a longer period of time, would reduce the moisture gradient between the center and ends of the pads. In addition, the oil loading process was done under vacuum to degas the oil, while previously, degassing depended on convection of the oil in the side loader while being heated under vacuum, and the exposure to vacuum during filling. This was a simple process improvement with consequences which are much more difficult to measure.

TABLE 38. NO₂ FILTRATION TEST RESULTS

DOP Sample	Date	Water Content ppm	Volume Resistivity ohm-cm	Dielectric Strength V/mil	Particulates, per 100 ml				
					5-10 μ m	10-25 μ m	25-50 μ m	50-100 μ m	>100 μ m
As delivered	8/13/81	272	$1.05 \cdot 10^{11}$	403	1,522	391	143	57	12
Unfiltered	7/11/83	341	$4.07 \cdot 10^{10}$	350	498,407	49,261	17,980	79	6
Filtered 72 Hrs.	7/11/83	59	$1.33 \cdot 10^{12}$	400	7,255	4,426	974	186	41
Filtered 261 Hrs.	7/19/83	48	$1.4 \cdot 10^{12}$	350	1,317	628	145	22	2
Filtered 168 Hrs.	7/28/83	44	$1.55 \cdot 10^{12}$	320	749	410	49	2	2
Lot 864041 - 1	9/8/83	80	$1.3 \cdot 10^{11}$	390	428,838	55,829	1,279	50	3
Lot 864043 - 1	9/9/83	32	$2.07 \cdot 10^{11}$	390	444,368	66,967	1,799	150	51
Lot 864042 - 1	10/26/83	33	$2.0 \cdot 10^{11}$	390	545,383	45,966	1,934	89	8
Lot 864046 - 1	1/24/84	24	$1.05 \cdot 10^{11}$	400	165,537	48,676	5,295	358	70
Lot 864051 - 1	2/9/84	28	$1.07 \cdot 10^{11}$	400	1,279	608	34	4	3

vacuum chamber with the capacitors and filling it prior to filling the units. Quality control tests were run on these samples and the results are presented in Table 38. It appears that the first lot of 864041 units received impregnation from DOP with a high water content of 80 ppm. All lots except for the 864051 units received oil which had a very high particulate content. The volume resistivity of all the oil samples taken was a factor of ten lower than expected based on the early test run, but this is predictable based on the fact that the DOP samples taken from the lots were exposed to the environment of the impregnator itself at temperature of up to 90°C. Some addition of ionic species has to be expected under these circumstances.

9.5 PRE-IMPREGNATION TESTING

Prior to the impregnation of each lot of capacitors, tests were conducted on each capacitor. These tests included capacitance and dissipation factor measurements, but did not include screening for dielectric strength or insulation resistance.

Results of these tests are presented in Section 10.1.

9.6 IMPREGNATION AND SEALING

The impregnation process is critical to the proper performance of high voltage capacitors. This step must assure the degassing of the oil as well as the complete penetration of the winding by the oil. The final drying of the capacitors themselves is probably the most critical portion of the whole process.

Oil from the filtration system reservoir was drawn into the side loader of a Red Point Oil Impregnation System under vacuum in order to degas it, prior to or at the same time as the capacitors were loaded into the main chamber. The oil was heated to 85°C \pm 5°C and kept under vacuum (about 250 microns of Hg due to boil-off) for at least 24 hours prior to the impregnation.

The can body includes a bellows for thermal expansion compensation. A "funnel" is attached to the fill port which permits sealing the capacitor with a screw-in plug and copper washer under about 1.5 inches of oil.

9.4 OIL FILTRATION AND TESTING

The dioctyl phthalate oil which was used for the pulse and high voltage filter capacitors built on this program is routinely filtered in a dedicated closed-loop system diagrammed in Figure 36. Separate systems are used for other oils. Filters in the system remove water, ionic species, and particulates. The pump is of the membrane type so as to avoid metal particles being introduced by vane or piston wear. Seals are of Teflon[®] or Viton[®].

In order to obtain high purity oil, tests were conducted prior to the first impregnation run to determine the filtering time required to achieve a water content of less than 50 ppm and the volume resistivity of greater than $1 \cdot 10^{12}$ ohm-cm. During the actual impregnation cycle, samples of the oil going into the capacitors were taken by placing a sample bottle into the

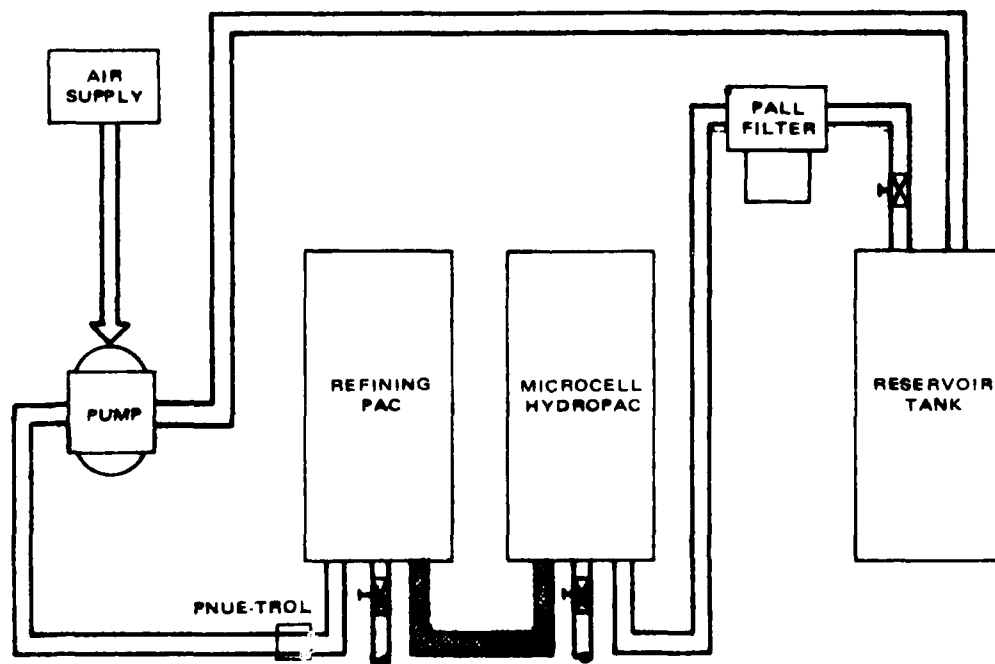
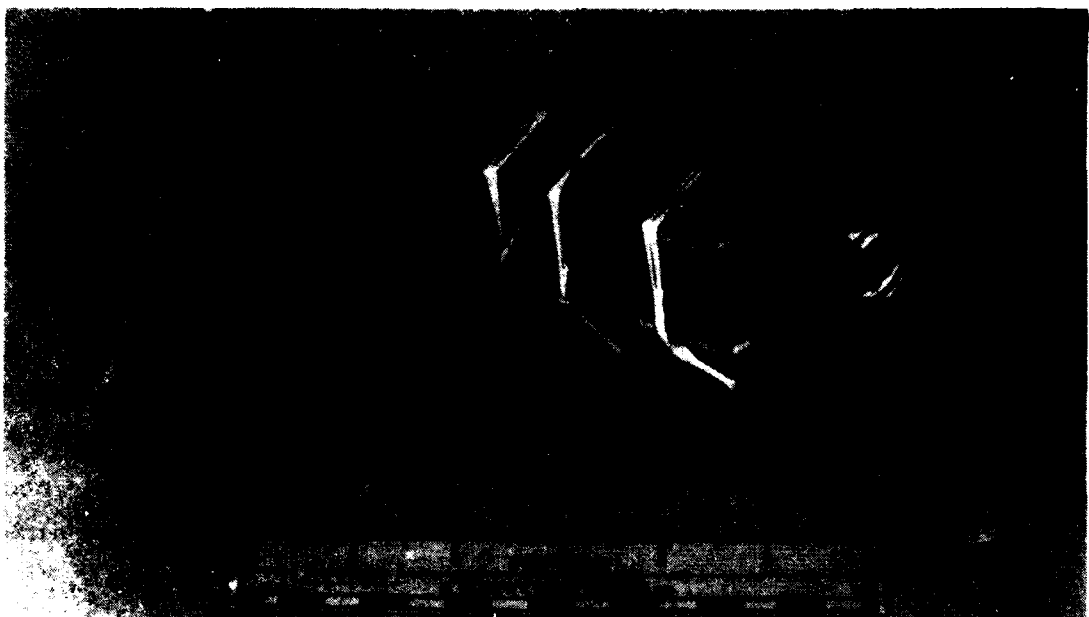


Figure 36. Oil filtration system.



76 50826

Figure 34. Pad test configuration.



76 50828

Figure 35. Reusable test vessel assembly.

fixture is removed from the oven. Immediately the nuts are tightened prior to cooling, to obtain the final pressing dimension.

After cooling, the pads are removed from the fixture and placed in a dry box maintained with dry desiccant. The pads are removed individually for further assembly operations and returned as each step is completed.

The next step is to clamp the pad to its final dimension between a pair of epoxy glass laminant boards of 0.062 inch thickness. These boards are cut to size depending on the pad width and height. While the pad and boards are held in a vise, the assembly is tied with three lengths of lacing cord. Proper dimensioning of the boards prevents distortion of the pad at the radius or fold. While this system admittedly applies little pressure to the center of the pad width, it has been found adequate to maintain the pad dimensions and capacitance during the assembly procedure.

9.3 ASSEMBLY INTO THE CAN

Once the pad is clamped to dimension as described above, termination can be carried out. At each end, several layers of 5 mil Kraft sheet cut to shape and with slits for the tabs are used to cover the ends of the pad and reduce the possibility of flashover across the pad dielectric margin to a tab or the case. The tabs can then be folded over and solder connections made to wires or the case. The test pads made for this program had a heavy braided conductor connected to the high voltage tabs, while the ground potential tabs were soldered directly to the copper strap which was part of the reusable vessel.

The pad was inserted into the U-shaped copper strap and any extra space taken up by sheets of 5 mil Kraft paper. This was then tied together with lacing cord to hold the pad in place. The ground tabs were soldered into the bottom of the strap where a slot had been cut for this purpose. As the strap was attached to the lid of the vessel, the high voltage conductor was fed through the hollow stud of the terminal and soldered at the top. Photographs of the pad test configuration and the reusable vessel are included as Figures 34 and 35.

The can assembly is completed by joining the copper strap to the can lid by means of two bolts in the lid, installing a Viton[®] O-ring in the lid groove, and fastening the lid to the body of the can by means of four bolts.

ground potential foil cut. Several turns of insulation are wound over this, per the winding instruction sheet, and then cut. A length of 5 mil Kraft paper is taped to the end of the winding with Kapton tape, and wrapped around the winding one and one-half turns. The end of this outer wrap is then taped with Kapton tape to complete the winding. The mandrel is pulled apart and the pad is slid off and put into a container and labelled.

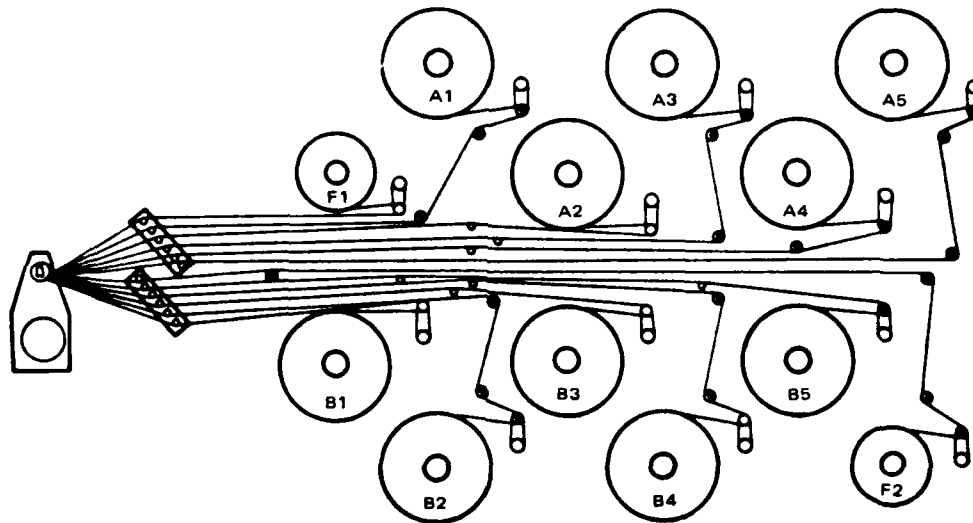
This work is performed by a skilled technician with several years of experience with the machine. The winding of a single pad, after setup is completed, may take as long as twenty minutes, but generally required about ten minutes.

Setup is basically common to all capacitor winding machines of this type, and involves putting the rolls of material on spindle adaptors and/or the spindles themselves, alignment of the rolls to get the proper margin width and alignment of foils, feeding the materials over the proper rollers and combs, and setting of the tension on each spindle. Generally, one or more test windings are made to determine the correlation of inches of length to number of turns, for the start, tab insertion, and end points in the winding.

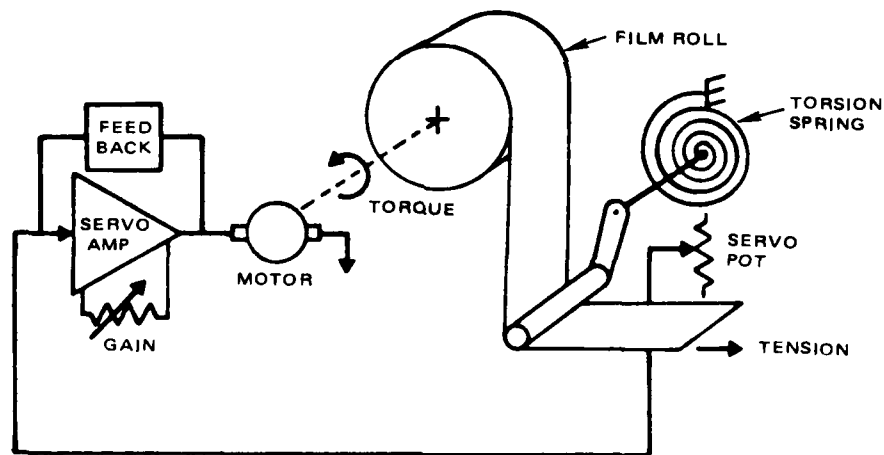
9.2 PAD PRESSING

After the pads have been wound, they may be stored indefinitely within the controlled environment of the winding room. When assembly continues, the remaining steps are done within a few days to avoid excessive water absorption by the Kraft paper in the winding. The first step is to press the pad to flatten it to a nearly rectangular form. The pressing is done in two stages.

The number of turns in the winding, combined with the desired dielectric thickness, is used to calculate the pressing dimension. The first step is to press the pad to within 10 percent of this dimension. Because of the water content of the paper and resistance to flattening of the winding, this requires several pounds of pressure. The pressing fixture consists of two aluminum plates, two Teflon® sheets between which the pads are sandwiched, and a number of studs with nuts used to apply the pressure. The fixture, with pads, is placed in a drying oven at 85°C for 16 hours at atmospheric pressure. When this period is over the oven is back-filled with dry nitrogen and the



a. Web paths shown.



b. Closed loop servo tension controls.

Figure 33. Capacitor winding machine.

the basic chassis, Figure 33b, is described in AFWAL-TR-80-2037. Detail drawings were included in Appendix B of that report.

Pads are wound on a removable split mandrel which is flat, rather than cylindrical. This reduces the distortion which occurs when a cylindrical pad is pressed flat, as is normal in the industry. To accommodate this, winding speed is relatively slow, and the torque motor is capable of reversing direction in order to maintain constant tension.

For this program, all pads tested were of buried foil, rather than extended foil, construction. Two folded flag tabs were inserted per foil and overlaid with an extra stack of insulation cut to size. Individual tabs for each foil in a pair were separated by one-half turn of the winding, and pairs were placed at the one-quarter and three-quarter length positions along the active foil length. In all cases, high potential and ground potential tabs extended from opposite ends of the pad.

The winding environment was a Class 100,000 clean room maintained at 50 to 60 percent relative humidity and 70 to 75°F temperature. Capacitor materials were stored adjacent to the winding machine under the same conditions.

The ground potential foil and both dielectric stacks start the winding. These are clamped in the mandrel and the excess cut off with scissors. Several turns of this arrangement are wound into the mandrel, as specified in the winding design sheet, to build up a radius on the mandrel and provide protection from distortion in the active dielectric when the mandrel is removed. The high potential foil is then added to the stack, having been cleanly cut with scissors and properly aligned. Winding proceeds to the first tab location. The tab is laid in with tweezers, covered with a 5-layer stack of insulation as found in each dielectric, and aligned and positioned near the center of a flat side of the pad. The mandrel is turned one-half turn, and the ground tab laid in, projecting out the other end of the pad, in the same way. Winding then proceeds to the next tab position and the process is repeated. The remainder of the high potential foil length is wound and then this foil is cut with scissors. Another half-turn is wound, and then the

9.0 MANUFACTURING PROCEDURES

The development of high energy density capacitors is limited more by manufacturing techniques than by engineering design. In order to properly ascertain any improvement in dielectric film quality, utmost care must be taken to control all manufacturing processes and eliminate flaws which may arise during these steps. The approach taken by Hughes in the fabrication of capacitors is generally applicable to any high reliability component, device, or system. A critical consideration is the avoidance of any type of contamination.

In this section the manufacturing steps which were used by Hughes to build capacitors on this program are described in some detail. The steps which are involved in the fabrication of single element test samples are:

1. Pad winding
2. Pad pressing
3. Assembly into the can
4. Oil filtration and testing
5. Pre-impregnation testing
6. Impregnation and sealing.

Descriptions of the equipment used are included or referenced below. The techniques described here are applicable to both pulse capacitors and the DC filter.

9.1 PAD WINDING

The winding machine used is a modified Hilton machine with 10 spindles for dielectric films and papers and 2 spindles for foils, as shown in Figure 33a. The closed loop servo tension control system which was added to

TABLE 41. RESISTANCE PARAMETER MEASUREMENTS

Dwg. No.	S/N	ESR (100 kHz)		Leakage (1000 VDC, 5 min) nA	Insulation Resistance $10^{10} \Omega \cdot \mu F$	DWV kV
		Pre m Ω	Post m Ω			
864041	3	46.8	51.5	200	1.17	7.5
	5	49.1	48.5	200	1.17	7.5
	6	47.3	46.3	170	1.38	7.5
	7	47.6	47.9	190	1.23	7.5
864042	5	76.5	47.8	140	1.56	8.0
	7	70.9	48.4	120	1.83	8.0
	8	73.0	44.2	135	1.60	8.0
864043	9	54.4	69.6	130	0.975	8.3
	10	64.3	76.2	120	1.08	8.3
	11	69.1	71.0	110	1.20	8.3
	12	51.1	76.6	100	1.30	8.3
864046	1	-	-	78.7	1.28	7.5
	2	-	-	65.0	1.55	7.5
	3	-	-	91.7	1.10	Fail
	4	-	-	77.4	1.30	7.5
	5	-	-	79.7	1.26	7.5
	6	-	-	69.3	1.45	7.5
864051	1	-	-	83.9	1.20	8.3
	2	-	-	80.0	1.3	8.3
	3	-	-	86.4	1.17	8.3
	4	-	-	78.9	1.28	8.3
	5	-	-	90.8	1.11	8.3
	6	-	-	81.1	1.24	8.3

The leakage current was measured at 1000 VDC after 5 minutes charging time, using the circuit shown in Figure 37.

This test is used to detect major flaws which are indicated by anomalously low IR values. This points to current flow through pinholes, conductive inclusions or along paths external to the bulk of the dielectric. Expected values of the insulation resistance were given for each design in Section 8.

10.1.4 Dielectric Withstand Voltage

This test was used to test the samples for major weak spots in the dielectric. The circuit in Figure 10-1 is used to charge the capacitor to the expected peak value of DC voltage or DC plus AC voltage, for a period of one minute. Greater voltages were not used because of the possibility of damage to the insulation system, which is already highly stressed at the normal operating voltage, and because the DC test does not always stress the insulation system as it was designed to be stressed.

One 864046 capacitor failed this test, as shown in Table 10-3. This capacitor was designed for the high repetition rate pulse service. The failure occurred at a film stress of 10.4 kV/mil, at room temperature, about 47 seconds into the test, and was probably caused by a flaw in the film.

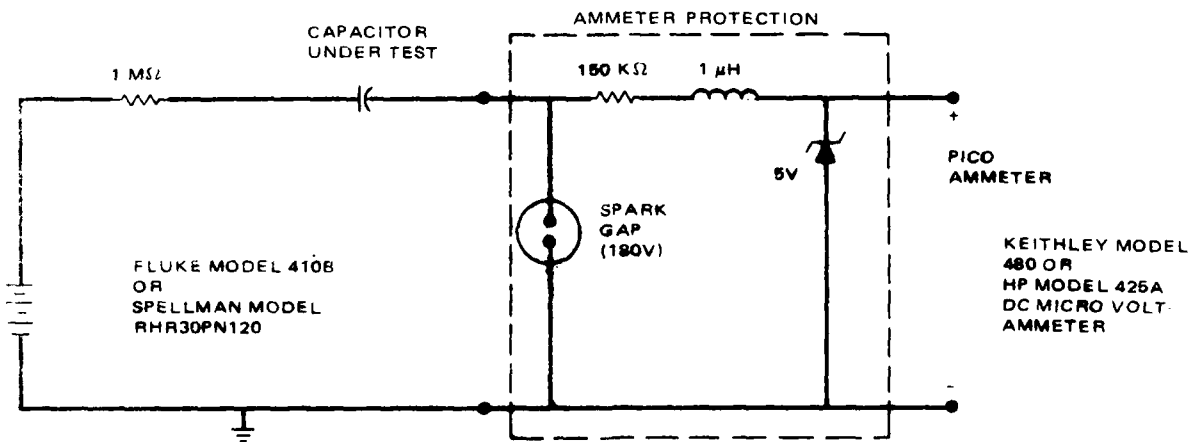


Figure 37. Leakage current and dielectric withstand voltage test circuit.

10.1.5 AC Filter Capacitor Tests

Component Research Company, who manufactured the metallized film capacitors for the 400 Hz AC application, performed capacitance, dissipation factor, leakage current, and AC dielectric withstand tests on these components. Capacitance and dissipation factor were measured at 1 kHz and 25°C with a 1 VRMS signal. Leakage current was measured at 200 VDC and 25°C after 5 minutes charging time. The AC hi-pot was at 168 VRMS 60 Hz for 1 minute and was also at 25°C. There were 216 Ultem[®] capacitors and 338 Kimfone polysulfone capacitors.

These capacitors have virtually zero space factor and are essentially all film between the electrodes. Because of this, a great deal can be learned about the relative merits of a film by studying the behavior of such capacitors, since material interactions are not a problem. While the metallized electrodes inhibit shorting and failure, damage caused by localized self-healing breakdowns is detectable as a change of electrical properties such as DF and insulation resistance. If breakdowns are very numerous, a change of capacitance may even be detectable as the result of the loss of electrode area.

The dissipation factor of the Ultem design ranged between 0.009 and 0.0011, and averaged 0.0010. By comparison, the Kimfone units exhibited dissipation factors ranging from 0.0006 to 0.0015 and an average of 0.0010. No correlation was observed between the DF and the leakage current in either set of capacitors. The Ultem units exhibited high leakage currents in a great many cases. The lowest leakage observed in each type was 600 pA for the Ultem and 100 pA for the Kimfone, corresponding to insulation resistance values of 6 and $36 \times 10^{12} \Omega\text{-}\mu\text{F}$. Leakage currents as high as 10 μA occurred frequently in the Ultem capacitors, while no leakage current greater than 1 μA was observed in the Kimfone type. A summary histogram of the data is shown in Figure 38. It can be seen that the majority of Ultem capacitors had about an order of magnitude less insulation resistance than the Kimfone capacitors. The leakier units probably had faults and had cleared incompletely, leaving high resistance current paths. (Both sets of metallized

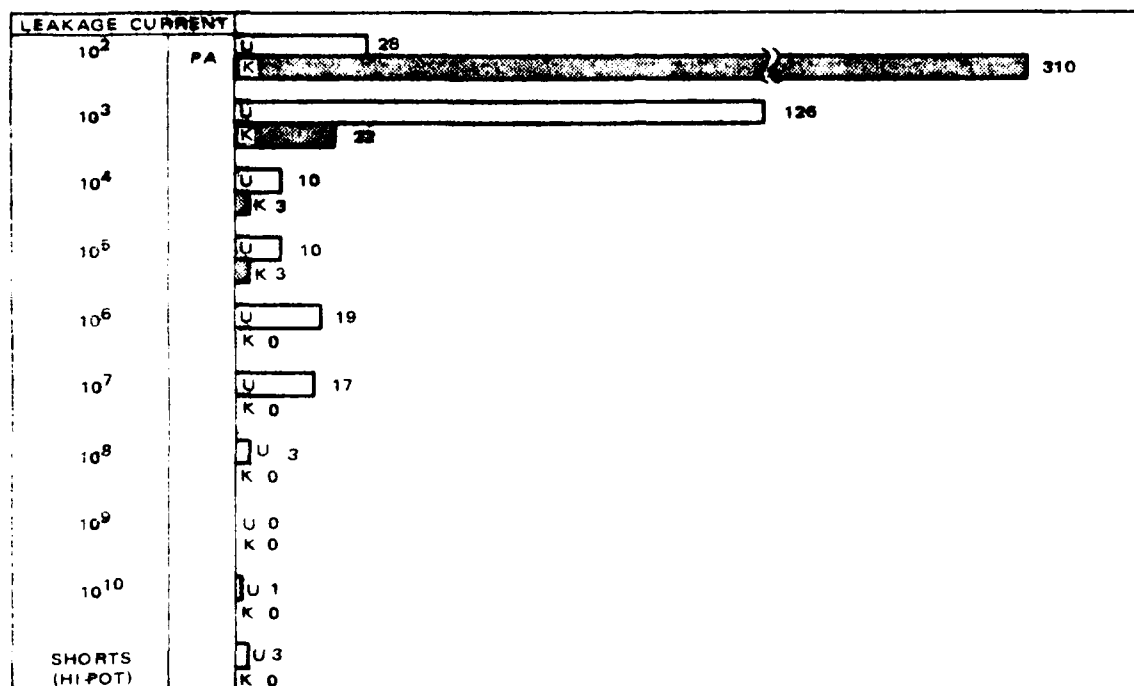


Figure 38. Histogram of leakage current data for Ultem and Kimfone metallized film capacitors.

film rolls were pre-cleared at 441 volts.) Three Ultem capacitors failed the AC hipot test, while no Kimfone capacitors failed.

The data may indicate that the 24 gauge Ultem film used here had a significantly greater fault count than the commercial polysulfone film of the same gauge. If this were true of the plain film used for the other capacitors, reduced lifetime would be expected.

10.2 LIFE TEST FIXTURES

10.2.1 Pulse Capacitors

A simplified system diagram depicting the pulse test circuit stand which was built during the previous AFWAL program at Hughes is given in Figure 39. The control system allowed the selection of peak voltage, pulse repetition rate, and duty cycle. Changes in the load inductance and resistance were made by inserting different coils and varying the number of value of the resistors paralleled in the load chassis. Such modifications were made when the capacitance value to be tested was changed from 2.2 μF to 1.1 μF .

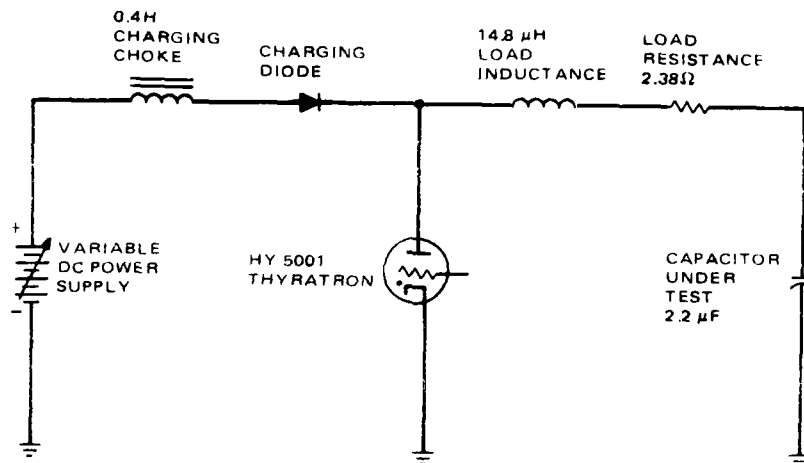
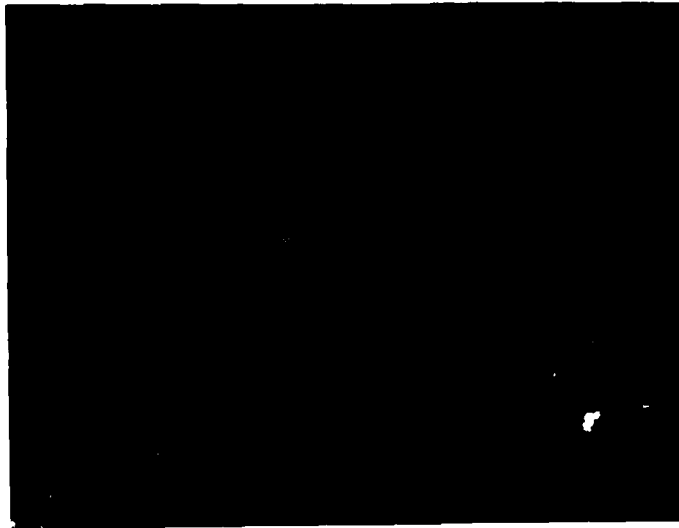


Figure 39. Pulse test circuit simplified diagram. Component values given for 2.2 μ F capacitor configuration.

This change in the value of the capacitor pad was necessitated by the DC power supply which would not provide sufficient power to test the 300 pps unit at full voltage. No problem was found in testing the 50 pps unit at full voltage on the original configuration. The modification made was to double the load inductance and resistance in order to obtain the same voltage waveform obtained on the larger capacitance samples. This meant a reduction in the peak current to approximately one-half the value for the 2.2 μ F pads.

Figure 40 shows oscilloscope photographs taken during pulse tests of both size capacitors, depicting the discharge waveforms. The scales are the same for each. The voltage trace starts at the peak charging voltage and drops during the discharge, reverses, and approaches zero potential before significant recharging takes place. The current trace is initially at zero, and rapidly peaks during the discharge. The non-sinusoidal nature of this peak is due to the effect of other parts of the circuit when the voltage reverses. The current also reverses slightly before returning to a zero level. Figure 40(a) is from a test of 864042 S/N 5 at 8.12 kV peak voltage.



(a)



(b)

Figure 40. Discharge voltage and current waveforms for (a) 2.2 μF and (b) 1.1 μF pad test configurations. Horizontal scale 10 $\mu\text{s}/\text{division}$, vertical scales 2000 V/division (voltage) and 400 A/division (current).

The peak current here from the 2.2 μF pad was 1554 amps. The rise time on the current pulse was 7.90 μs and the voltage reversal was 23 percent. Figure 40(b) is from a test of 864046 S/N 6 at 7.96 kV peak voltage. This 1.1 μF pad produced a peak current of 804 amps, with a current pulse rise time of 7.38 μsec . The voltage reversal was 24 percent.

Measurements of voltage were made using a Tektronix 468R oscilloscope with a Tektronix 6013A 1000/1 Ratio High Voltage Probe connected to the high voltage lead to the capacitor terminal and grounded at the grounding stud on the capacitor can. Current measurements used a Pearson Model 110 current transformer with a 0.1 volt/amp output and a Telonic Industries TG-950 50 Ω attenuator set at 20 dB (1/10) displayed on the same oscilloscope, which had very useful storage capability. Temperature measurements were made using copper-constantan TC junctions and a Bailey Instruments Model BAT-4 analog meter.

A complete description of the pulse test facility was given in the previous report AFWAL-TR-80-2037.²¹ Mr. Robert Gourlay described the low inductance load configuration in a paper presented at the 1976 IEEE International Pulse Power Conference.²²

An important point is that the capacitor cans were not cooled or heat sunk except for the static ambient air at 22°C. The baseplate was a plywood sheet.

10.2.2 DC Filter

The requirement for testing this capacitor called for a 20 kHz ripple signal superimposed on the DC voltage. The circuit used for this purpose is shown in Figure 41. This test fixture was capable of testing two 1.2 μF capacitors in parallel. A relay circuit was used to detect a power supply overload condition and shut off the supply when a failure occurred.

These capacitors were not cooled or heat sunk, other than by static ambient air at 22°C. No tests were performed at higher temperatures.

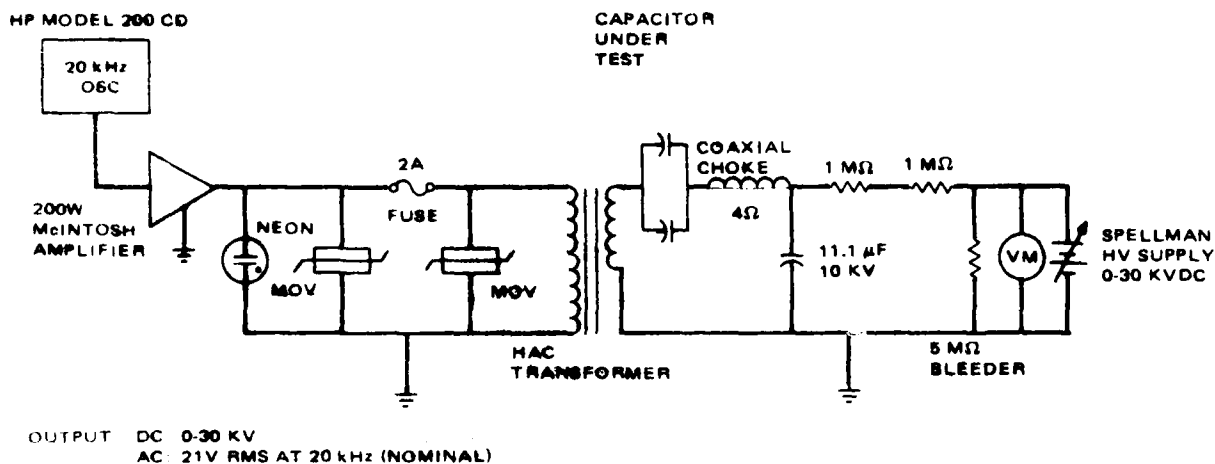


Figure 41. DC filter capacitor test fixture.

The capacitor DC voltage was measured using a Singer Company Model ESM High Voltage Electrostatic Voltmeter. The DC power supply was a Spellman Model RMR30PN120. The oscillator used was an HP Model 200 CD. The ripple voltage at 20 kHz was measured using a Triplet multimeter.

10.2.3 High Frequency AC

The test fixture for this unit presented some technical problems because the power amplifier intended for use could only supply 1500 watts. With a full 8 μF capacitor unit, or four 2 μF pads in parallel, a Q of ≥ 500 was required in a parallel resonant circuit in which the capacitors would be tested.

To obtain a Q of 500 at 10 kHz frequency, the first design utilized several parallel air coils and a conductor consisting of two layers of 10 mil soft annealed copper 0.625 inch wide. The inside diameter of the coil was 12 inches. This coil was fabricated and its Q measured by two different methods, and found to be in the range 40-50. This meant that the losses in

the complete coil would be too large to be supplied by the 1500 W amplifier at the test voltage.

The second design was a helical coil of 0.75 inch OD copper tubing, with a 22 inch diameter air core. This was found to have a Q of 90-120. The Q measurement was made using 8 μF of low dissipation factor polypropylene/foil capacitors in a resonant circuit and measuring the half amplitude width of the resonance peak, as well as by a voltage drop measurement with a resistor in series with the inductor.

A third design utilized a ferrite core made by stacking individual I-bar core pieces. A 0.625 inch OD copper tube helix with 6 inch inside diameter was wound for this inductor. The Q measured on this inductor was on the order of 170 after some additional ferrite material was added to the poles to reduce losses due to the magnetic field cutting through the end turns.

At this point, it was apparent that the effort to test four 2 μF pads in parallel was excessive. It was proposed that it would be more practical to test 2 μF pads singly, which could be done using the above inductor. A schematic diagram of the test circuit is shown in Figure 42.

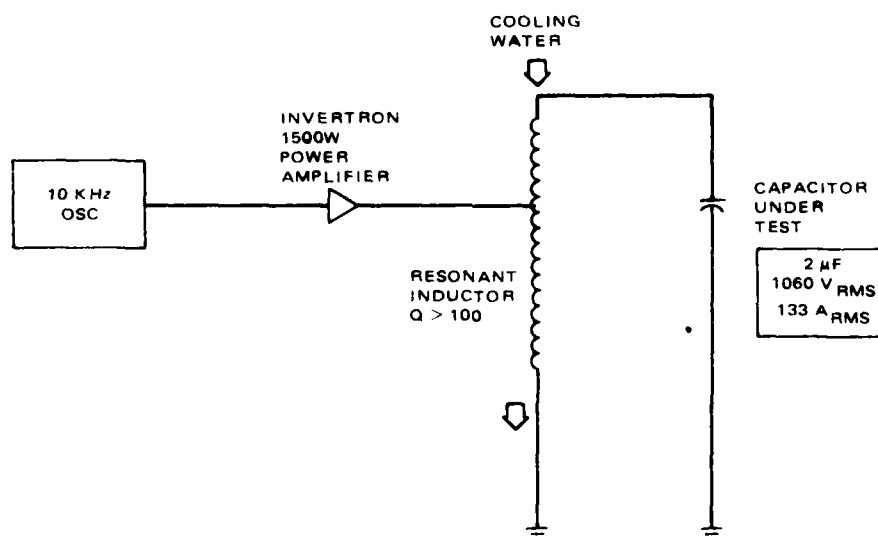


Figure 42. High frequency AC test fixture design.

Other options which were considered were the use of Litz wire for the inductor, and the possibility of installing a 60 kW power amplifier that was in storage for this test. Both these options were feasible, but both were considerably more expensive than had been originally planned.

One problem which was understood to be significant for this capacitor was the direct thermal path between the coil and the capacitor in the resonant circuit. The life of the capacitor may be critically dependent on whether heat flows into or out of the terminations, which in turn depends on the losses in the coil and the available cooling for the coil. The copper tube coil designs fabricated on this program would have had cooling water circulating through them in order to reduce this problem for the capacitor. It remains to be seen whether the energy density goal for this capacitor is meaningful in relation to the inductor mass and required cooling provisions.

10.2.4 AC Filter

In this case, a 400 Hz AC sine wave was to be applied to the capacitors at 140 Vrms level. Each pad would be individually fused. The life test would be carried out with the capacitors at 125 to 200°C, the higher temperatures permitting an accelerated stress on the performance of polysulfone versus polyetherimide film. A forced-air convection oven was used to provide the ambient environment. The power was supplied by a 400 Hz motor-generator set dedicated to the High Voltage Test Laboratory, and the proper voltage was obtained using three single-phase autotransformers designed and built by Hughes for this purpose. The test circuit is shown in Figure 43.

The high ambient temperature range proved to be a problem because some of the materials used in the pad fabrication did not have the same high temperature stability as the dielectric films themselves. These auxiliary materials, including a solid core of polycarbonate, start and end leaders of polyester, and a piece of polyester adhesive tape, caused fires at temperatures of about 150°C. The life test was therefore limited to a temperature of 125°C.

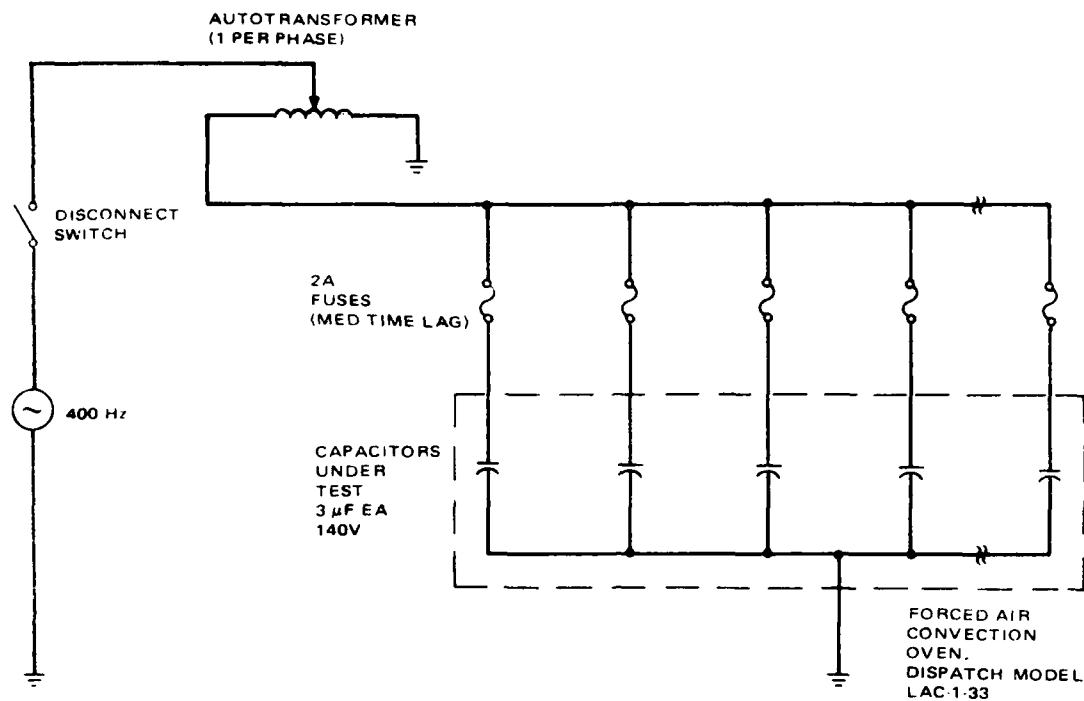


Figure 43. AC filter capacitor test circuit. Up to 300 capacitors could be tested at one time.

10.3 TEMPERATURE RISE STUDY

Prior to actual life testing, a series of pulse bursts were run on 864041 and 864042 pad samples in which thermocouples (TC) had been implanted for temperature measurements. These bursts were run at various voltages and pulse repetition rates to obtain useful information about the peak temperature rise within the capacitor pad and the time required for the pad to cool to 30°C or less. Because the 864041 and 864042 designs were exactly the same, the only difference between the samples was in the location of the thermocouple junction. In the 864041, the junction was located at the center of the winding, while in the 864042, the junction was outside the winding, half-way down its length, at one corner of the pad. Although one might have

expected the latter thermocouple to show consistently lower temperatures, in fact the reverse was true.

Most of the measurements were made on two samples, 864041 S/N 6 and 864042 S/N 5. Table 42 shows that there were no sizeable differences between the measured electrical parameters of the two samples which would indicate any major differences between the heat generated or the temperature rise.

The temperature rise in the capacitor pad, assuming adiabatic behavior during the one minute pulse train, should be proportional to the square of the RMS current and proportional to the equivalent series resistance:

$$\Delta T = BI_{\text{RMS}}^2 \cdot \text{ESR} \quad (10-3)$$

where B is a constant depending on the thermal mass of the pad. As shown in Figure 44, the temperature rise did not show this expected behavior across

TABLE 42. COMPARISON OF TC TEST CAPACITORS

Parameter	864041/6	864042/5
Capacitance	2.34	2.19
Dissipation Factor	0.005	0.005
ESR (mΩ)	46.3	47.8
Insulation Resistance (10 ¹⁰ ohm-μF)	1.38	1.56
Dielectric Withstand Test Voltage, kV	7.5	8.0
TC Location	Pad center	Pad exterior

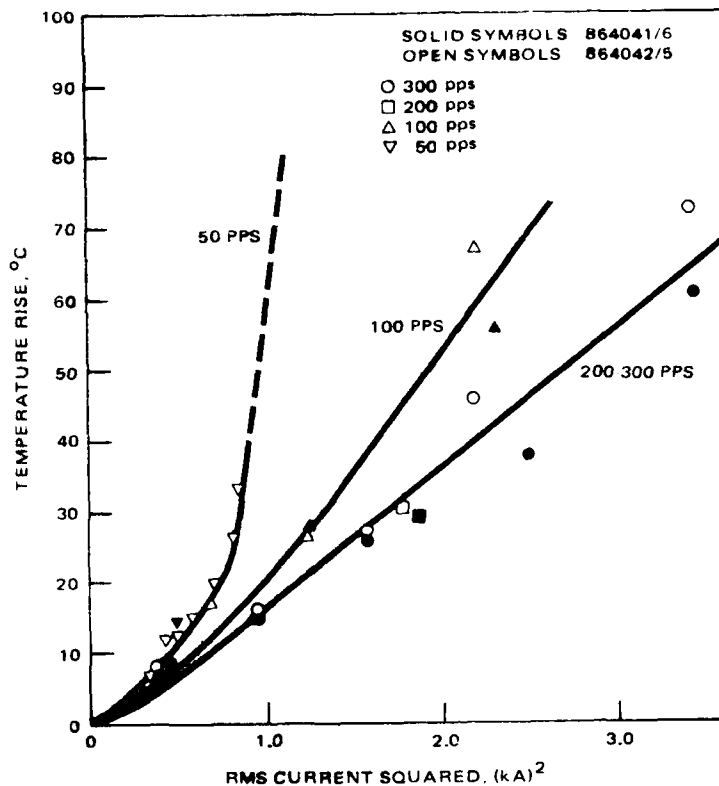


Figure 44. Temperature rise versus total power in pulse capacitors.

the entire range of test conditions. Temperature rise measurements were made at peak voltages from 2 to 8 kV and repetition rates of 50, 100, 200 and 300 pps. It would appear that the ESR is not a constant across this range, since the temperature rise depended strongly on the pulse frequency.

In fact, the apparent dependence of the effective ESR on frequency should have no basis in physical reality, but is only apparent. The RMS current was calculated using the equation:

$$I_{\text{RMS}} = I_p \left(\frac{\tau}{2T} \right)^{1/2} \quad (10-4)$$

here τ is the width of the current pulse, and $1/T$ is the repetition rate. The peak current, I_p , was linearly proportional to the charging voltage for each capacitor, with a measured ratio of 0.19 to 0.20 A/V for the two capacitor samples used. Thus, there is a possibility that the ESR was increasing with voltage or peak current. To test this hypothesis, the above equations were solved for the ESR times the constant B which depends upon the specific heat and mass of the pad.

$$\text{ESR} \cdot B = \frac{\Delta\theta}{(I_{\text{RMS}})^2} \quad (10-5)$$

If we plot the value of $\Delta\theta/(I_{\text{RMS}})^2$ versus voltage where θ is temperature, as shown in Figure 45, there does appear to be a dependence of ESR on voltage once a voltage of over 4 kV is reached. (Check runs showed that this was not an aging effect.) The decreasing value of the ESR below this voltage, if

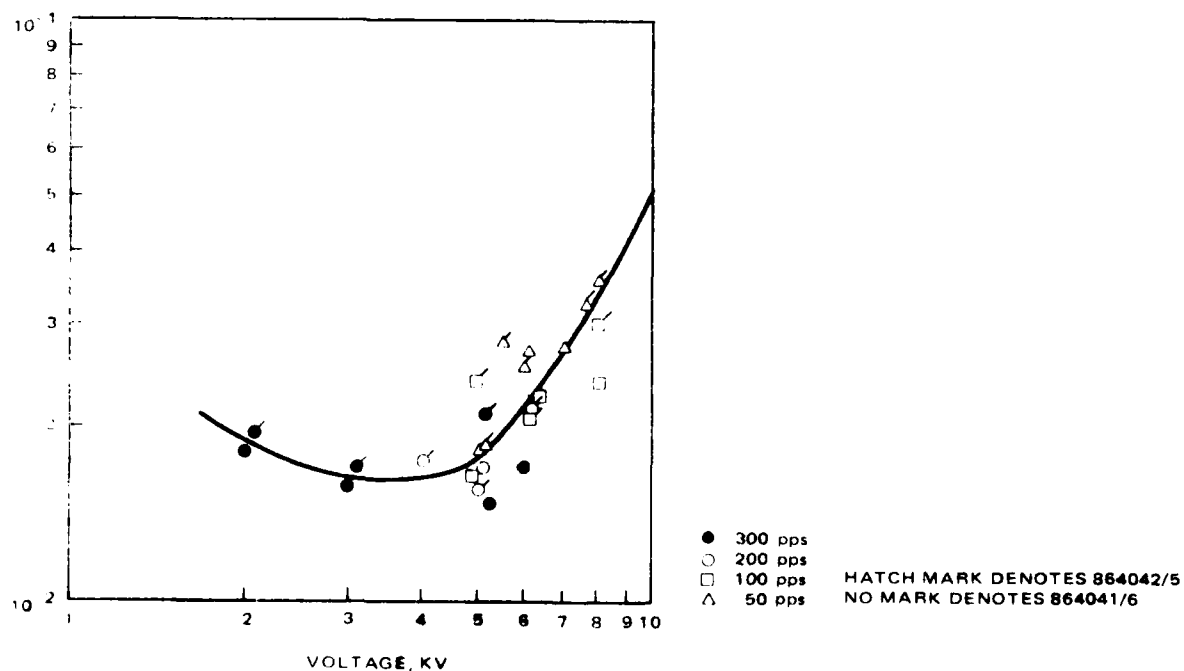


Figure 45. Dependence of ESR on voltage.

Another phenomena was observed at the interface between the tabs and foils. The current density at this location can be expected to be very large. Speckles appeared distributed over this interface such that the largest spots were at the place where the tab ribbon was against the foil and the current density highest. These spots appear to be the results of sparks jumping across a very small gap between the tab and the electrode. At the very edge of the foil, the aluminum had been notched, as though it had been welded to the tab ribbon and had been removed when the tab was lifted. On the inner tabs of 864041 S/N 7, light colored speckles appear on the foil side opposite the tab contacting it, but not on the opposite side of the folded foil flag of the tab. When a tab was lifted off, pinholes were left in the foil electrode where the stake points in the ribbon had been in contact with it. It would appear that localized spot welding may have been occurring. A peak current density of $640,000 \text{ Amps/in}^2$ ($99,200 \text{ Amps/cm}^2$) is expected in the tab ribbon, while the peak current density in the flag (assuming it is a constant over the hole area, which it is not) is 474 A/in^2 (73.5 amps/cm^2). If the mechanical contact between flag and foil is poor, localized current densities could obviously be quite large.

Pulse capacitors of high energy density should generally be made with extended foil terminations or with a large number of large area, single layer tabs. This will decrease the ESR and reduce the peak current densities in the terminations and thus eliminate this aging mechanism. It is difficult to show any relationship between the tab failures which did occur and this phenomenon, but it is obvious that the high current densities at these locations will cause heating and reduce the lifetime of the surrounding insulation. Perhaps more failures would occur at these locations if a double thickness of insulation were not present.

Discoloration spots were observed in several of these capacitor windings. These appeared to be deposits on the foil which could be wiped off. This is considered to be a product of deterioration of the dioctyl phthalate oil. The spots were light in color and appeared mainly along the upper half of the tabs. There seemed to be some correlation between the location of these spots and the location of discharge burns along the foil edges.

Degradation of the dioctyl phthalate impregnant had also occurred in S/N 5 and 6. This, unlike the wrinkling, was not observed in S/N 3 and was therefore not due to processing but due to life testing. No oil degradation was observed in S/N 1, 2, or 4, either. The degradation was detected by an adhesive-like behavior observed in unwinding the pad. Similar deterioration of mineral oil under pulse discharge conditions have been previously studied at Hughes. That liquid appears to polymerize and simultaneously give off H_2 gas in the presence of partial discharges and heat. The phenomenon occurs across the bulk of the winding and ceases at the ends of the active dielectric region and in the doubly-insulated area over the tabs.

10.5.2 Low Repetition Rate Pulse Capacitors

Capacitor designs 864041 and 864042 exhibited most of the phenomena observed in the high repetition rate components and on phenomenon which was not observed in those parts. Four of the six units which were life tested failed on a foil edge; three on the lower edge and one on the upper edge. The other two units failed on a positive potential and a ground potential tab where the strip passed through the margin.

Part 864041 S/N 5 was dissected prior to the end of life after a few thousand pulses at voltages between 5.0 and 6.0 kV at 300 pps. No corona damage was observed. Wrinkles were present in the folds of the pad, but crinkles were not observed in the flat portions of the pad. This was typical of the appearance of the pads which were life tested.

Partial discharge burns were observed at the foil ends, but not along the longitudinal edges, which were aligned within ten mils in most cases. The burns at the ends were darkest where notches were left in the foil edge by the scissoring operation. Although none of the failures occurred at this location, lifetime could eventually be limited by this mechanism. An easy solution would be to fold back the foil ends to form a smooth, curved edge at this point which would have a much higher corona inception voltage.

10.5 FAILURE ANALYSES

After each capacitor failed, it was dissected to determine the location of failure, any obvious causes, and any other evidence of degradation or contributing factors. No chemical analysis or other sophisticated methods were used to measure changes in the materials; all observations were visual.

10.5.1 High Repetition Rate Pulse Capacitors

The five 864046 capacitors which were life tested all failed at the foil edge, and in two cases the puncture was at one of the ground potential (lower end) tabs despite extra layers of insulation over the tabs. Of the remaining units, two failed on an upper foil edge and one on a lower edge. Serial number 3, which shorted during the 7.5 kV DC, one minute dielectric withstand test, failed in the body of the capacitor and not on a foil edge or tab.

Burns due to partial discharges were observed along the cut high potential foil ends in all of the life tested units. Comparatively little or no damage was observed along the longitudinal foil edges, although such damage did appear near the start of the high voltage foil in S/N 5, and there mainly along the upper edge. In this case, the ground potential foil was displaced about 0.033 in. below the high potential foil. Thus, the field at the ground foil edge was enhanced along the top, while the field at the high potential foil was enhanced along the bottom edge. The observed asymmetry in the damage may be explained by:

1. Differences in the edge profiles of the foils themselves
2. The asymmetry due to gravity
3. Negative charge injection from the ground foil due to the enhanced field.

No corona damage was observed in S/N 6, which had not survived as long.

The pads were wrinkled and "crinkled," meaning that both large and deep wrinkles were observed which repeated through many turns of the winding, and a fine pattern of very small "crinkles" were observed as well. No failures could be directly ascribed to this phenomenon, however.

TABLE 45. LIFE TEST RESULTS -- DC FILTER CAPACITORS

Part No.	DC Voltage, kV	AC RMS Voltage, V	Frequency kHz	Lifetime hrs.	Failure Mode
864043/9	8.3	21	20	148.8	Positive tab
864043/10	8.3	21	20	137.1	Bulk
864043/11	8.3	21	20	144.1	Positive tab
864043/12	8.3	21	20	420.0	Bulk
864051/1	8.3	21	20	89.0	
864051/2	8.3	21	20	171.1	
864051/3	8.3	7	20		
864051/4	8.3	7	20	173.6	
864051/5	8.3	0	20		
864051/6	8.3	21	20	226	

capacitor designs (polysulfone and polyetherimide) and the second used 25 of each. The cause of the fires is believed to have been one or more of the auxiliary materials used in the capacitor pad construction. In the first test, 37 Ultem capacitors survived the fire while only 9 Kimfone capacitors survived. This may have more to do with air draft patterns than with the materials themselves, however.

In the third configuration, ten capacitors of each type were tested. Fires were isolated using a Kapton outer wrap around each capacitor. The temperature was held at 125°C while a voltage of 140 VRMS at 400 Hz was applied. During the test, five of the polysulfone capacitors failed. The failures occurred after 0.3, 117, 258, 744, and 2664 hours. None of the Ultem capacitors failed. The remaining fifteen capacitors operated satisfactorily for 3408 hours at which time the life test was shut down.

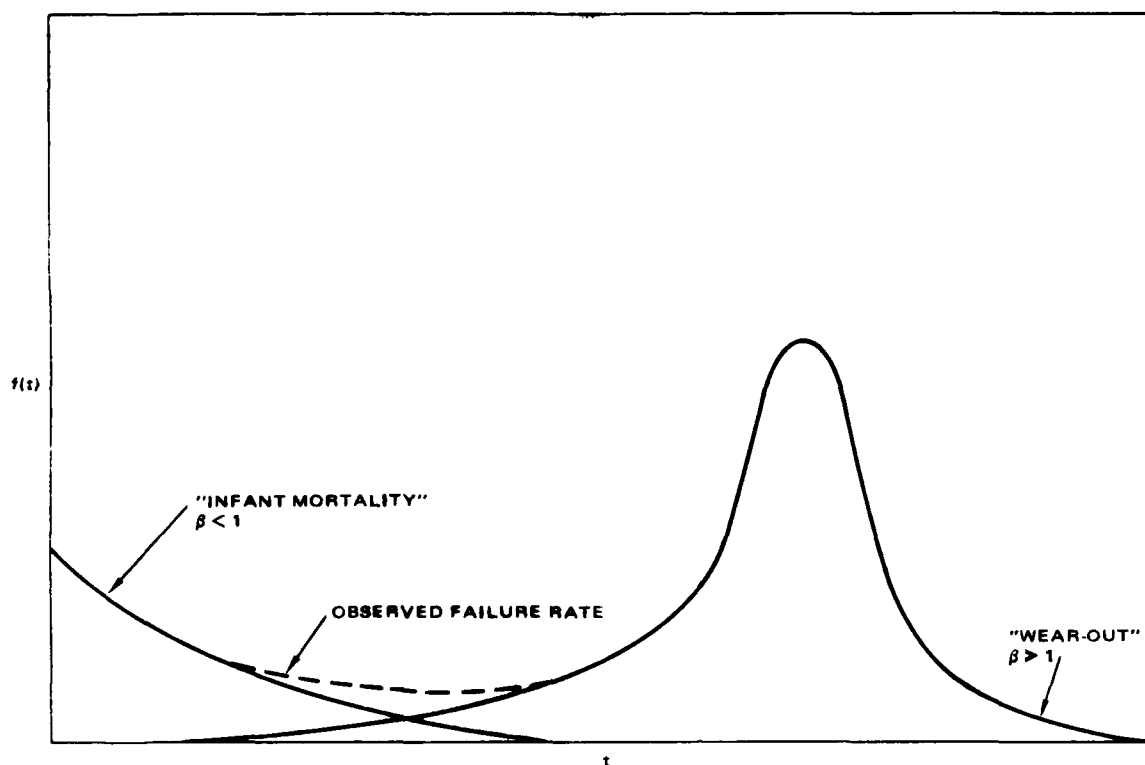


Figure 49. Capacitor failure rate distribution.

10.4.3 DC Filter Capacitor

For this application, two different designs were tested. The first was the 864043, and four units of this design were tested at 8.3 kV DC plus 21 V_{RMS} of 20 kHz AC ripple. As seen in Table 45, three of the four units failed between 137 and 149 hours, while a fourth survived nearly three times as long. Two different failure modes appear on the Weibull plot.

Six units of the 864051 design were tested. In all cases, 8.3 kV DC was applied, but the ripple voltage was varied.

10.4.4 AC Filter Capacitor

The first two attempts at testing the 400 Hz capacitors were accelerated tests using temperature as the accelerating stress. It was found that fires occurred and spread in the first two test configurations at a temperature around 150°C. The first configuration used 100 pieces of each of the two

and therefore the reliability is given by

$$R(t) = \exp \left\{ - \left(\frac{t - t_0}{\eta} \right)^\beta \right\} .$$

Of some interest to users is the failure rate function, $f(t)$, which is given by the derivative of $F(t)$ with respect to t :

$$f(t) = \frac{dF}{dt} = \left\{ \left(\frac{t - t_0}{\eta} \right)^{\beta-1} \right\} \cdot \exp \left\{ - \left(\frac{t - t_0}{\eta} \right)^\beta \right\}$$

This function can be used to determine the probability of a failure during some period of time during the operation life of a PFN, for example. A normal failure distribution ("bell curve") is a special case of the Weibull function, given by $\beta = 3.44$. The average time to failure, \bar{t} , and the variance, S^2 , are found from the Weibull parameters β and η using the gamma function Γ :

$$\bar{t} = \eta \Gamma(1 + 1/\beta)$$

$$S^2 = \eta^2 \Gamma(1 + 2/\beta) - \eta^2 (1 + 1/\beta)^2$$

For capacitors, there is generally expected to be a double failure rate distribution which is described by a curve similar to that shown in Figure 49. Such a distribution would appear on the Weibull plot as two-segmented lines, the first having a small slope and the second having a much larger slope. The two types of failures are often referred to as "infant mortality" and "wear-out." When "wear-out" times are very short, one might expect to see a mixture of distributions in the data, as has been observed here for the 864046 and 865043 capacitor designs. It is also possible that the competing forces of voltage stress and high temperature might cause different failure mechanisms to begin appearing concurrently, whereas normally one would predominate.

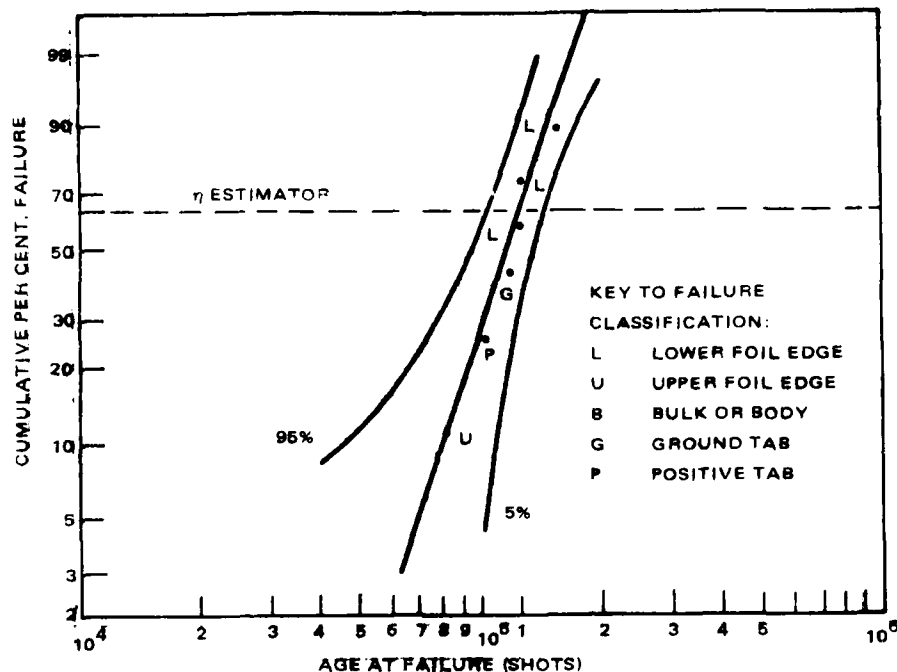


Figure 48. Weibull plot of low rep rate pulse capacitor life test data.
Confidence levels of 5% and 95% are also shown.

The Weibull distribution is a useful method for describing mathematically the cumulative probability of failure, $F(t)$, versus a random variable t , for such devices as capacitors. Here, the random variable is time. The Weibull equation,

$$F(t) = 1 - \exp \left\{ - \left(\frac{t - t_0}{\eta} \right)^\beta \right\},$$

uses three parameters to describe the failure distribution. The Weibull slope, β , gives the shape of the curve, while t_0 is the origin of the distribution and η the mean (63.7 percent failure level). The function $F(t)$ is related to the reliability, $R(t)$ by

$$R + F = 1$$

TABLE 44. LIFE TEST RESULTS -- LOW REPETITION RATE PULSE CAPACITORS

Part No.	Voltage kV	Frequency Hz	Duty Cycle	Lifetime Shots	Rise Time μ sec	Voltage Reversal %	Peak Current A	Failure Type
864041/3	7.90	50	1/60	81,000	7.90	20.7	1570	Upper foil edge
864041/6	(8.14)	50	1/60	99,000	7.73	21.5	1656	Positive tab
864041/7	7.90	50	1/60	150,000	7.90	20.7	1570	Ground tab
864042/5	(8.14)	50	1/60	122,000	7.73	21.5	1656	Lower foil edge
864042/7	7.96	50	1/60	123,000	7.65	22.9	1650	Lower foil edge
864042/8	7.96	50	1/60	115,000	7.65	22.9	1650	Lower foil edge

TABLE 43. LIFE TEST RESULTS - HIGH REPETITION RATE PULSE CAPACITORS

Part No.	Voltage kV	Pulses/ sec.	Duty Cycle	Lifetime Shots	Rise Time sec	Voltage Reversal, %	Peak Current, A	Failure Type
864046/1	7.80	300	1/60	52,000	7.38	25.4	800	Ground tab
864046/2	7.80	300	1/60	68,000	7.38	25.4	800	Ground tab
864046/3				Failed hi-pot				Bulk
864046/4	7.80	300	1/60	51,000	7.38	25.4	800	Upper foil edge
864046/5	7.96	300	1/60	54,000	7.38	24.1	804	Upper foil edge
864046/6	7.96	300	1/60	18,000	7.38	24.1	804	Lower foil edge

where L and V are the life and voltage under conditions not tested and L_o and V_o are the actual test conditions, we can get an idea of what the life would have been if $V = 7.5$ kV had been used. In this case,

$$\left(\frac{V_o}{V}\right)^n = \left(\frac{8.0}{7.5}\right)^{7.0} = 1.57$$

Thus we might expect a 50 to 60 percent increase in lifetime if the tests were repeated at 7.5 kV. The assumed exponent, however, may not be correct, and this calculation greatly depends on its determination. Unfortunately, life/stress tests were not performed over a range of voltages to obtain this exponent.

The results of the life tests are given in Table 43. The mean life was 4.9×10^4 shots, and this amounts to only about 3 bursts of the PFN. The life at 8.0 kV was two orders of magnitude below the 10^6 shot goal. The mean was calculated assuming a normal distribution. A Weibull plot of the data indicated a superposition of two or more failure mechanisms but there were insufficient data points to permit separating them.

10.4.2 Low Repetition Rate Pulse Capacitor

Testing of the low repetition rate pulse units was carried out at 8.0 kV and 50 pps. The duty cycle was one minute on and sixty minutes off. The voltage reversal was between 20 and 23 percent of the peak voltage. Peak currents in these 2.2 μ F units was approximately 100 amps and the current rise time was between 7.6 and 7.9 μ sec, measured from the 0 percent to the 100 percent points, and the reason for the wide variation in measurement was the flat top of the current waveform.

The data are presented in Table 44, and are plotted on Weibull distribution paper in Figure 48. The mean life taken from the plot was 1.23×10^5 shots and the shape of the curve given by $\beta = 2.99$. These data are consistent with a single cause of failure. The points on the plot are marked with the observed failure locations.

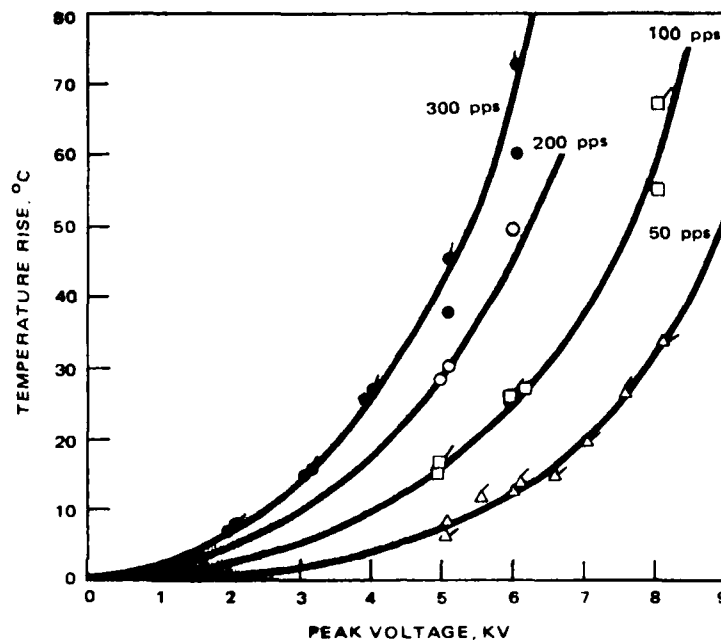


Figure 47. Temperature rise versus peak voltage.

The 864046 design was tested at 300 pps, after the load inductance and resistance had been changed to accommodate a 1.1 μF pad test. Under these conditions the current waveform would have a similar rise time and the voltage waveform a similar reversal to those observed on the 2.2 μF , 50 pps capacitors. This permitted testing at the high repetition rate by greatly reducing the required power output from the DC power supply.

The test was performed with an 8.0 kV peak voltage and a duty cycle consisting of one minute bursts followed by 60 minutes cooldown time. The peak voltage was 8.0 kV rather than the design voltage of 7.5 kV. This means that the low repetition rate and high repetition rate capacitors were tested at the same voltage, so that some information was obtained regarding lifetime versus frequency. If we assume an exponent of $n = 7.0$ in the life/stress equation:

$$\frac{L}{L_o} = \left(\frac{V_o}{V} \right)^n \quad (10-7)$$

minutes. Using this plot, it was possible to estimate the time required to cool to any given temperature between bursts, given the peak temperature expected at the peak voltage and frequency of operation. For a $\Delta\theta$ of 100°C , for example, the time required to cool to a $\Delta\theta$ of 5°C over an ambient of 25°C is 58 minutes.

This data applies only to the conditions of the life test on the single pads and will not be applicable to a full-size capacitor in a different can. The cooling rate will depend on the available paths for conduction out of the can and on the exterior environment. In this test, the reusable vessel had a large thermal mass and surface area relative to a typical capacitor can, and the grounding strap which fit around the pad provided a decent conduction path to the can walls. Cooling was therefore expected to be fairly rapid. However, a carefully laid out internal arrangement, with adequate means for the removal of heat, could improve the cooling characteristics of the complete capacitor considerably.

No temperature measurements were made on the 864046 design which was life tested at the high repetition rate. Very little difference in thermal behavior was expected. However, it is obvious from Figure 47 that the peak temperature rise above ambient at the operating voltage of 7.5 kV could be more than 120°C .

10.4 LIFE TESTS

The life testing performed is now described, with the results of the tests. Failure analysis information is provided in Section 10.5.

10.4.1 High Repetition Rate Pulse Capacitor

It was found during the temperature rise study reported above that the pulse test stand to be used on this program could not actually provide the power required to test the 300 Hz, 2.2 μF capacitor pads at voltages of more than about 6.0 kV. For this reason, the 864041 units, which were exactly identical to the 864042 units, were tested at the 50 Hz repetition rate and the results of those tests are described in a later section.

limited by the average power density during the burst. Thus, the difference between the energy densities which can now be attained at repetition rates of 50 and 300 pps are not as great as previously thought.

After many of the bursts run on these capacitors, temperature measurements were made during the cooling period to determine the time required to return to a temperature of 30°C or less. Some of this data is presented in Figure 46, in a normalized plot of temperature versus time. Peak temperatures were observed to be reached at the thermocouples approximately 90 seconds after the burst was ended. (This would indicate that the actual hot-spot temperatures within the dielectrics were somewhat higher than the temperatures recorded at the thermocouple junction locations.) As expected, the temperature profile during cooling fits an exponential decay curve:

$$\Delta\theta(t) = \Delta\theta(0) \exp(-0.516 \cdot t) \quad (10-6)$$

where $\Delta\theta$ is the difference between the temperature at the thermocouple after the burst and before the burst in degrees centigrade, and t is the time in

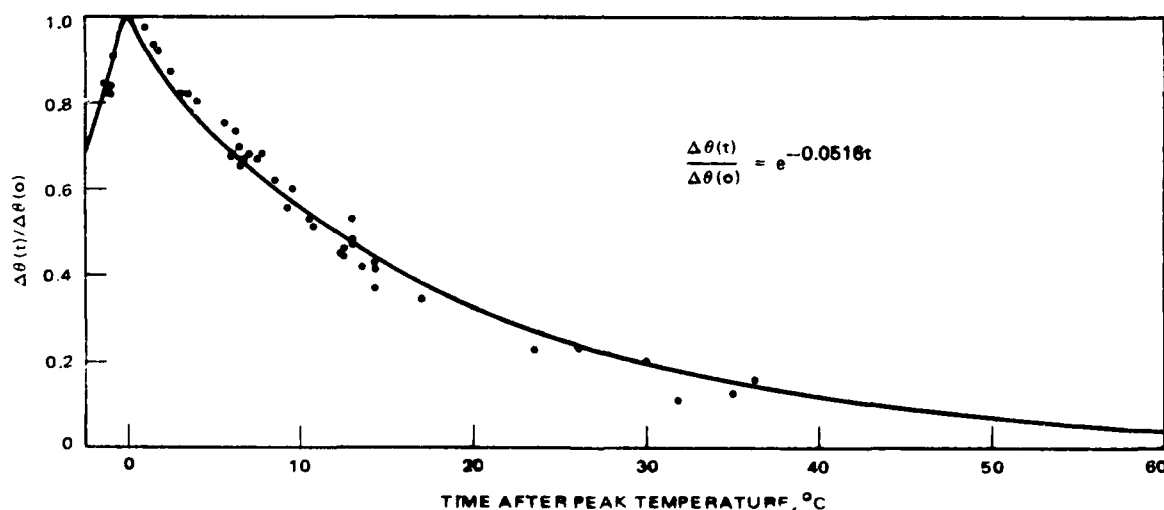


Figure 46. Normalized plot showing cooling of capacitors with time. Data taken on 864041/6 and 864042/5 samples after bursts of various voltages and frequencies.

real, might be the result of a known effect in which charged particles are trapped on the surfaces of the plastic film layers or within the cellulose matrix of the paper layers.

The increase in ESR with voltage might very well be related to the presence of partial discharges in the dielectric. The average dielectric stress at 4 kV is 2186 V/mil, and the transient field in the liquid impregnant (where discharges would first occur) is 3631 V/mil. Much larger fields would occur at the foil edges, due to field enhancement, and large gradients there might result in bubble formation as well. Failure analysis on these parts did show evidence of burns due to partial discharges along the foil edges, which provides circumstantial evidence in favor of this hypothesis.

The partial discharges would affect the ESR value because they dissipate energy which appears as a form of dielectric loss. The discharges would be expected to have an initiation or inception voltage which is characteristic of the dielectric system. In energy storage capacitors, such discharges are bound to occur at the operating voltage, especially when energy densities are high.

Another possible cause for the nonlinearity is a current and not voltage-related phenomenon. Observations made of the inserted tabs used to mechanically contact the foil electrodes after failure have uncovered an energy-intensive process going on between the tab flag foil and the actual electrode foil. It is possible that spot-welding might actually occur at small points over the flag surface. Such a phenomenon would depend heavily on the peak current, and not the peak voltage, and would involve the dissipation of substantial energy in melting aluminum. Since the peak current is linearly related to the peak voltage, it will be difficult to distinguish between these mechanisms.

The significance of these observations is that the heat generated in a pulse capacitor of this basic design or layout is not always directly proportional to the total energy throughput. This is important for the design engineer who is attempting to translate a design for a 300 pps capacitor to a design for a 50 pps capacitor, for example. This also means that the energy density of these repetition rate capacitors operating in burst mode is not yet

10.5.3 DC Filter Capacitors

Two designs were built and tested for this application. The first design, 864043, failed to meet a life goal of 1000 hours. Two of the four units tested failed at a high voltage tab, and two failed in the body of the capacitor. The puncture of S/N 9, occurred where the tab ribbon passed through the margin, which was confirmed to be 0.25 inch wide, as per the design. The extra insulation was present over the tab. Serial number 11 failed at the middle of the tab ribbon, 0.380 inch below the upper foil edge, possibly because of field enhancement or mechanical stresses around a staking point in the ribbon. Serial number 10 failed 0.094 inch below the top foil edge, in the center of the flat portion of the pad. The body puncture in S/N 12 occurred 0.25 inch below the top foil edge, on a wrinkle which had appeared in the flat portion of the pad. Wrinkles appeared in the other units as well, but those failures were not associated with them.

While there was no indication of partial discharge burns along the foil edges in these capacitors, S/N 12, which had lasted much longer than the other samples, was found to have some indications of oil degradation. Adhesion was noted in unwinding this pad.

The data for the second design 864051 are presented in Table 45, and are plotted on Weibull distribution paper in Figure 50. The mean life was 195 hours and the shape of the curve given by $\beta = 1.38$. These data are consistent with a single cause of failure. It became obvious that this design suffered the same deficiencies as had the 864043, and that the basic problem had not been addressed. The AC voltage compared to the DC voltage represents 0.35 percent at 21 VRMS or 0.12 percent at 7 VRMS. It would appear that the AC voltage stress is negligible. The current and power dissipated are also relatively small.

10.5.4 AC Filter Capacitors

The first test configuration provided for 100 capacitors of each design to be tested side-by-side. At a temperature of 150°C, a fire started and spread across the matrix of capacitors which were in close proximity to one another. After the fire was extinguished, 37 of the Ultem capacitors were

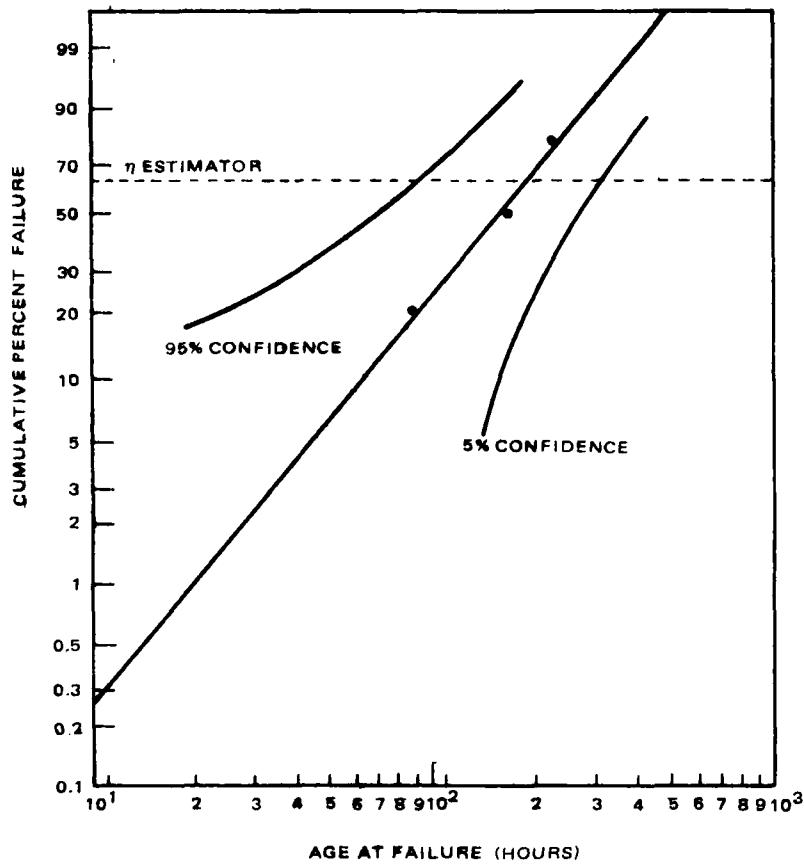


Figure 50. Weibull plot of DC filter capacitor life test data. Confidence levels of 5% and 95% are also shown.

still intact, and nine of the Kimfone capacitors remained. There was charring and carbonization of entire capacitors over most of the ground plane. Teflon wire insulation had been melted and removed above the capacitors, and solder connections to the ground plane had come free.

The second configuration involved only 25 of each design, separated by a much greater distance. A thermocouple was attached to the ground plane and another suspended above the capacitors for monitoring. Prior to applying heat, the capacitors were electrically stressed for several hours and the temperature rise determined to be negligible. The temperature was then increased to 50°C for four hours, then to 100°C, 125°C, and finally to 150°C before another fire started and spread. No excessive heating due to electrical power dissipation was observed at any temperature until the fire occurred.

Subsequently, one capacitor of each type was placed in an oven at 195°C without electrical stress. One capacitor, which happened to be polysulfone, distorted in shape and the end spray termination actually ruptured as the core material melted and expanded. Since both capacitors had the same core materials, it is probably just pure chance that the Ultem capacitor did not also rupture during the short test.

The third test configuration involved only ten capacitors of each type. Each capacitor was individually wrapped in a three inch wide piece of Kapton-M polyimide to prevent the spread of fire. The test temperature was restricted to 125°C.

11.0 CONCLUSIONS

This program provided a great deal of information about the nature of dielectric films in general and polysulfone film in particular. Initially, it was thought that a superior dielectric film could be produced by merely eliminating as much of the particulate contamination as possible. Relatively little attention was given to the dissolved ionic impurities present in the film, which have been shown to play a significant role in dielectric breakdown. Since these contaminants were found to enter the films via the resin and the solvent, they can be removed, at least partially, by appropriate treatment of the polymer solution. Unfortunately, no current treatment was found which significantly improved the breakdown characteristics. A number of experiments showed time-dependent breakdowns which occur because of migration of the ionic impurities and the resulting field distortion. A remaining problem, therefore, is to determine to what extent the impurities must be removed and to develop a practical technique for doing so.

The technique of casting films on a roughened casting drum was proved useful for preparing textured films. Further work is necessary in this area to better define the extent and nature of the roughness required to make an impregnable capacitor. This work is the first practical demonstration of a general process for making films that could be used in large high-voltage capacitors without Kraft paper. The elimination of Kraft paper will allow higher operating temperatures, lower the dissipation factor, permit higher average fields, and simplify assembly processes.

This development work has also led to proposing a new material for use in high energy density capacitors. While many of the same problems of particulate and ionic contamination must be considered for this material, tests have shown some promising results. This new material, Ultem, a polyetherimide

developed by General Electric, should be suitable for many military capacitor applications. This material has a higher temperature capability than any other film material except Kapton or Teflon, but since it is solution-cast it can be made at any thickness desired with very high film quality. It has a high ultimate tensile strength and generally excellent mechanical properties. Although its dissipation factor is higher than polysulfone, it is still only one-third that of Mylar.

Model capacitors were built and life tested to study the new Ultem film and determine whether large increases in capacitor energy density could be achieved. The electrical stresses varied from a DC voltage with a small ripple superposed to 300 pulse per second energy discharge. It was hoped that Ultem film would allow nominal lifetime goals to be achieved even when relatively high electric fields were generated across the dielectrics.

The practical goal of this program was to substantially increase the energy density of several types of capacitors while maintaining some minimum lifetime. The values of energy density which are stated as goals in the Statement of Work are quite ambitious targets, and should be put into perspective. In the case of pulse capacitors, the highest energy density components currently being produced have energy densities of 150-200 j/lb. However, they are designed for short lifetimes of $10^3 - 10^4$ shots when operated single-shot or at very low repetition rates. Higher repetition rate units must be considerably larger simply due to the dielectric heating. They must be larger still for reasonable lifetimes. Similar high frequency AC capacitors, designed for long lifetimes have energy densities about two orders of magnitude less than the stated goals.

Table 46 summarizes the performance of the various capacitors tested during the program. For comparison the program goals are also displayed.

In pulse capacitors, where the Ultem film was used in a system also containing Kraft paper and an impregnating oil, the superior temperature characteristic of the Ultem was actually offset by its greater losses. When large temperature rises resulted from these losses, the oil and paper deteriorated and the lifetimes were short of the goals set for the pulse capacitors. Average electric fields of 4.2 to 4.4 kV/mil were obtained.

TABLE 46. COMPARISON OF PROGRAM GOALS AND VALUES ACHIEVED

High Repetition Rate Pulse Capacitors	Program Goal	Value Achieved	Unit
Capacitance	1.1	1.1	μ F
Capacitor Voltage	7.5	8.0	kV
Pulse Repetition Rate	300	300	pps
Capacitor Energy Density Goal	≥ 200	90	J/lb
Capacitor Voltage Reversal	> 20	24	%
Life	10^6	5×10^4	pulses
<u>Low Repetition Rate Pulse Capacitors</u>			
Capacitance	2.2	2.2	μ F
Capacitor Voltage	8.0	8.0	kV
Pulse Repetition Rate	50	50	pps
Capacitor Energy Density Goal	≥ 500	114	J/lb
Capacitor Voltage Reversal	> 20	22	%
Life	10^6	1.2×10^5	pulses
<u>High Voltage Filter Capacitors</u>			
Capacitance	1.2	1.2	μ F
Working Voltage	8.3	8.3	kV
Dissipation Factor	< 0.2	0.18	%
Energy Density Goal	100	124	J/lb
<u>High Frequency AC Capacitors</u>			
Capacitance	2.0	2.0	μ F
Dissipation Factor	< 0.01	0.01	%
Energy Density Goal	≥ 50	2.6*	J/lb
<u>AC Filter Capacitors</u>			
	Polysulfone	Ultem	
Capacitance	3.0	3.0	μ F
Capacitor Voltage	140	140	Volts
Dissipation Factor	0.08	0.12	%
Operating Temperature	125	125	$^{\circ}$ C
Life Test, 3408 hours	50	0	failures, %
* Design Value only.			

Similar dielectrics were stressed with essentially a steady state DC field averaging 4.5 to 5.2 kV/mil. Lifetimes were also short, although thermal degradation was not the cause. In this case, it appeared that the breakdown characteristics of the Ultem film were not as superior as had been hoped. Nevertheless, lifetimes of hundreds of hours were achieved with the film stressed at more than 9.9 kV/mil. This can be translated to much longer lifetimes at lower stresses.

Its loss factor rendered the polyetherimide film unsuitable for use in very high average power capacitors. Lower loss factor materials such as polypropylene and the fluorocarbons were selected for use in the 10 kHz AC inverter capacitor application for this reason. Although even moderate energy densities will be very difficult to achieve; in this case, size and weight can be reduced substantially using advanced termination techniques. This will also reduce ohmic losses and temperature gradients within the capacitor.

Ultem polyetherimide film was also compared to polysulfone film in a life test at 125°C, using metallized film capacitors made of each material. As expected, the polyetherimide exhibited superior performance at the high temperature - there were no failures in ten Ultem capacitors after 3400 hours, while there was a forty percent failure rate in the same number of polysulfone capacitors in only 800 hours. This result is important, since a substitute for polysulfone is badly needed in military applications where high temperature operation is required. Polyetherimide is easily solution cast into thin films which have excellent mechanical properties, and it should therefore be a viable alternative to the more expensive Kapton or Teflon materials for temperatures up to about 140°C.

Unfortunately, lifetime data were not obtained over a range of conditions for each type of electrical stress: DC, AC, and pulse. Such information is needed before the limitations of the new material can be defined. Also additional data are needed to design high energy density capacitors which will have long lifetimes.

The polyetherimide material has good potential where high temperatures are encountered in the ambient environment but its use in high average power capacitors is limited, unless the Kraft paper can be eliminated from the dielectric. The concept of texturing the film during the casting process needs further development and evaluation.

REFERENCES

1. R. D. Parker, "Capacitors for Aircraft High Power," United States Air Force Report AFWAL-TR-80-2037, Air Force Aero Propulsion Laboratory, Wright-Patterson AFB, Ohio, January 1980.
2. C.L. Dailey and C.W. White, "Capacitors for Aircraft High Power," United States Air Force Report AFAPL-TR-74-79, Air Force Aero Propulsion Laboratory, Wright-Patterson AFB, Ohio, July 1974.
3. J.E. Creedon and R.A. Fitch, "A Half-Megawatt Pulse Forming Network," Proc. IEEE International Pulse Power Conference, paper IIIB-1, 1976.
4. J.E. Creedon, et al, "Compact Megawatt Average Power Pulse Generator," 13th Pulse Power Modulator Symposium, p. 264, 1978.
5. G.H. Mauldin, et al, "The Performance of the Perfluorocarbon Liquid/Plastic Film Capacitor Technology in Pulse Power Service — A Current Status Report," Conference on Electrical Insulation and Dielectric Phenomena, p. 54, 1983.
6. P. Hoffman and J. Ferrante, "Energy Storage Capacitors of High Energy Density," IEEE Trans. Nuclear Science, Vol. NS-18, p. 235, 1971.
7. P.S. Hoffman, "Capacitors for Aircraft High Power," United States Air Force Report AFAPL-TR-74-79, Air Force Aero Propulsion Laboratory, Wright-Patterson AFB, Ohio, February 1975.
8. General Electric Capacitor Data Book CPD-275, p. 55, July 1982.
9. W. White and I. Galperin, "Material Considerations for High Frequency, High Power Capacitors," Conference on Electrical Insulation and Dielectric Phenomena, p. 60, 1983.
10. W. White, personal communication, February 13, 1984.
11. R.J. Hopkins, et al, "Development of Corona Measurements and Their Relation to the Dielectric Strength of Capacitors," AIEE Transactions, 70, II, 1951.
12. J.R. Nye and W.R. Wilson, "Physical Concepts of Corona in Capacitors," AIEE Transactions, 72, III, 1953.

13. M. Kanazashi, "Deterioration of Polymer Films by Corona Discharge," 7th Electrical Insulation Conference, 1967.
14. A.G. Vail, "Dielectrics for DC and Energy Storage Capacitors," 4th Electrical Insulation Conference, 1963.
15. M. Fox, et al, "Theory of Discharges at the Foil Edge in Capacitors," IEE Proceedings (BG), 115, #7, 1968.
16. T.E. Springer, et al, "Field Grading in Capacitor Margins," 3rd IEEE Pulsed Power Conference, 1981.
17. R.D. Parker, "Air Force Aero Propulsion Laboratory Report AFWAL-TR-80-2037," Wright-Patterson AFB, OH, January 1980.
18. G.P. Boicourt and E.L. Kemp, "A Newly Discovered Failure Mode in High Energy Density, Energy Storage Capacitors," Los Alamos Scientific Laboratory Report LA-7376-MS, 1978.
19. P.J. Dynes and D.H. Kaelble, "Plasma Polymerization of Metals", Journal of Macromolecular Science - Chemistry, Vol A10, p. 535, 1976.
20. David H. Kaelble and Paul J. Dynes, "Surface Energetics Analysis of Lithography, Adhesion Science and Technology, (Plenum Press) Vol 9B, p. 735-761, 1975.
21. R.D. Parker, "Capacitors for Aircraft High Power," United States Air Force Report AFWAL-TR-80-2037, Air Force Aero Propulsion Laboratory, Wright-Patterson AFB, Ohio, January 1980.
22. R.D. Gourlay, "A Compact Low Inductance Load for Pulse Tests," Proc. IEEE International Pulsed Power Conference, p. IIE-6, 1976.

APPENDIX
CAPACITOR PAD TEST PLAN

HUGHES

HUGHES AIRCRAFT COMPANY

AEROSPACE GROUPS
CULVER CITY, CA 90230

ADVANCED CAPACITORS

Contract F33615-79-C-2081

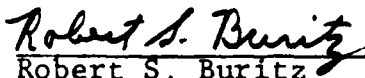
Capacitor Pad Test Plan

Addendum to Interim Technical Report


Robert S. Buritz
Power Devices Department
Developmental Products Laboratory
Technology Support Division
Electro-Optical and Data Systems Group

Prepared for:

United States Air Force
Air Force Systems Command
Aeronautical Systems Division
Air Force Wright Aeronautical Laboratories
Aero Propulsion Laboratory
Capt. Gerald Clark, Project Engineer


Robert S. Buritz
Program Manager

Approved:


Karl C. Hurley, Acting Manager
Power Devices Department

TEST PLAN

This document contains the plan for test of four different types of capacitor pads developed under Contract F33615-79-C-2081. This plan has been tailored to provide maximum utilization of the pulse test facility developed under Contract F33615-75-C-2021, to expedite the program while saving substantial costs.

1.0 PARAMETER MEASUREMENTS

All capacitor pads shall undergo the following parameter tests before any other testing is performed.

- 1.1 Capacitance. Capacitance shall be measured at 1.0 KHz and 25°C.
- 1.2 Dissipation Factor. Dissipation Factor shall be measured at 1.0 KHz and 25°C.
- 1.3 Insulation Resistance. Insulation Resistance shall be determined at 1 kV, with a 5-minute wait before current measurement.
- 1.4 DC Withstand. DC Withstand shall be conducted in accordance with MIL-STD-202, Method 301. The DC voltage used shall be equal to the peak AC voltage or the AC plus DC peak voltage of the design.

2.0 HIGH REPETITION RATE PULSE CAPACITORS

This section covers the test of 2.20 μ F 7.5 kV capacitor pads designed to the requirements of paragraph 4.3.1 of the Statement of Work.

- 2.1 Specimen Mounting. A minimum of 6 pads but not more than 20 pads will be tested. These pads shall be mounted in reuseable test cans per the general description in AFWAL-TR-77-40, page 68. At least 2 pads shall have a thermocouple at the center of the winding.

2.2 Test Fixture. The test apparatus described in the referenced report, pages 69-75, shall be used for these tests without modification.

2.3 Test Sequence

2.3.1 Order of Test. The capacitors with thermocouples shall be tested first.

2.3.2 Initial Tests. A 300 pps 1 minute burst shall be run at 5 kV. The following parameters shall be closely observed.

- o pad temperature (after burst)
- o charging current

If pad internal temperatures does not rise above 70°C, wait 2 hours and run another burst 500V higher. Continue this sequence until 7.5 kV or 100°C is reached. During this sequence, observe how long it takes the pad to cool to 30°C.

2.3.3 Pad Tests. Test each pad at rated parameters or those determined in the previous paragraph. Set the timing between bursts to the time determined above. Test to 10⁶ shots only.

2.4 Failure Analysis. Disect each pad after testing. Classify the failure as: edge or body, infant or wear-out.

3.0 LOW REPETITION RATE PULSE CAPACITORS

Test these components to the requirements of Sections 2.1 through 2.4, but using the requirements of paragraph 4.3.2 of the Statement of Work.

4.0 DC CAPACITORS

This section covers the test of 1.2 µF 8.3 KV pads designed to the requirements of paragraph 4.3.3 of the Statement of Work.

AD-A151 709 ADVANCED CAPACITORS(U) HUGHES AIRCRAFT CO EL SEGUNDO CA 3/3

ELECTRO-OPTICAL AND DATA SYSTEMS GROUP
J B ENNIS ET AL. OCT 84 HAC-FR84-76-621

UNCLASSIFIED AFMAL-TR-84-2058 F33615-79-C-2081

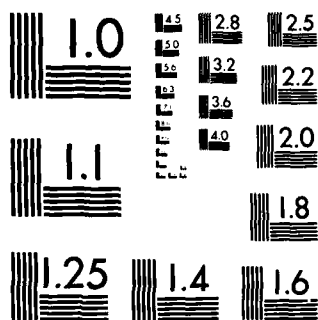
F/G 9/1

NL

END

FILED

DTIC



MICROCOPY RESOLUTION TEST CHART
NATIONAL BUREAU OF STANDARDS-1963-A

- 4.1 Specimen Mounting. At least 10 pads but not more than 20 pads will be tested. These pads shall be mounted in reusable test cans per Section 2.1. The thermocouple shall be omitted.
- 4.2 Test Fixture. A fixture capable of supplying 8300 VDC plus 21 VAC (rms) at 20 KHz shall be used. All capacitors may be tested at one time on the same fixture if sufficient AC power (400 W) is available, but each capacitor shall be wired in series with a small resistor to protect the test circuitry if the capacitor shorts. A temperature of 25°C shall be maintained.
- 4.3 Test Sequence. The DC voltage shall be applied in a smooth ramp over a period of 1 minute. Following the application of the DC voltage, the AC voltage shall be applied. If the test is shut down for any reason, this sequence must be used each time it is restarted. Since no life requirement is given, the test will be continued for 1000 hours total time.
- 4.4 Failure Analysis. Failure analysis per paragraph 2.4 shall be performed on each pad at the conclusion of the test.

5.0 AC CAPACITORS

This section covers the test of 120 µF, 400 Hz capacitor pads designed to the requirements of the amended Statement of work.

5.1 Test Sequence

- 5.1.1 Breakdown Tests. Fabricate not less than 20 pads each of polyetherimide and polysulfone film. Perform breakdown tests.
- 5.1.2 Life Tests. Conduct accelerated life tests at 125°C. Tests will be limited to 2000 hours or less.
- 5.1.3 Failure Analyses. Each pad shall be dissected after test, and the failure mechanism determined. All anomalies shall be reported.

END

FILMED

4-85

DTIC